THERMODYNAMIC AND ECONOMIC ANALYSIS OF A SOLAR THERMAL POWERED ADSORPTION COOLING SYSTEM

A THESIS SUBMITTED TO
THE GRADUATE SCHOOL OF NATURAL AND APPLIED SCIENCES
OF
MIDDLE EAST TECHNICAL UNIVERSITY

BY

DERVİŞ EMRE DEMİROCAK

IN PARTIAL FULFILLMENT OF THE REQUIREMENTS
FOR
THE DEGREE OF MASTER OF SCIENCE
IN
MECHANICAL ENGINEERING

OCTOBER 2008

Approval of the thesis:

THERMODYNAMIC AND ECONOMIC ANALYSIS OF A SOLAR THERMAL POWERED ADSORPTION COOLING SYSTEM

submitted by **DERVİŞ EMRE DEMİROCAK** in partial fulfillment of the requirements for the degree of **Master of Science in Mechanical Engineering Department, Middle East Technical University** by,

Prof. Dr. Canan Özgen
Dean, **Gradute School of Natural and Applied Sciences** _____

Prof. Dr. Süha Oral
Head of Department, **Mechanical Engineering** _____

Assist. Prof. Dr. Derek Keith Baker
Supervisor, **Mechanical Engineering Dept., METU** _____

Prof. Dr. Bilgin Kaftanoğlu
Co-supervisor, **Mechanical Engineering Dept., METU** _____

Examining Committee Members:

Assoc. Prof. Dr. Cemil Yamalı
Mechanical Engineering, METU _____

Assist. Prof. Dr. Derek Keith Baker
Mechanical Engineering, METU _____

Prof. Dr. Bilgin Kaftanoğlu
Mechanical Engineering, METU _____

Assist. Prof. Dr. İlker Tarı
Mechanical Engineering, METU _____

Dr. Merih Aydınalp Köksal
Environmental Engineering, Hacettepe Univ. _____

Date: 16.10.2008

I hearby declare that all information in this document has been obtained and presented in accordance with academic rules and ethical conduct. I also declare that, as required, I have fully cited and referenced all material and results that are not original to this work.

Name, Lastname : DERVİŞ EMRE DEMİROCAK

Signature :

ABSTRACT

THERMODYNAMIC AND ECONOMIC ANALYSIS OF A SOLAR THERMAL POWERED ADSORPTION COOLING SYSTEM

Demirocak, Derviş Emre

M.Sc., Department of Mechanical Engineering
Supervisor: Assist. Prof. Dr. Derek Keith Baker
Co-supervisor: Prof. Dr. Bilgin Kaftanoğlu

October 2008, 166 pages

In this thesis, yearly performance of the solar adsorption cooling system which is proposed to be installed to a residential building in Antalya is theoretically investigated in detail. Firstly, thermodynamic designs of the adsorption cooling cycle for three different types of cycles which are intermittent, heat recovery and heat & mass recovery cycles are presented. Secondly, adsorption characteristics of three adsorbent/adsorbate pairs which are zeolite-water, silica gel-water and activated carbon-methanol are given. Following this, load side (i.e., building) of the system is designed and parameters that should be considered in building design are presented. Then, solar-thermal cooling system design methodology with an emphasis on solar fraction is presented. In addition, system parameters effecting the performance of the adsorption cooling system are analyzed and results are presented. Finally, economic analysis is done in order to understand the economic feasibility of the solar-thermal cooling systems compared to conventional cooling systems. TRNSYS is used for the yearly simulations

and an integrated model of the overall system is developed in TRNSYS. Since energy consumption and performance investigations of environment-dependent systems such as building HVAC, refrigeration systems and solar collectors usually require weather information, typical meteorological year (TMY) data for Antalya is also generated in order to be used in the analysis of the system parameters.

Keywords: Adsorption Cooling, Typical Meteorological Year (TMY), Economic Analysis, Thermodynamic Design, Zeolite, Silica Gel, Activated Carbon.

ÖZ

ISIL GÜNEŞ ENERJİSİ İLE ÇALIŞAN ADSORBSİYON SOĞUTMA SİSTEMİNİN TERMODİNAMİK VE EKONOMİK ANALİZİ

Demirocak, Derviş Emre

Yüksek Lisans, Makina Mühendisliği Bölümü
Tez Yöneticisi: Yrd. Doç. Dr. Derek Keith Baker
Ortak Tez Yöneticisi: Prof. Dr. Bilgin Kaftanoğlu

Ekim 2008, 166 sayfa

Bu tez çalışmasında, Antalya'daki bir yazlık evde kurulu olduğu kabul edilen ısıl güneş enerjisi ile çalışan adsorbsiyon soğutma sisteminin yıllık performansı teorik olarak detaylı bir şekilde incelenmiştir. Öncelikle, üç farklı adsorbsiyon soğutma çevriminin termodinamik tasarımı sunulmuştur. Bunlar aralıklı, ısı geri kazanımlı ve ısı & kütle geri kazanımlı çevrimlerdir. Bundan sonra zeolit-su, silika jel-su ve aktif karbon-metanol adsorban/soğutucu çiftlerinin adsorbsiyon karakteristikleri sunulmuştur. Bunu takiben, sistemin yük kısmı olan binanın tasarımı yapılmıştır ve bina tasarımında göz önünde tutulacak parametreler açıklanmıştır. Daha sonra güneş-ısıl soğutma sistemlerinin tasarım metodolojisi, güneş kullanma miktarı vurgulanarak açıklanmıştır. Buna ilaveten, adsorbsiyon soğutma sisteminin performansını etkileyen sistem parametreleri analiz edilmiş ve sonuçlar sunulmuştur. Son olarak, güneş-ısıl soğutma sistemlerini ekonomik yönden konvansiyonel soğutma sistemleriyle kıyaslayabilmek için ekonomik analiz yapılmıştır. Yıllık benzetimler için TRNSYS kullanılmıştır

ve ayrıca entegre sistem modeli TRNSYS'de geliştirilmiştir. Çevre ile doğrudan ilgili sistemlerin (bina ısıtma, soğutma ve havalandırma sistemi, güneş kollektörleri, vb.) enerji tüketimleri ve performans incelemeleri genellikle hava verisine ihtiyaç duyar. Sistem parametrelerinin analizinde kullanılmak üzere, Antalya için tipik meteorolojik yıl (TMY) verisi de oluşturulmuştur.

Anahtar kelimeler: Adsorpsiyon Soğutma, Tipik Meteorolojik Yıl (TMY), Ekonomik Analiz, Termodinamik Tasarım, Zeolit, Silika Jel, Aktif Karbon.

Dedicated to pioneers of science whom always inspired and excited me

ACKNOWLEDGMENTS

I would like to thank to my supervisor Assist. Prof. Dr. Derek Keith Baker for his continuous support, contributions and valuable guidance throughout my study.

I also would like to thank to my co-supervisor Prof. Dr. Bilgin Kaftanoğlu for his precious advices.

I wish to express my gratitude to my parents Yılmaz and Sabire Demirocak who always support me during my life.

TABLE OF CONTENTS

LIST OF FIGURES

FIGURES

LIST OF TABLES

TABLES

LIST OF SYMBOLS

β	Collector slope
β'	Similarity (affinity) coefficient
ϕ	Latitude of the location
η	Efficiency of the natural gas plant
κ	Characteristic parameter for a given adsorbent/adsorbate pair
A	Adsorption potential
A_c	Total collector area dependent cost
A_{spec}	Specific collector area
C_S	Total cost of installed solar energy equipment
C_E	Total cost of equipment which is independent of collector area
C_{p_l}	Specific heat of adsorbate in liquid phase
C_{p_w}	Specific heat of adsorbate in adsorbed phase
C_{p_z}	Specific heat of adsorbent
$CDFs$	Cumulative distribution functions
COP	Coefficient of performance
$elec_u$	Unit price of electricity
E_0	Characteristic energy of adsorption for a reference vapor
E_{cool}	Yearly total cooling load of the building
F	Future value of money
FS	Finkelstein-Schafer
$G_\perp$	Normal incident solar radiation on the collector
H_L	Heat added into the boiler/heater
i	Percent interest per time period
L	Heat of evaporation of adsorbate

LCC	Life-cycle cost
$\dot{m}_{pl}$	Primary loop mass flow rate
$\dot{m}_{sl}$	Secondary loop mass flow rate
m_z	Mass of adsorbent
$Mtoe$	Million ton of equivalent oil
$M_{tot,conv}$	Yearly electricity bill of the conventional cooling system
$M_{tot,sol}$	Yearly electricity bill of the solar assisted cooling system
n	Heterogeneity factor
ng_u	Unit price of natural gas
NG	Yearly natural gas consumption
P	Equilibrium vapor pressure at temperature T
Pr	Present value of money
P_0	Saturated vapor pressure
PV	Photovoltaic
Q_L	Heat transfered from the low temperature space
Q_{gen}	Heat input to the generator
Q_{ih}	Heat of isosteric heating
Q_{des}	Heat of desorption
Q_{ref}	Heat of refrigeration
Q_{reg}	Recovered heat
Q_{sa}	Sensible heat obtained from cooling of adsorbent and adsorbate
Q_{sve}	Energy needed to heat up the vapor from evaporation to adsorption temperature
Q_{ads}	Enthalpy of adsorption
Q_{aux}	Rate of energy delivered to the secondary loop fluid stream
$Q_{cooling}$	Nominal cooling capacity
Q_{coll}	Useful energy gain of the collector
Q_{tot}	Total cooling load
R	Gas constant
SCP	Specific cooling power
SF	Solar fraction
T	Temperature

T_{cool}	Temperature of the cool adsorbent bed
T_{hot}	Temperature of the hot adsorbent bed
TMY	Typical meteorological year
V_{tank}	Volume of the storage tank
w	Equilibrium adsorption capacity
w_0	Maximum equilibrium adsorption capacity
w_{cool}	Equilibrium adsorption capacity of the cool adsorbent bed
w_{hot}	Equilibrium adsorption capacity of the hot adsorbent bed
W	Volume of the adsorbate condensed in micropores
W_0	Maximum volume adsorbed in micropores
W_{pump}	Work input to the pump
WS	Weighted sum

CHAPTER 1

INTRODUCTION

1.1 Renewable Energy

Today, renewable energies supply 14% of the world primary energy demand. These renewable energies include biomass, hydro and other renewables. Other renewables include solar, wind, tidal, geothermal and wave energy and are approximately 1% of the world primary energy demand. However, the utilization of these other renewables is increasing faster (5.7% annually) than other primary energy sources (International Energy Agency(IEA), 2004). Threats of climate change, exhaustion of fossil fuels and the need for secure energy supply stimulate the utilization of renewable energies. In short, today's global energy system is unsustainable in economic, social and environmental terms. In the near term renewable energies may be a solution for the problems mentioned above although they have some drawbacks.

The primary source of all renewable energies except geothermal energy is solar radiation. The amount of solar energy striking the earth's surface is $5.4 \cdot 10^{24}$ J per year (Sϕrensen, 2004). The world primary energy demand is approximated to be 11000 Mtoe (million ton of equivalent oil) in 2006 (IEA, 2004). Thus the solar energy intercepted by the earth is approximately 11500 times greater than the world's total primary energy demand in the year 2006. Solar energy should

be transformed into usable energy forms in order to be utilized. Solar energy is mainly exploited in two ways. It can be converted to either heat or electricity. Converting solar energy to heat is possible by using solar thermal energy technologies. Converting solar energy directly to electricity is achievable by using photovoltaic cells (PV). Also there are indirect ways of converting solar energy into electricity by using solar thermal energy technologies. Energy (heat or electricity) obtained from solar energy technologies can be used for many purposes including the following: drying, heating, cooking, cooling, desalination (Kalogirou, 1997) and generating electricity (Mills, 2004), (Trieb, Lagniβ & Klaiβ, 1997).

Solar thermal energy describes all technologies that collect sunlight and convert their electromagnetic energy into heat, either for directly satisfying heating/cooling needs or for producing electricity. In order to increase efficiency, high temperatures are necessary for electricity generation from solar thermal processes. These high temperatures can be obtained by using concentrating solar power technologies (Philibert, 2005).

Key advantages of solar thermal systems are as follows (European Solar Thermal Industry Federation [ESTIF], 2006);

- reduces the dependency on imported fuels
- improves the diversity of energy supply
- saves scarce natural resources
- saves CO_2 emissions at very low costs
- curbs urban air pollution
- is proven and reliable
- is immediately available
- owners of systems save substantially on their heating/cooling bills
- creates local jobs and stimulates the local economy

- inexhaustible

In this study cooling and refrigeration by using solar energy technologies are emphasized. Solar cooling and refrigeration can be done by using electricity generated by PV cells or by employing solar thermal technologies which will be considered in detail in the literature review.

1.2 Solar Cooling

The idea of solar cooling is not a new one. Passive cooling of buildings dates back to ancient times (Florides, Tassou, Kalogirou & Wrobel, 2002). Passive cooling is defined as attaining comfort by means of evaporative cooling, thermal inertia of the building, ventilation and shading (Sayigh & McVeigh, 1992). The passive cooling capacity of a building has a very close relation with its architecture. Considerable amounts of energy savings can be obtained by an appropriate design (Santamouris & Asimakopoulos, 1996). However, passive solar cooling alone is not enough to obtain thermal comfort always. Active solar cooling technologies are used to complement it. Active solar cooling systems became important after the 1973 oil crisis. Active solar cooling systems are driven by cost effective heat sources. Mostly with solar energy, but also waste heat from many industrial processes can be utilized for driving active solar cooling systems. Passive solar cooling is out of the scope of this study and only active solar cooling technologies will be discussed, with an emphasis on solar thermal powered technologies. In the rest of the text active solar cooling will be called **solar cooling**.

Usage of solar energy for cooling has been considered for two related purposes, to provide refrigeration for food preservation and to provide comfort cooling (Duffie & Beckman, 2003). Cooling, refrigeration and air conditioning are actually encouraging and bright future applications for solar energy technologies. It was estimated that approximately 15% of all electricity produced worldwide is used for refrigeration and air conditioning processes of various kinds (Lucas,

1988). Nowadays electricity used for refrigeration and air conditioning processes should be higher than 15% due to increasing thermal comfort expectations and global warming. Also increasing thermal comfort expectations, lower initial costs for air conditioning equipment and heat island effects in urban areas create peaks in electricity demand during the summer (Papadopoulos, Oxizidis & Kyriakis, 2003). Since the demand for air conditioning and cooling is in phase with the supply of solar energy from the sun, peak demand reduction is possible by using solar thermal technologies. Thus, idle investments for electricity generation can be reduced.

Solar cooling systems can be classified into two main categories according to the energy used to drive them:

1. Electrical systems
    - Vapor compression systems
    - Thermoelectric systems
    - Stirling systems[1]
2. Thermal systems
    - Absorption systems
    - Adsorption systems
    - Desiccant systems
    - Ejector systems
    - Rankine systems

Electrical systems utilize PV cells. On the other hand, thermal systems utilize solar thermal collectors of various types. Detailed information about solar

[1]Stirling systems can be categorized under either electrical or thermal systems, because Stirling systems can be driven by thermal energy for generating electricity or vice versa. In the context of solar energy, Stirling systems are used for generating electricity by using parabolic dish collectors (Infinia Corporation, 2007). Stirling systems are one of the main competitors of PV cells.

collectors can be found in the literature (Kalogirou, 2004). Adsorption and desiccant cooling technologies are appropriate for utilization of low temperatures (45°C - 95°C). Absorption, Rankine cycle and ejector cooling technologies are more favorable for high temperature applications (100°C - 350°C).

In recent years, solar thermal powered cooling systems have been successfully implemented all around the world. In order to reduce global warming and to reduce electricity peak demands occurring in summer months, solar cooling applications will become widespread at an increasing rate.

1.3 Objectives of the Thesis

In this thesis, yearly performance of the solar adsorption cooling system which is proposed to be installed to a residential building in Antalya will be theoretically investigated in detail. First, thermodynamic design of the adsorption cooling cycle for three different types of cycles which are intermittent, heat recovery and heat & mass recovery cycles will be presented. Second, the adsorption characteristics of three adsorbent/adsorbate pairs which are zeolite-water, silica gel-water and activated carbon-methanol will be given. Following this, the load side (i.e., building) of the system will be designed and parameters that should be considered in building design will be presented. Then, solar-thermal cooling system design methodology with an emphasis on solar fraction will be presented. In addition, system parameters effecting the performance of the adsorption cooling system will be analyzed and results will be presented. Finally, economic analysis will be done in order to understand the economic feasibility of the solar-thermal cooling system compared to conventional cooling systems. TRNSYS will be used for the yearly simulations and an integrated model of the overall system will be developed in TRNSYS. Since energy consumption and performance investigations of environment dependent systems such as building HVAC and refrigeration systems, solar collectors and cooling towers, usually require weather information, typical meteorological year (TMY) data will be generated in order to be used in the analysis of the system parameters. Inte-

grated model of the overall system is given in Figure 1.1 below.

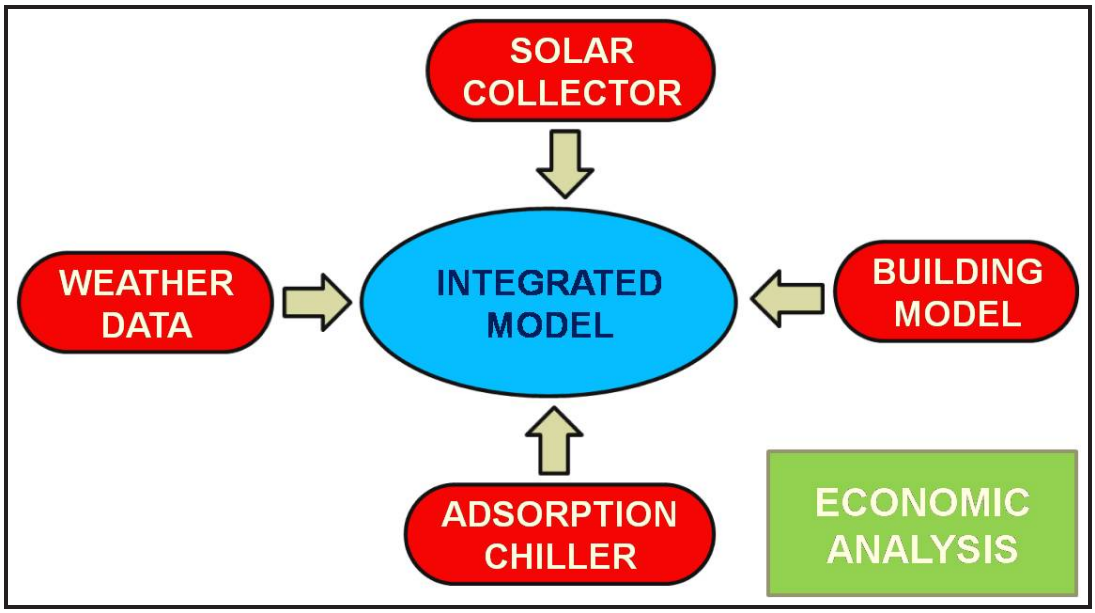

Figure 1.1: Integrated Model.

CHAPTER 2

LITERATURE SURVEY

Encyclopedia Britannica defines refrigeration as *"the process of removing heat from an enclosed space or from a substance for the purpose of lowering the temperature"*. Before going further it is appropriate to clarify the meanings of the terms solar cooling, solar refrigeration and solar air-conditioning. Generally solar cooling or solar air-conditioning terms are used for the systems which are used for obtaining thermal comfort conditions in buildings or vehicles, whereas solar refrigeration term is more likely to be used for the systems which are used for food preservation, vaccine storage or ice production. Chiller term is also used for air-conditioners which are working on absorption or adsorption refrigeration cycles (i.e. absorption chiller).

As stated in the Introduction, solar energy can be converted either to thermal energy or electricity. Theoretically speaking, all the refrigeration technologies can be driven by heat or electricity, but not all of them are feasible to be driven by solar energy. For example, solar thermal driven cooling technologies cannot compete with grid electricity driven room air conditioners which are working on vapor compression cycle, because solar thermal driven cooling technologies are more expensive per unit cooling power, bulkier (usually requires separate places for installation) and heavier than room air conditioners. Also electricity generated by PV cells is not economically competitive with grid electricity due

to high investment cost of PV cells. But these fields have a promising future. For instance in 1970s PV cells had an efficiency of 5%, today PV cells with 15% efficiency are commercially available, and moreover PC cells with up to 25% efficiencies have been developed, but are not available in the market yet.

2.1 Solar Refrigeration Systems

As mentioned in the Introduction, it is appropriate to divide solar refrigeration systems into two categories: electricity driven and thermal driven systems. Although solar thermal driven systems (specifically adsorption refrigeration) will be emphasized in this study, brief overviews of the other cooling technologies are given for completeness. First electricity driven refrigeration systems will be introduced, then thermal driven refrigeration systems will be explained in detail.

2.1.1 Electricity Driven Solar Refrigeration Systems

2.1.1.1 Vapor Compression Refrigeration Systems

Vapor compression systems are the most widely used technology for air conditioning and refrigeration today (Rona, 2004). First, the main features of vapor compression system will be explained, then differences between PV powered and grid electricity powered vapor compression systems will be discussed.

Carnot cycle is a reversible cycle and all processes in this cycle can be reversed. The reversed Carnot cycle is the most efficient refrigeration cycle operating between two temperature reservoirs. The mechanical vapor compression cycle is the reverse of Rankine cycle. The turbine in the Rankine cycle is replaced by an expansion valve or a capillary tube in the vapor compression cycle, since keeping the turbine makes the system complicated and expensive and increases the coefficient of performance (COP) of the system by only a very small amount.

In the vapor compression cycle the working fluid remains in the vapor phase during one part of the cycle and in the liquid phase during another part of the cycle (Çengel & Boles, 2002). A schematic of the vapor compression cycle is given in Figure 2.1.

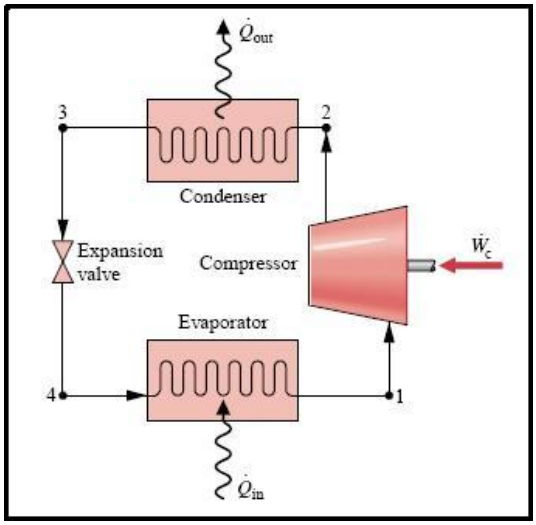

Figure 2.1: Vapor compression cycle (Moran, Shapiro, Munson & DeWitt, 2003)

As seen from Figure 2.1, the ideal vapor compression cycle consists of four processes:

1-2 → Isentropic compression in a compressor
2-3 → Constant pressure heat rejection in a condenser
3-4 → Throttling in an expansion valve
4-1 → Constant pressure heat absorption in an evaporator

The efficiency of a refrigerator is expressed in terms of COP which is the ratio of energy sought from the refrigerated space to the work input. According to Figure 2.1;

$$COP = \frac{Q_{in}}{W_c} \tag{2.1}$$

Typical COPs for vapor compression cycles are around 3 (Jensen, 2008).

2.1.1.2 Thermoelectric Refrigeration Systems

Thermoelectric cooling is different from the vapor compression cycle and does not work on a thermodynamic cycle. The thermoelectric effect or Peltier-Seebeck effect is the direct conversion of temperature differentials to electrical energy or vice versa. The main disadvantage of thermoelectric cooling is its low COP which is near 0.1. So, thermoelectric cooling is usually used for lower (under 25W) cooling demands, when their low COP is not a serious drawback (Riffat & Ma, 2003). Thermoelectric cooling also has some advantages.

- Thermoelectric devices have no moving parts, so require less maintenance.
- Thermoelectric devices have longer life times (above 100,000 h).
- Precise temperature control (0.1) is possible by thermoelectric devices.
- Thermoelectric devices can be used for both heating and cooling by changing the direction of the current.
- Thermoelectric devices can operate in any environmental conditions.
- Thermoelectric devices can be operated directly by using electricity supplied from PV panels without any conversion from AC to DC.

Detailed information on thermoelectric cooling can be found in literature (Riffat et al., 2003).

2.1.1.3 Stirling Refrigeration Systems

Consider a piston cylinder arrangement containing gas (usually helium, nitrogen or hydrogen). When the gas is compressed, the temperature inside the

cylinder rises. On the other hand, if the gas is expanded the temperature inside the cylinder drops. Stirling coolers are working on this basic principle.

Stirling coolers work on a reversed Stirling power cycle. A T-s diagram of the Stirling cycle is shown in Figure 2.2. As for the vapor compression cycle, the Stirling cycle consists of four thermodynamic processes (Haywood, Raine & Gschwendtner, 2002):

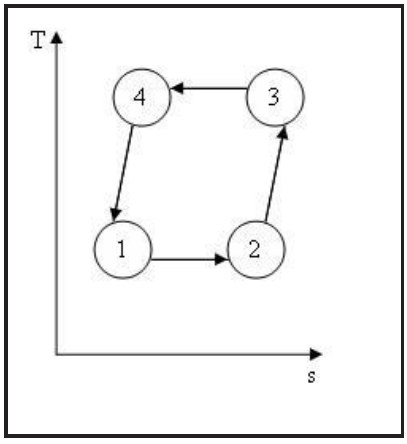

Figure 2.2: Stirling cycle

1-2 → Isothermal expansion
2-3 → Isochoric (constant volume) displacement
3-4 → Isothermal compression
4-1 → Isochoric (constant volume) displacement

COP's of Stirling coolers are close to vapor compression cycles for moderate temperature differences between the heat sink and heat source. As the temperature difference between sink and source increases, the Stirling coolers perform better than vapor compression cycles (Rona, 2004). In addition, very low temperatures (10 K) can be maintained by using Stirling coolers.

More detailed information can be found in the literature (e.g., Haywood et al., 2002; Rona, 2004).

2.1.2 Solar Thermal Driven Refrigeration Systems

Thermal driven cooling systems are usually feasible when a low temperature (below 200°C) and/or cost efficient heat source is available. In general, solar energy is the most widely available heat source for solar thermal driven cooling applications. Also waste heat from industrial processes can be an alternative to solar energy whenever it is available.

There are four major solar thermal driven cooling systems today. These are absorption, adsorption, desiccant and ejector cooling systems. In addition to these, the Rankine power cycle can be driven by solar thermal energy to produce work output, and then this work can drive any mechanical refrigeration cycle.

2.1.2.1 Absorption Refrigeration

According to International Energy Agency (IEA), absorption cooling system is the most widely used solar thermal driven cooling system today (IEA, 2002). Absorption cooling dates back to the 1700s, and the first ammonia-water refrigeration system was patented by Ferdinand Carre in 1859 (Srikhirin, Aphornratana & Chungpaibulpatana, 2001).

The main difference of the absorption refrigeration cycle from the vapor compression cycle is the replacement of the compressor with a thermally driven absorption mechanism. The absorption mechanism includes an absorber, pump, expansion valve, regenerator and generator. According to the working fluid used in the absorption system, the components of the absorption mechanism may change.

The working fluid in absorption refrigeration cycles is a solution of two or more materials. Usually water-ammonia (water/NH_3) or lithium bromide-water (LiBr/water) solutions are used. In water/NH_3 systems, water is the absorbent and NH_3 is the refrigerant. Since the freezing point of NH_3 is -77°C, water/NH_3 systems can be used for low temperature applications. On the other

hand, in LiBr/water systems LiBr is the absorbent and water is the refrigerant. Since the freezing point of water is 0°C, LiBr/water systems are only appropriate for air conditioning applications. A simple single effect water/NH_3 absorption refrigeration cycle is shown in Figure 2.3 below. In this configuration, a rectifier is used in the absorption cooling system in addition to the components mentioned above. Since water is highly volatile, the rectifier is used to separate water vapor from the NH_3. Without a rectifier, the water vapor would freeze and accumulate in the evaporator and would decrease the system performance.

In the absorption refrigeration cycle, the only work input is for the pump. Since the pump increases the pressure of a liquid and work input is proportional to specific volume, the work input for the pump is very small compared to the compressor in the vapor compression cycle and is on the order of 1% of the heat supplied from the generator (Çengel et al., 2002).

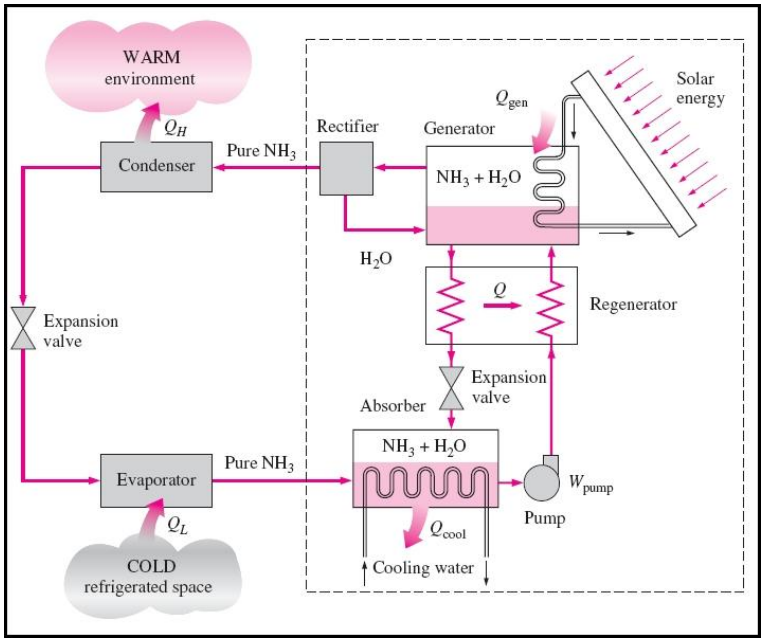

Figure 2.3: Mechanism of absorption refrigeration cycle (Çengel et al., 2002)

The COP of the absorption refrigeration cycle is defined as;

$$COP = \frac{Q_L}{Q_{gen} + W_{pump}} \cong \frac{Q_L}{Q_{gen}} \tag{2.2}$$

where Q_L is the heat transfered from the low temperature space (refrigerated space), Q_{gen} is the heat input to the generator and W_{pump} is the work input to the pump which is neglected. The COP for a single effect absorption refrigeration cycle is approximately 0.6. This is low compared to a vapor compression cycle, but if Q_{gen} is supplied from solar energy, the operational cost of the absorption refrigeration system is smaller than vapor compression system powered with grid electricity. On the other hand, the investment cost of absorption refrigeration system is higher than the vapor compression system. Also absorption chillers are heavier and bulkier than the conventional vapor compression chillers.

In order to increase the COP of the absorption chillers, multi-effect absorption refrigeration cycles can be utilized. Today double-effect refrigeration cycles are commercially available with COPs ranging from 0.8 to 1.2[1]. Also triple-effect and quadruple-effect absorption refrigeration cycles are in development with COPs up to 2. In addition to multi-effect absorption cycles, there are other options available in order to increase absorption system's performance. Generator/absorber heat exchanger (GAX) absorption refrigeration cycle and absorption refrigeration cycle with absorber heat recovery are just two of them. Interested readers may find detailed information in the literature (e.g., Srikhirin et al., 2001).

2.1.2.2 Desiccant Refrigeration

Desiccant cooling system has its root in the evaporative cooling concept. Evaporative cooling is based on a physical phenomenon in which evaporation of a liquid absorbs heat from the substances in contact with it. Heat absorbed dur-

[1]http://www.robur.com, http://www.broad.com, http://www.york.com

ing evaporation is related to the latent heat of vaporization of that liquid. The potential of evaporative cooling is associated with the difference between wet bulb and dry bulb temperatures. As this difference increases the potential of evaporative cooling increases.

Desiccants are defined by Daou, Wang & Xia (2006) as *"natural or synthetic substances capable of absorbing or adsorbing water vapor due the difference of water vapor pressure between the surrounding air and the desiccant surface"*. Thus, in desiccant cooling systems desiccants are used to dehumidify the inlet air and then this dry air is cooled and humidified by evaporative cooling and followed sometimes by a vapor compression system (or any other cooling system) for sensible cooling. Since desiccant cooling is utilized to handle latent loads, the vapor compression system's energy demand decreases. Although the desiccant cooling system's performance is strongly dependent on weather conditions, energy savings may reach up to 80% for dry climates. Energy savings decrease as humidity ratio increases (Daou et al., 2006).

A schematic of a desiccant cooling system is presented in Figure 2.4. The outside air stream at state 1 is passed through the desiccant wheel. Humidity of the air stream at state 2 is significantly decreased. Since adsorption or absorption of water vapor by the desiccant substance is an exothermic reaction, temperature of the air stream increases. Then by heat wheel the temperature of the air stream is decreased. If heat wheel is not enough for required cooling, vapor compression system should be used in conjunction with heat wheel. Finally the temperature of the air stream is further decreased and humidity ratio of the air is increased by evaporative cooling according to thermal comfort conditions.

A heater is used between state 7 and 8 in order to obtain high temperatures required for regeneration of the desiccant material. Solar energy or waste heat can be used for heating the exhaust air stream.

Assuming no need for a vapor compression system, the COP of the desiccant

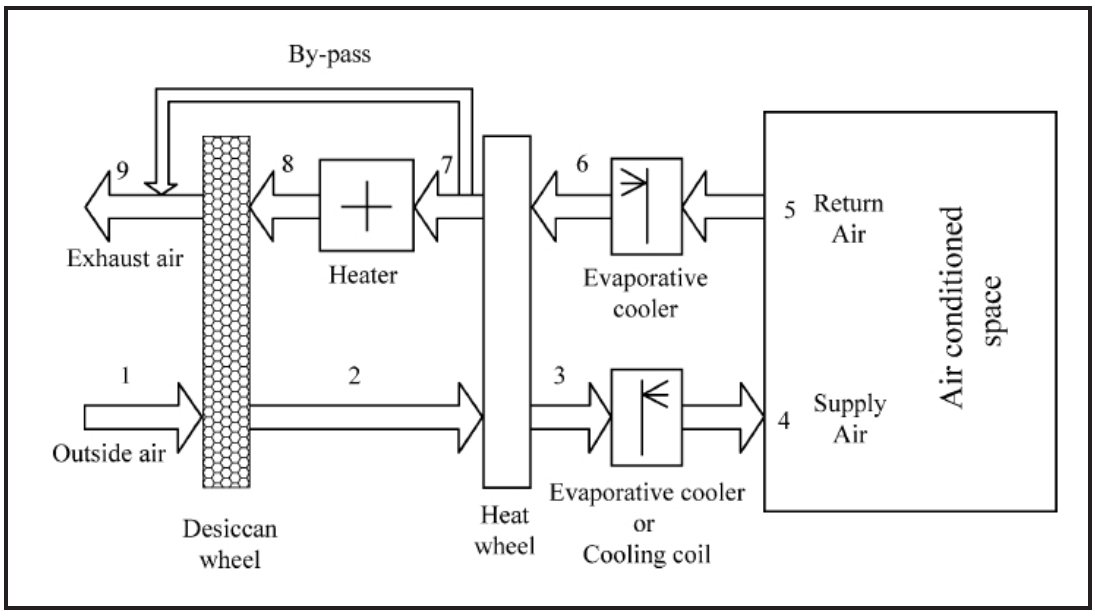

Figure 2.4: Desiccant cooling system (Daou et al., 2006).

cooling system is defined as:

$$COP = \frac{Q_L}{Q_H} \tag{2.3}$$

where Q_L is the heat extracted from the conditioned space and Q_H is the heat added into the heater.

The system shown in Figure 2.4 is utilizing solid desiccants. Also systems utilizing liquid desiccants are available. Detailed discussion of solid and liquid desiccant cooling systems and other system parameters can be found in Daou et al. (2006).

2.1.2.3 Ejector Refrigeration

An ejector refrigeration system, which can be driven by low grade thermal energy, is another alternative to the conventional vapor compression cycle. In this system the compressor of the vapor compression cycle is replaced by a boiler, an ejector and a pump. Detailed information about the theory, types

and working principles of ejectors can be found in the literature (Chunnanond & Aphornratana, 2004). A schematic of the system is given in Figure 2.5. COP of the ejector refrigeration system is defined as:

$$COP = \frac{Q_L}{Q_H} \tag{2.4}$$

where Q_L is the heat extracted from the evaporator and Q_H is the heat added into the boiler.

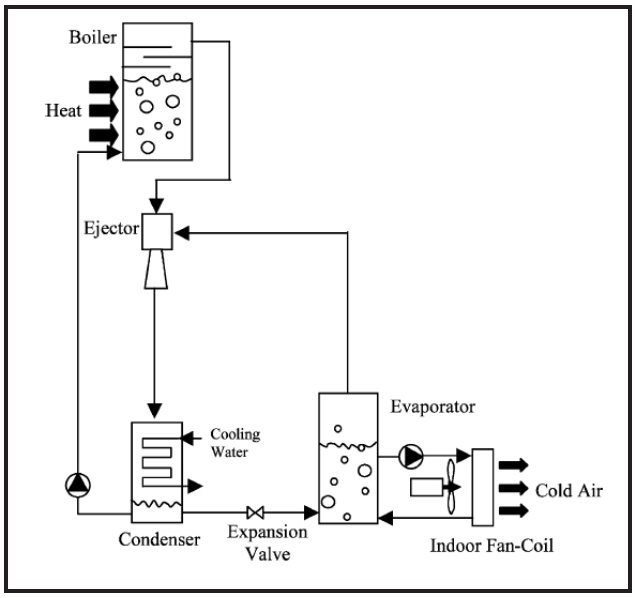

Figure 2.5: Ejector refrigeration system (Chunnanond et al., 2004).

The major disadvantage of the ejector refrigeration cycle is its low COP which is usually under 0.3. On the other hand, ejector refrigeration systems have high reliability, low operating and installation cost and require less maintenance (Pridasawas, 2006).

2.1.2.4 Rankine Refrigeration

The Rankine refrigeration system is the combination of the Rankine power cycle and vapor compression refrigeration cycle. The turbine work obtained from the Rankine cycle is used to drive the compressor in the vapor compression cycle. A schematic of a Rankine refrigeration cycle is given in Figure 2.6.

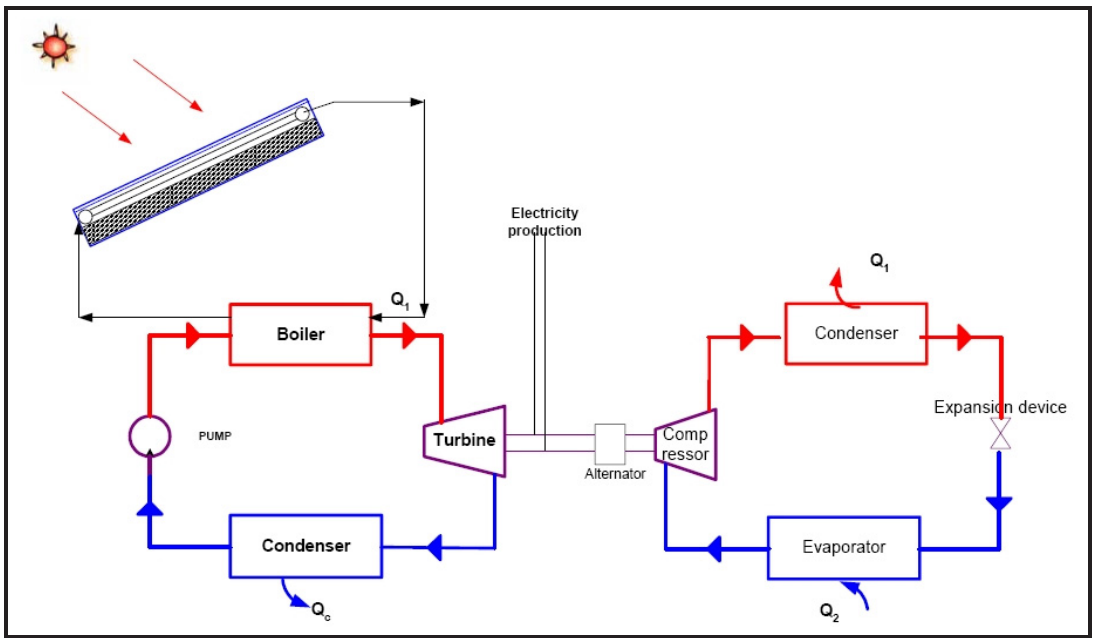

Figure 2.6: Rankine refrigeration system (Pridasawas, 2003).

Rankine refrigeration system's COP is same as vapor compression cycle, but the efficiency of Rankine power cycle is directly related to the temperatures of the sink and source. In order to increase the overall system's performance, high efficiency flat plate collectors, evacuated tube collectors or parabolic trough collector can be used. In general Rankine refrigeration systems are complex and suitable for large air conditioning applications (Pridasawas, 2006).

2.1.2.5 Adsorption Refrigeration

The first adsorption cooling system, which utilized ammonia and silver chloride (AgCl) as the working pair, was developed by Michael Faraday in 1848. The first commercial products became available at the beginning of the 20th century, but the invention of cheap and reliable compressors in the following decades made sorption systems unfeasible (Critoph et al., 2005). It was not until the 1970s energy crisis that a renewed interest in sorption systems began.

Adsorption refrigeration is similar to absorption refrigeration, so first of all it is better to emphasize the difference between absorption and adsorption refrigeration systems. In basic adsorption refrigeration systems, there is no need for a pump and a rectifier. The evaporation and condensation processes are driven by the pressure difference arising inside the system. This pressure difference is caused by adsorption phenomena which is the transfer of a substance from one phase (i.e. vapor) followed by its accumulation or concentration on the surface of another. On the other hand in absorption refrigeration systems, the substance is transferred from one phase to another and penetrates the second substance to form a solution. Adsorption refrigeration systems are explained in greater detail in the following section.

2.2 Thermodynamics of Adsorption Refrigeration Systems

Adsorption refrigeration cycles can be classified as follows: basic cycle (intermittent cycle), continuous heat recovery cycle, mass recovery cycle, thermal wave cycle, convective thermal wave cycle and cascade multi effect cycle. In addition, there are hybrid heating and cooling cycles and also there are combined refrigeration cycles like adsorption-ejector refrigeration cycle or adsorption-vapor compression refrigeration cycle (Ma, Wang, Dai & Zhai, 2006), (Zhang & Wang, 2002). Although these hybrid and combined cycles have promising

advantages, they are outside the scope of this thesis. In this study only intermittent, heat recovery and heat & mass recovery adsorption refrigeration cycles will be discussed.

2.2.1 Basic Adsorption Cycle (Intermittent Cycle)

The basic adsorption cycle relies on the adsorption of a refrigerant vapor (adsorbate) into an adsorbent bed at low pressure and subsequent desorption at a high pressure by heating the adsorbent bed. In the simplest case an adsorption refrigerator can be considered as two vessels connected to each other, one of which is filled with consolidated or granular adsorbent and both of which contain refrigerant as show in Figure 2.7.

At the beginning, the system is at a low pressure and temperature. The adsorbent bed is ideally always satuarted with vapor at this point. The adsorbent bed is heated and refrigerant starts to desorb from the adsorbent bed, which raises the system pressure. Desorbed refrigerant condenses in the second vessel and rejects heat as a result of condensation. Finally the adsorbent bed is cooled back to ambient temperature causing refrigerant to readsorb on the bed.

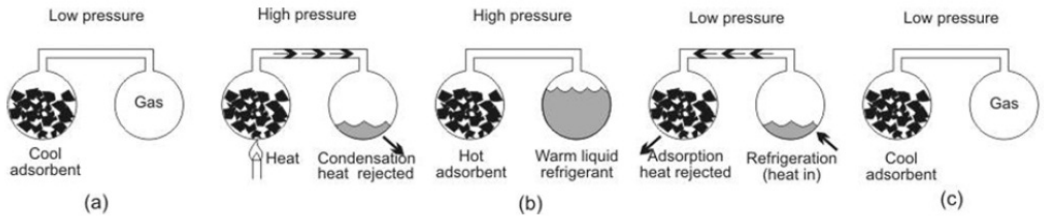

Figure 2.7: Basic adsorption cycle, (Critoph et al., 2005)

The basic adsorption refrigeration cycle consists of four thermodynamic steps. The variation in the amount of refrigerant adsorbed on the adsorbent (w)

throughout the cycle can be clearly represented by a Clapeyron diagram (ln P vs -1/T) which is shown in Figure 2.8. The cycle begins at point 1 where the maximum amount of refrigerant is adsorbed. The adsorbent is at a low temperature and at a low pressure at point 1. Along line 1-2, the adsorbent is heated and desorbs refrigerant vapor isosterically (i.e., at constant total adsorbed mass on the adsorbent). This step is isosteric, because there will be no refrigerant flow until the pressure inside the adsorbent bed becomes equal or greater than the pressure of the condenser and the amount of desorbed refrigerant is small relative to the total amount adsorbed; i.e., $(\Delta m_{ads}/m_{ads}) \approx 0$. Continued heating (line 2-3) desorbs more refrigerant, forcing it to the condenser until state 3 is attained, at which desorption ceases. This second step is isobaric desorption. Then the hot adsorbent is cooled isosterically causing adsorption and depressurization (line 3-4). When the pressure drops below P_{evap}, refrigerant in the evaporator starts to boil and then it flows to the adsorbent bed, producing the cooling effect. Cooling of the adsorbent continues until the bed is saturated with refrigerant, hence completing the cycle. This process (line 4-1) is also isobaric adsorption.

Coefficient of performance of the basic adsorption cycle can be expressed as,

$$COP = \frac{Q_{ref}}{Q_{ih} + Q_{des}} \tag{2.5}$$

The basic adsorption cycle is inherently intermittent due to the required time for the regeneration of the adsorbent bed (adsorbent/adsorber reactor). By using at least two adsorbent beds this basic cycle becomes a continuous basic adsorption cycle with one reactor being regenerated while refrigerant is adsorbed on the other one.

2.2.2 Heat Recovery Adsorption Refrigeration Cycle

For obtaining continuous refrigeration two or more adsorbent beds are necessary. In a simple heat recovery adsorption system two beds are operated out

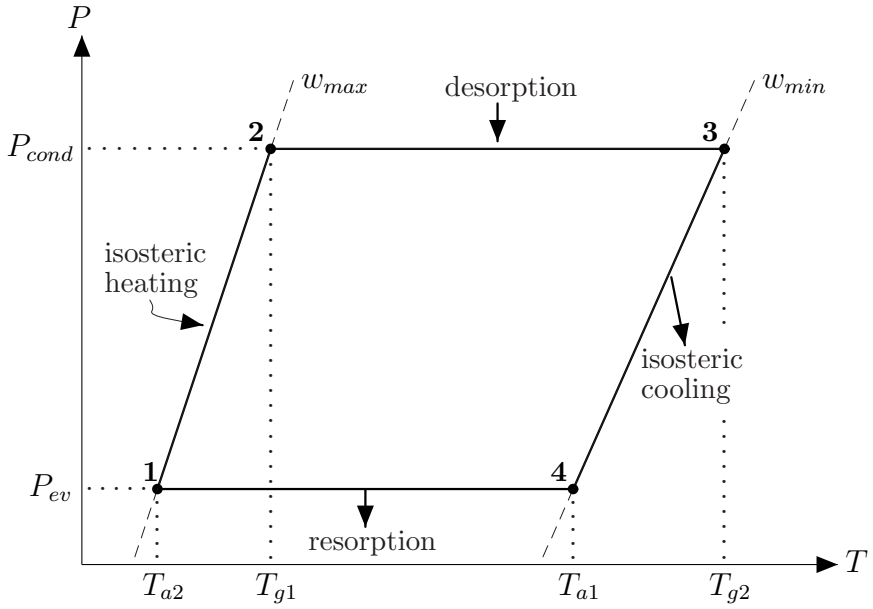

Figure 2.8: P-T-w diagram of basic adsorption cycle

of phase; one bed is heated (regenerated) while the other one is cooled. In order to increase the performance of continuous adsorption refrigeration systems heat recovery is essential. In a heat recovery cycle heat is transferred from the adsorber being cooled to the adsorber being heated. Recovered heat for a two adsorption bed system can be some part of sensible heat and heat of adsorption as shown in Figure 4.3 below. The COP of the system can be increased more than 25% by the heat recovery process (Wang, 2001b).

The COP of the heat recovery adsorption cycle can be expressed as,

$$COP = \frac{Q_{ref}}{Q_{ih} + Q_{des} - Q_{reg}} \tag{2.6}$$

where Q_{reg} is the heat recovered.

For real systems, the benefit of heat recovery process is strongly dependent

on decreasing dead weights (mass of heat transfer fluid and adsorbent bed material).

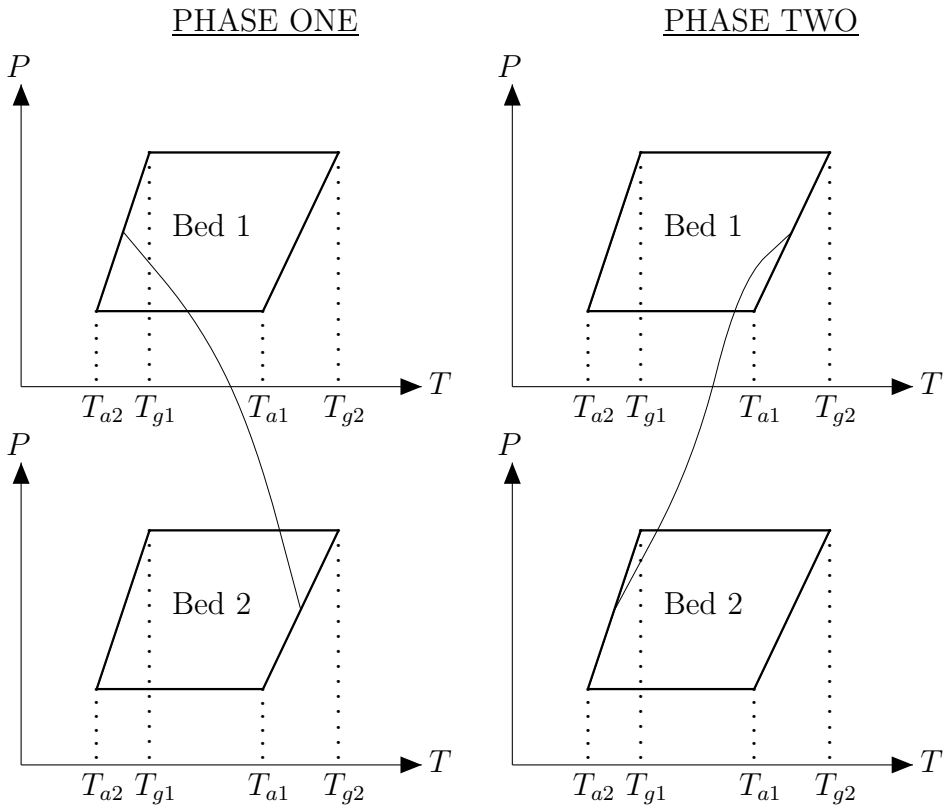

Figure 2.9: Two-bed adsorption refrigeration system with heat recovery. Phase 1: adsorbent bed 1 for heating and bed 2 for cooling, Phase 2: adsorbent bed 1 for cooling and bed 2 for heating (Wang, 2001b).

2.2.3 Heat & Mass Recovery Adsorption Refrigeration Cycle

Mass recovery is proved to be useful for increasing cooling power of the basic adsorption refrigeration cycle. In this process at the end of each half cycle, one

adsorber is cold and at a low pressure (P_{ev}) while other one is hot and at a high pressure (P_{cond}). Meanwhile the hot adsorber must be depressurized to the evaporator pressure, and the cold adsorber must be pressurized to the condenser pressure. Thus by connecting the two adsorbers with a simple pipe, part of this pressurization-depressurization can be done by transferring vapor from the hot adsorber to the cold adsorber. The mass outflow from the hot adsorber will cause more desorption and mass inflow into the cool adsorbent will cause more adsorption as shown in Figure 2.10. The mass recovery process continues until the beds reach an equilibrium pressure of approximately $P_m=(P_{ev}+P_{cond})/2$. Then the connection between two adsorbers is broken and each bed goes on with heating and cooling process. The mass recovery process is usually before heat recovery process. By combining heat and mass recovery, the COP of the adsorption refrigeration system can increase significantly. For an activated carbon-methanol pair, a COP close to 0.8 can be obtained (Wang, 2001b).

2.3 Adsorption Phenomenon

Adsorption is a surface phenomenon which can be classified into two groups; physical adsorption (physisorption) and chemical adsorption (chemisorption). Physisorption is a reversible process and mainly caused by dispersion-repulsion (van der Waals) forces and electrostatic forces between adsorbate (usually liquid or gas) molecules and the atoms which compose the adsorbent (porous substance) surface. On the other hand, chemisorption is an irreversible process and it will not be discussed in this study, but the interested reader should refer to Wongsuwan, Kumar, Neveu & Meunier (2001). Since physical adsorption is a reversible process, most of the adsorption processes applicable to the thermal or cooling systems mainly utilize physisorption. The adsorbing phase is the adsorbent and the material concentrated or adsorbed at the surface of that phase is the adsorbate (refrigerant) (Dieng, 2001). Adsorption is an exothermic process and the heat of adsorption is usually 30% to 100% higher than the heat of condensation (Suzuki, 1990).

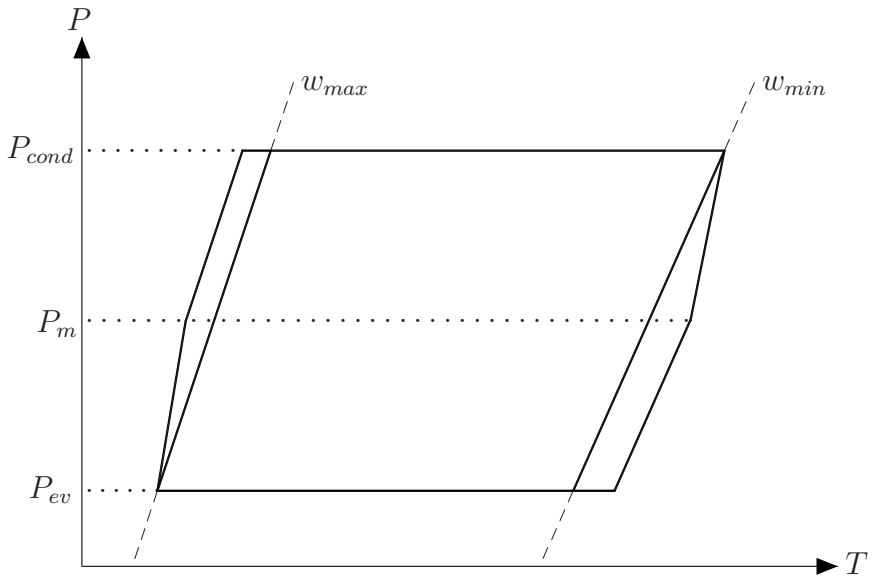

Figure 2.10: Two-bed adsorption refrigeration system with heat & mass recovery (Wang, 2001b).

2.3.1 Adsorption Equilibrium

In order to understand the adsorption phenomenon thoroughly, adsorption equilibrium should be introduced. Adsorption equilibrium is the state in which adsorption and desorption rates are the same. **Desorption** is the reverse process of adsorption, namely adsorbate molecules are separated from adsorbent atoms by heating. Investigation of adsorption equilibrium is crucial in determining the performance limitations of the adsorption refrigeration cycles. In practice, the maximum capacity of adsorbent cannot be fully utilized because of mass transfer effects involved in actual fluid-solid interaction processes. However, for modeling of adsorption processes related to low-grade energy sources, adsorption equilibrium assumption is usually valid. Moreover, instantaneous

equilibrium between the adsorbed and gaseous phases exists (Leite, 1998). If adsorption equilibrium assumption is not valid, **kinetics of adsorption** should be considered.

Adsorption equilibrium of an adsorbent-adsorbate pair can be described by adsorption isotherms. Adsorption isotherms correlate temperature, pressure and amount adsorbed. Adsorption isotherms of water vapor on a zeolite at various temperatures are shown in Figure 2.11.

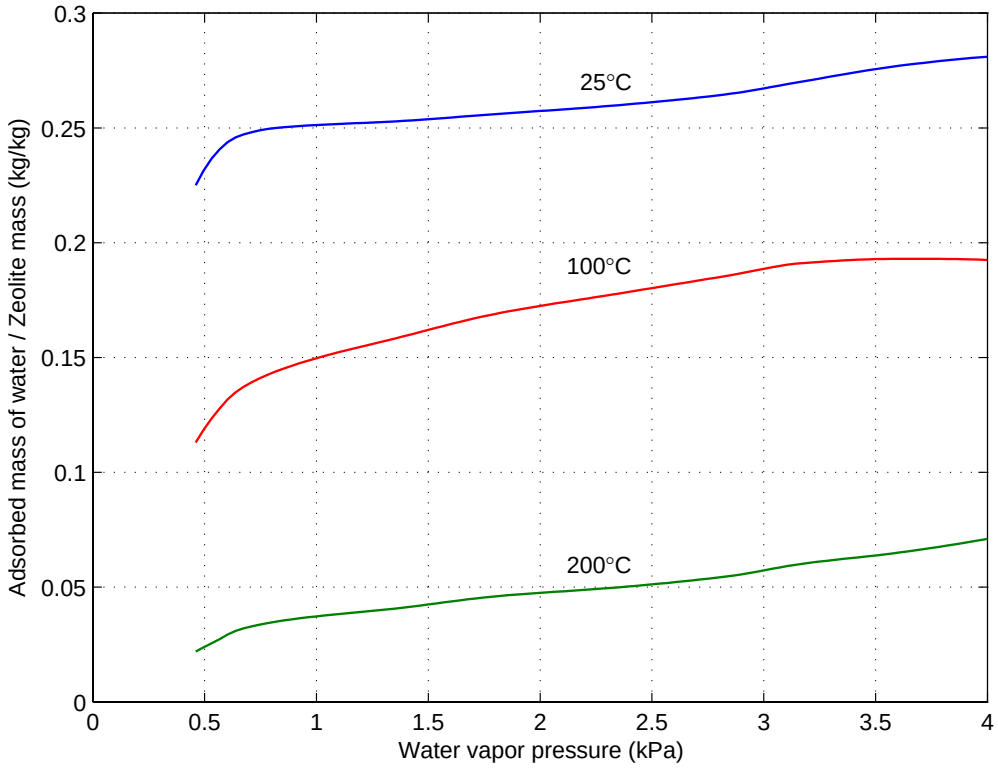

Figure 2.11: Adsorption isotherms of water vapor on zeolite. (adapted from (Tchernev, 1978))

Adsorption isotherms can be defined in many mathematical forms based on

either purely empirical or semi-empirical equations. The main drawback of purely empirical correlations is their inability to have physical meaning. Moreover these equations are usually valid for a limited range of variables where the parameters have been determined. On the other hand purely empirical equations are necessary for most cases, because each adsorbent has lots of types. For instance there are approximately 50 types of natural and 150 types of synthetic zeolites available worldwide. Their physical and chemical characteristics are different from each other, (Wikipedia, 2008).

The semi-empirical explanation of adsorption of vapors and gases on microporous solids was first given by Dubinin and Radushkevitch (D-R) (Dubinin & Radushkevitch, 1947).

$$W = W_0 \exp(-\kappa A^2) \tag{2.7}$$

where W is the volume adsorbed in micropores (m^3), W_0 is the maximum volume adsorbed in micropores (m^3), κ is the characteristic parameter for a given adsorbent/adsorbate pair and A is the adsorption potential defined by Polanyi[2] (Hutson & Yang, 1997).

$$A = RT \ln\left(\frac{P^0}{P}\right) \tag{2.8}$$

where T is the temperature of the adsorbent, P is the equilibrium pressure at temperature T, P^0 is the saturated vapor pressure and R is the gas constant.

Adsorption on non-porous solids is different than adsorption on porous solids; surface adsorption dominates the former one whereas micropore adsorption dominates the latter one. This is the reason that prompted the development of the D-R equation 2.7, but the D-R equation has several limitations (Hutson & Yang, 1997);

[2]Originally the *adsorption potential* term was first introduced by Eucken (Polanyi, 1963).

- mostly applicable for microporous solids with practically homogeneous or uniform micropore structures
- deviates from Henry's law at low pressures (not valid for zero loading case; i.e., w→0).
- valid for degrees of micropore filling higher than 0.15.

Later Dubinin and Astakhov (D-A) generalized the D-R equation. The D-A equation can be expressed as:

$$W = W_0 \exp\left(-\left(\frac{A}{\beta E_0}\right)^n\right) \tag{2.9}$$

where E_0 is the characteristic energy of adsorption for a reference vapor (usually benzene), β is termed the similarity (affinity) coefficient (β=1 for the reference vapor) and n is a heterogeneity factor (related to heterogeneity of pore distribution) depending on the type of the adsorbent. For carbonaceous adsorbents n≈2, and for zeolites n≈4-6 (Hutson et al., 1997).

Even the D-A equation does not fully agree with the experimental data. This discrepancy is associated with the heterogeneity of the system, in which the characteristic energy varies with the different regions in the solid (Sumathy, Yeung & Yong, 2003). Thus many researchers extended the D-R/D-A equations to overcome their drawbacks (Hutson et al., 1997). One of the most important extension is the Dubinin-Stoeckli (D-S) equation which considers the micropore size (Dubinin & Stoeckli, 1980). Also the non-ideal nature of the gas phase can be taken into account by replacing P and P^0 by fugacities f and f^0 respectively (Bering, Dubinin & Serpinsky, 1972); (Wang & Wang, 1999b).

Although the D-A equation has some limitations, it is extensively used in modeling the adsorption refrigeration systems because the D-A equation has only three unknown parameters which can be determined easily by experiments. In general, as the adsorption equilibrium equations become more accurate, the number of parameters used in the equations increases, hence the complexity in-

creases (detailed experiments should be carried). As a result the D-A equation is sufficient for most practical purposes.

2.3.2 Adsorbents and Refrigerants

Adsorbents and refrigerants (adsorbates) are one of the most important elements of any refrigeration and heat pump system, because the working conditions and the environmental considerations mainly depend on them.

Generally speaking, the ideal refrigerant has the following characteristics (Sumathy et al., 2003); (Cacciola & Restuccia, 1994);

- High latent heat per unit volume[3]
- Good thermal stability
- High thermal conductivity
- Low viscosity
- Low specific heat[4]
- Non-toxic, non-flammable, non-corrosive
- Chemically stable in the working temperature range
- Molecular dimension should be small enough to allow easy adsorption
- Vapor pressure should be near atmospheric pressure for the prescribed operating temperature (from technical and safety points of view)

Based on the above criteria, the main candidates are water, ammonia and methanol. Characteristics of these refrigerants are presented in Table 2.1.

[3]Good for obtaining high refrigerating effect per unit mass of refrigerant. But, heat of adsorption/desorption is linearly proportional to latent heat, so as latent heat increases the required heat input for desorption increases. As a result, high latent heat is desirable for **intermittent** systems where the most important aim is obtaining the maximum possible refrigeration effect.

[4]Unfortunately, low specific heat requirement for refrigerant tends to contradict with high latent heat per unit volume requirement, so a high specific heat must be tolerated (Critoph, 1988).

Table 2.1: Refrigerant properties

Ammonia	**Methanol**	**Water**
Toxic	Toxic	Non-Toxic
Flammable in some concentrations	Flammable	Non-Flammable
Not compatible with copper	Not compatible with copper at high temperatures	Compatible with copper
High operating pressure	Low pressure	Extremely low operating pressures
Good latent heat	Good latent heat	High latent heat
Thermally stable	Unstable beyond 393K	Thermally stable
Non polluting	Polluting	Polluting

On the other hand, the ideal adsorbent has the following characteristics (Sumathy et al., 2003); (Cacciola et al., 1994);

- High adsorption and desorption capacity, to attain high cooling effect
- Good thermal conductivity, in order to shorten the cycle time
- Low specific heat capacity
- Chemically compatible with the chosen refrigerant
- Low cost and widely available
- Wide concentration change in a small temperature range
- Reversibility of adsorption process for many cycles.

Based on these criteria zeolite, silica gel and activated carbon are the most

appropriate adsorbents. For detailed discussion of adsorbents, adsorbates and suitable adsorbent refrigerant pairs used in solid-vapor adsorption systems, interested readers are referred to Srivastava & Eames (1997); Srivastava & Eames (1998).

Considering appropriate adsorbents and refrigerants, well-suited pairs are zeolite-water, silica gel-water and activated carbon-methanol. All these pairs have weaknesses and strengths. In this study all of these pairs are investigated. First, while zeolite-water systems can be used for air conditioning and ice production, they are not adequate for freezing purposes (below 0°C) due to the freezing point of water. Zeolites have a unique property, which is very important for solar applications, which is that their adsorption capacity is a weak function of vapor pressure above some critical vapor pressure (Figure 2.11) (Tchernev, 1978). In addition, natural zeolites such as clinoptilolites are widely available in Turkey. On the other hand, zeolites have low thermal conductivity (0.1-1.0 W/mK) which slows the adsorption and desorption process, thereby limiting the rate of cooling per unit adsorbent mass referred to as specific cooling power (SCP). Enhancement of thermal conductivity is possible without sacrificing permeability much and more detailed information can be found in Critoph & Zhong (2005).

CHAPTER 3

WEATHER DATA

The performance of environment related systems, such as heating, ventilating, air conditioning and refrigeration (HVAC&R) systems, solar collectors, PV cells, and cooling towers are closely dependent on weather variables like dry bulb temperature, wet bulb temperature, wind speed, solar radiation (beam and diffuse), etc (Üner, 1998). Thus in designing and/or predicting the yearly performance of environment related systems, weather data should be used as an input. In this study adsorption refrigeration systems are emphasized, so in the forthcoming chapters the effects of the environment dependent parameters like evaporator temperature (T_{ev}) and condenser temperature (T_{cond}) on the adsorption refrigeration systems performance will be investigated. Weather data has a strong effect on the performance of the solar collector and the building cooling load (the hourly cooling load of the building fixes the adsorption system's size and operating hours, solar collector area, etc.) which will be discussed in the following chapters.

In general there are two methods for developing annual weather data;

- Synthetic generation of weather variables
- Selection among real data

Synthetic generation of weather variables are useful when there are no (or

insufficient) recorded weather data for a specific location. The aim in these methods is representing weather variables by mathematical functions. But since weather variables are neither completely random nor deterministic, it is very difficult to represent all the variance (Üner, 1998). In this study, since weather data are available for Antalya starting from 1975, the second approach (selection among the real data) is adopted and discussed below. For more information on synthetic generation of weather variables, the reader should refer to Üner (1998).

Selection among the real data is widely used for simulation of building energy systems whenever weather data is available for that location. The idea is selecting the most representative weather data set by comparing the long term recorded weather data statistically. Statistical means are necessary for handling recorded weather data, because just taking long term averages of the recorded weather data variables may be misleading for annual simulations. This is because taking the average of variables smooths the peaks, hence generated data sets can not fully represent extremes of the actual weather variables.

In 1976, Klein developed the concept of a design year which was useful for simulating solar heating systems (Duffie et al., 2003). More detailed studies conducted in Sandia National Laboratories has led to the generation of a typical meteorological year (TMY) (Hall, Prairie, Anderson & Boes, 1978). A TMY is a data set of hourly values of solar radiation and meteorological elements for a one-year period. It consists of months selected from individual years and concatenated to form a complete year (National Renewable Energy Laboratory (NREL), 1995). For example, if 30 years data are available, all 30 Januarys are examined and the one considered to be most typical is selected to be included in TMY. Other months are also treated in the same manner. TMY represents typical rather than extreme conditions, so it is not appropriate for designing systems to meet the worst-case conditions occurring at a location. TMY is useful for representing a long period of time, such as 30 years (NREL, 1995).

More recently TMY data sets are replaced by TMY2 data sets which are based

on more recent and accurate data (NREL, 1995). Another weather data set is the International Weather for Energy Calculations (IWEC) which was a result of ASHRAE research project 1015. Additionally there are many other different weather data sets available worldwide. Some of these data sets and their explanations can be found in the following website (US DOE, Energy Efficiency and Renewable Energy, 2007). However TMY/TMY2 and IWEC methods are extensively used by researchers and designers (Üner, 1998).

The main difference between these data sets is the assigned weights to the weather variables. Weather variables included in TMY and IWEC are maximum, minimum and mean dry bulb and dew point temperatures; maximum and mean wind velocity; and the total global horizontal solar radiation. In TMY2, in addition to these weather variables direct solar radiation is also used. Since direct solar radiation is not measured by the Turkish State Meteorological Service (DMİ), the TMY method is preferred to generate weather data set for Antalya. Although weather data is available starting from 1975, there are big gaps in weather data until 1983, so weather data starting from 1983 to 2005 is used to generate TMY for Antalya.

Weights used in TMY, TMY2 and IWEC are given in Table 3.1. Since wet bulb temperature is measured by DMİ, dew point temperature is replaced by wet bulb temperature.

3.1 TMY Generation Methodology

The generation of TMY is quite long and very well explained by Üner (1998), NREL (1995) and Sawaqed, Zurigat & Al-Hinai (2005). For completeness, the solution procedure is explained here again and interested readers are referred to these references for more information. In this study, a new TMY data set is generated using 23 years of data for Antalya following the procedure explained in Sawaqed et al. (2005). The steps followed in the development of TMY are explained below.

Table 3.1: Weights given to weather variables for different formats

Weather Variable	**TMY**	**TMY2**	**IWEC**
Max Dry Bulb Temperature	1/24	1/20	5/100
Min Dry Bulb Temperature	1/24	1/20	5/100
Mean Dry Bulb Temperature	2/24	2/20	30/100
Max Wet Bulb Temperature	1/24	1/20	2.5/100
Min Wet Bulb Temperature	1/24	1/20	2.5/100
Mean Wet Bulb Temperature	2/24	2/20	5/100
Max Wind Speed	2/24	1/20	5/100
Mean Wind Speed	2/24	1/20	5/100
Total Horizontal Solar Radiation	12/24	5/20	40/100
Direct Normal Solar Radiation	-	5/20	-

3.1.1 Step 1

In this step raw weather data obtained from DMİ is checked for missing data. If there are more than three consecutive days of data are missing, that month in that year is removed from the data set. This is why, although weather data between 1975 and 2005 was obtained from DMİ, only weather data between 1983 and 2005 is used in the TMY analysis. Missing data up to three consecutive days is generated by interpolation.

3.1.2 Step 2

For each month of the calendar year, cumulative distribution functions (CDFs) for both short term[1] and long term[2] daily mean values for each of the parameters (maximum, minimum and mean dry bulb and dew point temperatures; maximum and mean wind velocity; and the total global horizontal solar radiation) are calculated. The CDFs gives the proportion of values that are less

[1]The daily mean values for a given month in a given year are termed short term daily averages.

[2]When short-term daily averages are averaged over the years for each day in a given month, long-term daily averages are obtained.

than or equal to a specified value of a variable. In order to calculate CDFs the data are sorted in ascending order, then using j as the rank index of the sorted data the CDFs are obtained as follows:

$$CDF_j = \frac{1}{n} j, \quad j = 1, 2, ..., n \tag{3.1}$$

where n is the number of days in a given month.

3.1.3 Step 3

For each month of the year five candidate months are selected within the years considered in TMY generation. These candidate months are the months with the CDFs closest to long-term CDFs over all parameters. The selection is done by comparing the short-term CDFs with the long-term CDFs by using the Finkelstein-Schafer (FS) statistics (Finkelstein & Schafer, 1971) for each parameter as follows:

$$FS = \frac{1}{n} \sum_{i=1}^{n} \delta_i, \quad i = 1, 2, ..., n \tag{3.2}$$

where δ_i is the absolute difference between the short-term and the long-term CDFs for day i in the month. FS statistics are calculated for all parameters used in generating TMY.

Four CDFs for average dry bulb temperature for January are given in Figure 3.1. When all years' CDFs are compared to the long-term CDF by using FS statistics, CDF of the year 1988 is the best[3] and CDF of the year 2003 is the worst[4]. Although the year 1983 is not the best month compared to the long-term in terms of dry bulb temperature, it is selected for the TMY because selection of the TMY also depends on the CDFs of the other parameters.

[3]All years FS statistics is compared with the long term average for each variable. The year with the minimum FS statistics is defined as the **best year** for the concerning variable.

[4]All years FS statistics is compared with the long term average for each variable. The year

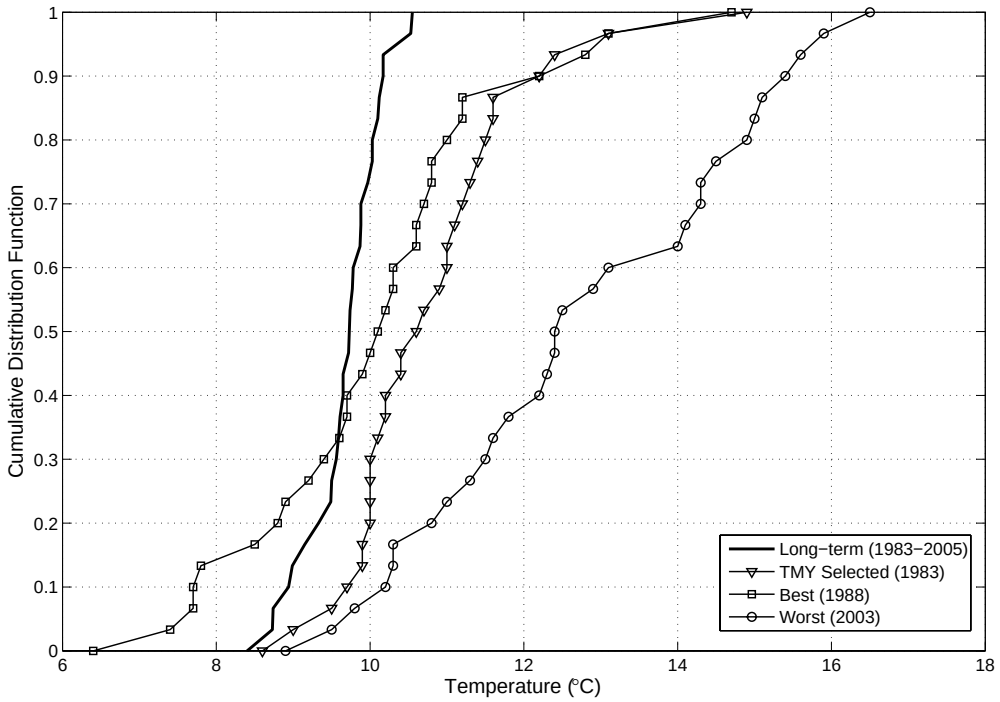

Figure 3.1: CDFs for January average dry bulb temperarure.

The selection of the five candidate months is based on the evaluation of the all parameters described previously and the weights associated with these parameters are given in Table 3.1. Therefore in order to select the five candidate months, the weighted sum (WS) of the FS statistics considering all parameters is calculated for each month. The WS is expressed as follows:

$$WS = \sum_{i=1}^{k} w_i FS_i, \quad i = 1, 2, ..., k \tag{3.3}$$

where k is the number of parameters used in the analysis, w_i is the weighting

with the maximum FS statistics is defined as the **worst year** for the concerning variable.

factor for the parameter i and FS_i is the FS statistics for the parameter i. The weighted sums for the calendar months for the years considered are given in Table 3.2.

The WS of the months are sorted in ascending order and the five years with the smallest weighted sums are selected to be used in further analysis.

3.1.4 Step 4

The five candidate months are ranked with respect to closeness of the month to the long-term mean and median for the mean ambient temperature and the global radiation. Details of this calculation are given in Sawaqed et al. (2005). For brevity, only results of this step are given in Table 3.3.

3.1.5 Step 5

The persistence of mean dry bulb temperature and daily global horizontal radiation are estimated by determining the frequency and run length above and below fixed long-term percentiles. For mean daily dry bulb temperature, the frequency and run length above 67th percentile (consecutive warm days) and below 33rd percentile (consecutive cool days) were determined. For global horizontal radiation, the frequency and run length below 33rd percentile (consecutive low radiation days) were determined. Details of this step can be found in Sawaqed et al. (2005).

3.1.6 Step 6

Based on the above persistence evaluation the month to be used in the TMY is selected. In this step the month with the longest run, the month with the most runs, and any months with zero runs are excluded, and the highest ranked month remaining from step 3 is chosen to be used in the TMY. Details of this step can also be found in Sawaqed et al. (2005).

Table 3.2: Weighted sum of FS statistics for each month of the years considered for Antalya.

Year	Months											
	1	**2**	**3**	**4**	**5**	**6**	**7**	**8**	**9**	**10**	**11**	**12**
1983	21.85	30.72	38.58	34.72	21.08	21.93	14.18	13.12	7.75	17.43	21.58	20.26
1984	13.11	28.38	41.72	23.26	20.11	20.88	24.51	8.13	5.70	7.66	23.94	28.88
1985	28.74	43.21	28.32	29.51	31.41	14.72	4.98	12.72	12.37	14.60	18.34	20.74
1986	38.07	36.44	15.12	27.49	20.90	23.48	22.15	27.67	30.62	12.20	18.34	22.48
1987	24.86	20.97	48.11	36.77	37.20	12.94	6.47	10.63	5.17	20.79	20.07	28.86
1988	32.82	33.03	36.86	35.73	35.85	14.97	30.04	14.12	16.51	25.01	24.45	32.10
1989	39.21	34.00	37.31	31.25	31.25	21.56	24.59	10.26	22.07	24.48	33.50	33.05
1990	37.44	47.96	44.11	39.95	30.25	32.94	20.13	25.32	20.69	30.75	22.04	27.59
1991	32.89	38.31	49.33	41.87	46.67	23.62	23.04	14.04	16.94	21.23	27.40	34.25
1992	37.26	37.30	37.07	49.19	39.80	29.22	23.18	19.86	18.10	12.13	29.86	32.32
1993	35.39	35.27	52.02	33.68	51.65	26.47	20.32	15.87	15.78	22.71	32.69	22.61
1994	28.50	45.93	52.23	40.24	41.02	32.49	22.36	13.53	11.88	29.26	36.92	32.02
1995	17.59	43.20	49.32	41.15	37.83	21.57	14.60	11.26	14.78	29.61	22.13	29.32
1996	31.67	43.03	44.90	46.99	19.21	24.00	14.60	5.39	11.07	20.03	31.14	17.67
1997	32.20	37.44	45.53	42.04	24.67	30.11	19.72	16.20	23.88	30.41	16.08	21.46
1998	22.62	43.47	34.99	42.34	36.10	13.72	18.46	12.75	9.17	18.99	10.50	28.07
1999	23.86	33.62	38.84	29.76	13.97	16.15	14.72	15.18	6.44	16.35	23.83	20.26
2000	24.73	26.13	39.79	34.45	49.63	52.65	34.98	34.74	20.14	28.15	33.39	29.26
2001	25.33	29.38	22.50	32.25	44.48	26.02	15.12	8.09	8.25	19.03	34.11	31.56
2002	22.64	24.85	24.12	44.17	13.13	18.64	22.43	13.79	29.13	6.55	13.37	35.13
2003	30.03	38.23	35.25	40.73	23.78	32.59	14.26	11.74	17.71	15.75	13.28	19.54
2004	37.17	30.69	25.82	24.48	25.96	41.37	24.92	31.29	25.80	25.23	16.35	20.46
2005	29.08	30.54	38.79	33.99	39.89	46.85	54.33	40.93	39.75	27.57	20.51	17.45

Table 3.3: The selected candidate years for the calendar months of the year. (First two digits of the years are not shown (i.e., 98 refers to 1998))

Months											
1	**2**	**3**	**4**	**5**	**6**	**7**	**8**	**9**	**10**	**11**	**12**
98	00	86	85	86	99	85	96	99	02	02	96
84	87	04	84	02	87	87	01	87	85	97	83
95	02	85	99	84	98	95	84	84	84	98	03
83	84	01	86	99	85	83	87	83	86	03	99
02	01	02	04	96	88	03	89	01	92	04	05

3.1.7 Step 7

Finally the 12 selected months are concatenated to make a complete year and discontinuities at the month interfaces for 6 hours each side are smoothed by using curve fitting techniques. Table 3.4 shows the newly generated TMY data set for Antalya.

Table 3.4: TMY for Antalya

Months	**Years**
January	1983
February	1987
March	1984
April	1986
May	1986
June	1985
July	1985
August	1987
September	1986
October	1987
November	1985
December	1987

CHAPTER 4

THERMODYNAMIC ANALYSIS OF ADSORPTION REFRIGERATION CYCLES

In this chapter it is aimed to give the thermodynamic design procedure in detail for the adsorption refrigeration cycles which are working with the most commonly used adsorbent/adsorbate pairs like zeolite-water, silica gel-water, activated carbon-methanol, activated carbon-ethanol, activated carbon fiber-ethanol and activated carbon fiber-methanol. All these pairs have weaknesses and strengths and the selection of the working pairs is strongly dependent on operating conditions (i.e., evaporator, condenser and regeneration temperature). It is aimed to determine the selection guidelines for each pair at the end of this chapter. For example, regeneration temperature is an important measure in choosing the appropriate heat source. If solar collectors are to be used for the heat source, then selection of the solar collector type (flat plate, evacuated, parabolic, etc.) is firmly dependent on regeneration temperature. Moreover, if using solar collectors of any type is found to be unfeasible (economic point of view) and impractical (technical point of view, i.e, it is impossible to obtain temperatures above 200°C with flat plate collectors) at the end of the eco-

nomic analysis chapter, other options (i.e., natural gas fired heaters) should be considered as a heat source. All these options will be discussed at the end of this chapter from the technical point of view. Later in the economic analysis chapter, technical and economical points of view will be examined together to reach a general conclusion.

Starting with the basic intermittent adsorption refrigeration cycle, heat recovery and heat & mass recovery adsorption refrigeration cycles will be examined successively.

4.1 Zeolite-Water Pair

4.1.1 Intermittent Adsorption Refrigeration Cycle

The basic adsorption refrigeration cycle's operating principles are discussed in the literature survey. In this section a thermodynamic model of the intermittent adsorption cycle will be explained. A P-T-w diagram of the basic adsorption refrigeration cycle is given in Figure 2.8.

As seen from Figure 2.8, the thermodynamic cycle consists of 4 processes;

- $1 \rightarrow 2$ isosteric heating (constant concentration)
- $2 \rightarrow 3$ isobaric desorption (heat of desorption + sensible heating)
- $3 \rightarrow 4$ isosteric cooling (constant concentration)
- $4 \rightarrow 1$ isobaric adsorption (heat of adsorption + sensible cooling)

In order to calculate the COP of the basic adsorption cycle, heat input to the system and the useful refrigeration effect must be calculated. Although detailed thermodynamic models are available in the literature (Cacciola et al., 1995), (Critoph, 1988) for the sake of completeness, the thermodynamic model is included here again.

Considering Figure 3.1, in isosteric heating (1 → 2) and isobaric desorption (2 → 3) heat is added to the adsorbent bed. The heat that must be supplied to the adsorbent bed for its isosteric heating (1 → 2) is given as

$$Q_{ih} = m_z(C_{p_z} + C_{p_w} w_{max})(T_{g1} - T_{a2}) \tag{4.1}$$

where m_z is the mass of adsorbent in kg, C_{p_z} is the specific heat of adsorbent in kJ/kg·K and C_{p_w} is the specific heat of adsorbate in adsorbed phase in kJ/kg·K.

The heat necessary for the desorption phase (2 → 3) has two components;

$$Q_d = Q_{des} + Q_{sd} \tag{4.2}$$

where Q_{des} is the heat of desorption which is given by;

$$Q_{des} = m_z \int_{w_{max}}^{w_{min}} \Delta H dw \tag{4.3}$$

and Q_{sd} is the sensible heat of adsorbent plus its adsorbate content,

$$Q_{sd} = m_z C_{p_z}(T_{g2} - T_{g1}) + m_z C_{p_w} \int_{T_{g1}}^{T_{g2}} w(T) dT \tag{4.4}$$

The useful refrigeration effect which is the energy that must be supplied to the evaporator, Q_e, is calculated as the latent heat of evaporation of the cycled adsorbate, minus the sensible heat of the adsorbate that is entering the evaporator at condensation temperature.

$$Q_e = m_z(w_{max} - w_{min}) \left[L(T_e) - \int_{T_e}^{T_c} C_{p_l}(T) dT \right] \tag{4.5}$$

where C_{p_l} is the specific heat of adsorbate in liquid phase[1] and L is the heat of evaporation of adsorbate in kJ/kg.

[1] C_{p_l} is assumed to be equal to C_{p_w}. See item 2 above.

On the basis of the previous equations, the COP for cooling operation can be calculated as the ratio of useful refrigeration effect produced and heat input to the adsorbent bed.

$$COP = \frac{Q_e}{Q_{ih} + Q_d} \tag{4.6}$$

In order to evaluate the equations above to find the COP of the basic adsorption refrigeration cycle, some assumptions must be made and some other auxiliary equations must be used. These assumptions and equations are as follows;

1. Specific heat of the dry adsorbent is assumed to be constant[2].

2. Specific heat of the refrigerant in adsorbate phase is assumed to be equal to the specific heat of the bulk liquid phase[3] (Critoph, 1988); (Pons & Grenier, 1986)[4].

3. Heat of adsorption is assumed to be equal to the heat of desorption which can be expressed by the following equation (Cacciola, Restuccia & Benthem, 1997),

$$\Delta H(w) = (B_0 + B_1 w + B_2 w^2 + B_3 w^3) \cdot \frac{R}{MM_{H_2O}} \cdot 1000 \tag{4.7}$$

   where B_0, B_1, B_2 and B_3 are constants and their numerical values are given in Table 3.1. R is the universal gas constant and MM_{H_2O} is the molar mass of water in kg/kmol.

4. Heat of evaporation of water is assumed to be equal to the heat of condensation of water and can be expressed by the following equation where T is in K (Cacciola et al., 1997),

$$L(T) = 3172 \cdot 10^3 - 2.4425 \cdot 10^3 T \tag{4.8}$$

[2]Specific heat of zeolite is taken as 920 J/kg·K

[3]Specific heat of water, C_{p_w}, is assumed to be constant and taken as 4187 J/kg·K

[4]Other approaches in the literature for the refrigerant in the adsorbate phase are, neglecting it's thermal contribution and considering it's specific heat is equal to the specific heat of the gas at a given temperature and pressure (Cacciola et al., 1995).

5. Thermal contribution of refrigerant vapor, metal parts and additives are neglected.

6. Equilibrium equation which relates the amount adsorbed, w, and pressure of adsorbate, P, at temperature T of a zeolite-water pair is necessary. Equilibrium equations for different kinds of zeolites can be found in the following literature;

   - Zeolite 4A-water → (Cacciola et al., 1997), (Gorbach, Stegmaier & Eigenberger, 2004)
   - Zeolite 13X-water → (Cacciola et al., 1995), (Wang, Zhu & Tan, 1999a)
   - Zeolite MgNaA-water → (Miltkau & Dawoud, 2002)

   In this study Zeolite 4A-water pair will be explored. The equilibrium equation is given by the following equation (Cacciola et al., 1997),

$$\ln(P) = \left(A_0 + \frac{B_0}{T}\right) + w\left(A_1 + \frac{B_1}{T}\right) + w^2\left(A_2 + \frac{B_2}{T}\right) + w^3\left(A_3 + \frac{B_3}{T}\right) \tag{4.9}$$

   where A_0, A_1, A_2 and A_3 are constants and their numerical values are given in Table 3.1. The pressure (P) is expressed in mbar and temperature (T) is in Kelvin.

Table 4.1: Numerical values of A_i and B_i (i=0,1,2,3) constants, which appear in the equation 4.7 and 4.9.

$\mathbf{A}_0$	14.8979	$\mathbf{B}_0$	-7698.85
$\mathbf{A}_1$	95.4083	$\mathbf{B}_1$	21498.1
$\mathbf{A}_2$	-636.658	$\mathbf{B}_2$	-184598
$\mathbf{A}_3$	1848.84	$\mathbf{B}_3$	512605

Now it is possible to calculate the COP of the intermittent adsorption cycle

for different operating conditions. In Figure 4.2(a), evaporator temperature (T_{ev}) and condenser temperature (T_{cond}) are kept constant at 10°C and 30°C respectively and dependence of the COP on the regeneration temperature (T_{g2}) for the zoelite 4A-water pair is shown. As seen from Figure 4.2(a), zoelite 4A-water pair has a maximum COP at approximately 180°C.

In Figure 4.2(b), effect of the T_{ev} on the COP of the intermittent cycle is shown. T_{g2} and T_{cond} are kept constant at 110°C and 30°C respectively. As expected, as T_{ev} increases, COP of the system increases.

In Figure 4.2(c), effect of the T_{cond} on the COP of the intermittent cycle is shown. T_{g2} and T_{ev} are kept constant at 110°C and 10°C respectively. As expected, as T_{cond} increases, COP of the system decreases.

4.1.2 Heat Recovery Adsorption Refrigeration Cycle

As seen from the previous section, intermittent adsorption refrigeration cycle has a COP of $0.5 \sim 0.55$. For air conditioning applications, COP must be higher than 1 and possibly higher than 1.2, to compete favorably with a vapor compression unit (COP=3) powered with electricity provided by a thermal power plant ($\eta \sim 1/3$)[5] (Wang & Wang, 2005). Thus the heat recovery process can be utilized to increase the COP of the adsorption system. In addition, intermittent cycle is not appropriate for air conditioning purposes because the refrigeration effect is obtained during night when cooling demand is low. Hence, by the heat recovery process two adsorbent beds can be operated out of phase for obtaining a quasi continuous cycle. As expected, the heat recovery adsorption refrigeration cycle will be more complicated than intermittent cycle, as it has several valves, pumps, auxilary heaters/coolers, cooling tower and control unit.

A schematic of heat recovery process is given in Figure 4.3. Possible heat recovery for a two bed adsorption system will be some part of sensible heat

[5] η is the conversion efficiency of a thermal power plant from primary energy to electricity. Today up to 55% efficiency is possible (Hondeman, 2000).

and heat of adsorption depending on the mass of adsorbent, T_{a1}, T_{a2}, T_{g1} and T_{g2}.

In order to calculate the COP of the heat recovery adsorption system, recovered heat (Q_{reg}) should be calculated. Q_{reg}[6] is dependent on the heat released in isosteric cooling phase ($3 \rightarrow 4$) and isobaric adsorption phase ($4 \rightarrow 1$). Equations necessary in modeling these two phases are as follows (Cacciola et al., 1995);

During isosteric cooling phase ($3 \rightarrow 4$), only sensible heat is withdrawn from the adsorbent bed,

$$Q_{ic} = m_z(C_{p_z} + C_{p_w} w_{min})(T_{g2} - T_{a1}) \tag{4.11}$$

while during the adsorption phase ($4 \rightarrow 1$), total energy (Q_a) released is equal to the enthalpy of adsorption (Q_{ads}) plus the sensible heat (Q_{sa}) obtained from cooling of adsorbent and adsorbate from the temperature T_{a1} to T_{a2}, minus the energy (Q_{sve}) needed to heat up the vapor from evaporation to adsorption temperature.

$$Q_a = Q_{ads} + Q_{sa} - Q_{sve} \tag{4.12}$$

where

$$Q_{ads} = -m_z \int_{w_{min}}^{w_{max}} \Delta H dw \tag{4.13}$$

[6] Q_{reg} is calculated iteratively by using energy balance equation between hot and cool adsorbent beds as per below in equation 4.10:

$$\int_{T_{cool}}^{T} (m_z C_{p_z} + w_{cool} m_z C_{p_w}) \cdot dT = \int_{T_{hot}}^{T} (m_z C_{p_z} + w_{hot} m_z C_{p_w}) \cdot dT \tag{4.10}$$

where T_{cool} is the temperature of the cool adsorbent bed at the end of the adsorption process ($4 \rightarrow 1$), T_{hot} is the temperature of the hot adsorbent bed at the end of the regeneration process ($2 \rightarrow 3$), T is the final equilibrium temperature of the cool and hot adsorbent beds, w_{cool} is the equilibrium adsorption capacity of the cool adsorbent bed and w_{hot} is the equilibrium adsorption capacity of the hot adsorbent bed. Details of the calculation can be found in Matlab code given in Appendix A.

$$Q_{sa} = m_z C_{p_z}(T_{a1} - T_{a2}) + m_z C_{p_w} \int_{T_{a2}}^{T_{a1}} w(T)dT \tag{4.14}$$

$$\begin{aligned} Q_{sve} &= m_z \sum_{i=1}^{n} (w_i - w_{i-1}) C_{p_w}(T_e) \\ &\times \left[\frac{1}{2} \left(\frac{b(w_i)}{\ln(P_e) - a(w_i)} + \frac{b(w_{i-1})}{\ln(P_e) - a(w_{i-1})} \right) - T_e \right] \end{aligned} \tag{4.15}$$

where

$$a(w) = A_0 + A_1 w + A_2 w^2 + A_3 w^3 \tag{4.16}$$

$$b(w) = B_0 + B_1 w + B_2 w^2 + B_3 w^3 \tag{4.17}$$

$$n = \frac{w_{max} - w_{min}}{k} \tag{4.18}$$

k $\ll 1$ is a constant related to the accuracy of the model.

T_{ev} and T_{cond} are kept constant at 10°C and 30°C respectively and dependence of the COP of the heat recovery adsorption refrigeration cycle on T_{g2} for the zoelite 4A-water pair is shown in Figure 4.3(a). Dependence of the COP on T_{ev} and T_{cond} is similar to the intermittent adsorption cycle (i.e., as $T_{ev} \uparrow$ COP$\uparrow$ and as $T_{cond} \uparrow$ COP$\downarrow$).

In Figure 4.3(b), effect of the T_{ev} on the COP of the heat recovery cycle is shown. T_{g2} and T_{cond} are kept constant at 110°C and 30°C respectively.

In Figure 4.3(c), effect of the T_{cond} on the COP of the heat recovery cycle is shown. T_{g2} and T_{ev} are kept constant at 110°C and 10°C respectively.

As seen from Figure 4.3(a), COP of the intermittent adsorption refrigeration system is significantly improved with the heat recovery process. The maximum COP obtained by the heat recovery process is approximately 0.8 which is 33%

higher than the maximum COP (0.53) that can be obtained by intermittent cycle.

4.1.3 Heat & Mass Recovery Adsorption Refrigeration Cycle

The mass recovery process is utilized for obtaining higher cooling capacity. As discussed in literature survey, mass recovery process is very simple to operate, but very effective. It is recommended for operating conditions such as high condensing temperatures, low evaporation temperatures, or low generation temperatures (Wang, 2001c). P-T-w diagram of mass recovery process followed by heat recovery process is given in Figure 4.1 below. Effect of the mass recovery process on the COP depends on the operating conditions (Qu, Wang & Wang, 2002). Model required for the simulation of the mass recovery process is proposed by Szarzynski, Feng & Pons (1997) and Pons & Poyelle (1999).

Simulation model and required assumptions are described as follows:

1. The vapor desorbed from the hot adsorbent bed (high pressure bed) is completely readsorbed by the cool adsorbent bed (low pressure bed). That is:

$$\Delta W_{a2-a3} = \Delta W_{g2-g3} \tag{4.19}$$

2. The mass recovery process is an adiabatic process. In other words, the temperature variation is merely caused by adsorption or desorption in each bed.

$$\int_{T_{a3}}^{T_{a2}} (C_{p_z} + X \cdot C_{p_w}) dT = \int_{T_{a3}}^{T_{a2}} H \cdot dW \tag{4.20}$$

$$\int_{T_{g2}}^{T_{g3}} (C_{p_z} + X \cdot C_{p_w}) dT = \int_{T_{g2}}^{T_{g3}} H \cdot dW \tag{4.21}$$

3. The final pressure of the two adsorbers are equal to each other[7].

$$P_{a3} = P_{g3} = P_m \tag{4.22}$$

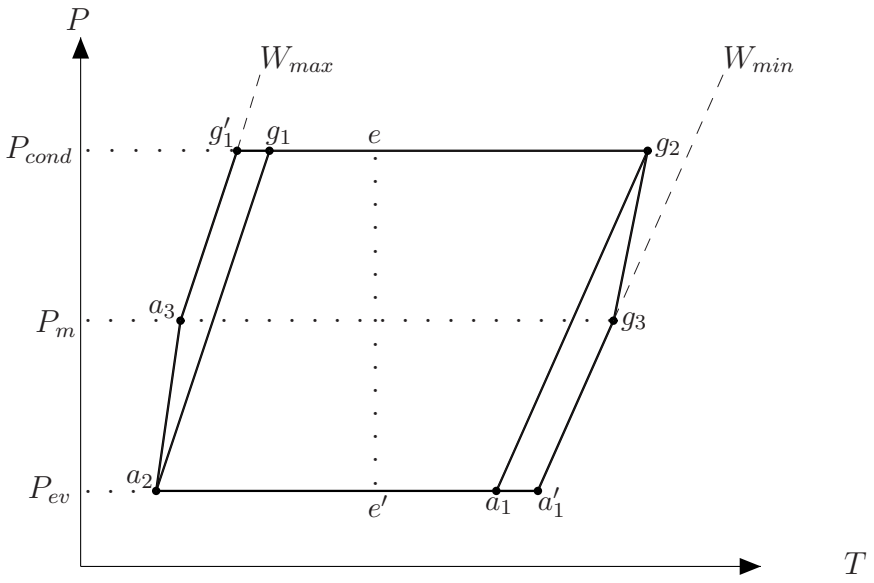

Figure 4.1: Two-bed adsorption refrigeration system with heat & mass recovery (Wang, 2001b).

The COP of the heat & mass recovery adsorption cycle for different regeneration temperatures is shown in Figure 4.4(a) below. As seen from Figure 4.4(a), the COP of the heat & mass recovery cycle is slightly higher than the heat recovery cycle. The maximum COP is approximately 0.82 at regeneration temperature of 150°C for zeolite 4A-water pair. Dependence of the COP on T_{ev} and T_{cond} is similar to the intermittent adsorption cycle (i.e., as $T_{ev} \uparrow$ COP$\uparrow$ and as $T_{cond} \uparrow$ COP$\downarrow$).

In Figure 4.4(b), effect of the T_{ev} on the COP of the heat & mass recovery cycle

[7] P_m does not necessarily equal to $(P_{ev} + P_{cond})/2$

is shown. T_{g2} and T_{cond} are kept constant at 110°C and 30°C respectively.

In Figure 4.4(c), effect of the T_{cond} on the COP of the heat & mass recovery cycle is shown. T_{g2} and T_{ev} are kept constant at 110°C and 10°C respectively.

Up to now three major types of adsorption refrigeration cycles (intermittent, heat recovery and heat & mass recovery) are examined. The complete models are presented for the simulation of these cycles. Matlab code for the simulation of the heat & mass recovery adsorption refrigeration cycle is given in Appendix A.

When simulation results are compared with the experimental results found in the literature, it is clearly seen that COP of the real systems are significantly lower than the ideal cycle. This is mainly a consequence of the heat & mass transfer resistances in the bed, effect of dead weights and heat exchanger losses.

As seen from the simulation results, zeolite-water pair usually requires high regeneration temperatures depending on the type of the system:

- $\sim$ 170°C for the intermittent cycle
- $\sim$ 150°C for the heat recovery cycle
- $\sim$ 140°C for the heat & mass recovery cycle

Since solar collectors will be used for heat source in this study, selection of the appropriate collector type is extremely important in order to obtain the required regeneration temperature. Selection of the collector type and the economics of this selection will be discussed in the forthcoming chapters. But now it is useful to examine the other popular working pairs in order to understand which pair is the most appropriate for a given regeneration temperature.

4.2 Silica gel-Water Pair

Another strong alternative for adsorption refrigeration cycles is silica gel-water pair. Silica gel has a relatively lower regeneration temperature (below 100°C, typically 85°C) than the other adsorbents (Saha, Boelman & Kashiwagi, 1995). All the equations used for the simulation of zeolite-water pair are also valid for the silica gel-water pair, but the adsorption equilibrium and the heat of adsorption equations should be replaced. Several different adsorption equilibrium equations are available in the literature Saha et al. (1995), Ng, Chua, Chung, Loke, Kashiwagi, Akisawa & Saha (2001), Chua, Ng, Wang, Yap & Wang (2004) and Di, Wu, Xia & Wang (2007). In addition, heat of adsorption is given for different types of silica gel by Sakoda & Suzuki (1984) and Ng et al. (2001). The heat of adsorption for silica gel on water is taken as 2800 kJ/kg and constant in the simulations. The heat of adsorption is assumed to be equal to the heat of desorption. In addition specific heat of silica gel is assumed to be constant and taken as 924 J/kg·K.

The adsorption equilibrium equation[8] which is used in the simulations is as follows (Saha et al., 1995):

$$w = A(T_s) \cdot \left[\frac{P_s(T_w)}{P_s(T_s)}\right]^{B(T_s)} \tag{4.23}$$

where $P_s(T_w)$ and $P_s(T_s)$ are the saturation vapor pressures at temperatures T_w(refrigerant temperature) and T_s(silica gel temperature) respectively. $A(T_s)$ and $B(T_s)$ are given as follows:

$$A(T_s) = A_0 + A_1 T_s + A_2 T_s^2 + A_3 T_s^3 \tag{4.24}$$

$$B(T_s) = B_0 + B_1 T_s + B_2 T_s^2 + B_3 T_s^3 \tag{4.25}$$

The saturation vapor pressure and temperature are correlated as follows (Wang,

[8]Type of the silica-gel used in the simulations is NACC Type RD.

Xia, Wu, Wang, Zhai & Dou, 2005):

$$P_s = C_0(T - 273.15)^3 - C_1(T - 273.15)^2 + C_2(T - 273.15) + C_3 \qquad (4.26)$$

where P_s in Pa and T in K.

The numerical values of A_i, B_i and C_i (i=0,1,2,3) are given in Table 4.2 below.

Table 4.2: Numerical values of A_i, B_i and C_i (i=0,1,2,3) constants, which appear in the equations 4.23, 4.24 and 4.25.

A_0	-6.5314	B_0	-15.587	C_0	0.0000888
A_1	$0.72452 \cdot 10^{-1}$	B_1	0.15915	C_1	0.0013802
A_2	$-0.23951 \cdot 10^{-3}$	B_2	$-0.50612 \cdot 10^{-3}$	C_2	0.0857427
A_3	$0.25493 \cdot 10^{-6}$	B_3	$0.53290 \cdot 10^{-6}$	C_3	0.4709375

4.2.1 Intermittent Adsorption Refrigeration Cycle

T_{ev} and T_{cond} are kept constant and dependence of the COP of the intermittent adsorption refrigeration system on T_{g2} for the silica gel-water pair is shown in Figure 4.2(a).

As seen from Figure 4.2(a), silica gel-water intermittent cycle has a much lower regeneration temperature ($\sim$ 110°C) than zeolite 4A-water intermittent cycle for the same operating conditions. Moreover silica gel-water intermittent cycle has a higher COP.

As expected as T_{cond} increases COP of the system decreases and as T_{ev} increases COP of the system increases. Effect of the evaporator and condenser temperature on the COP of the silica gel-water intermittent cycle is shown in Figure 4.2(b) and in Figure 4.2(c) respectively. T_{g2} and T_{ev} are kept constant at 110°C and 10°C respectively in condenser temperature analysis and

T_{g2} and T_{cond} are kept constant at 110°C and 30°C respectively for evaporator temperature analysis.

4.2.2 Heat Recovery Adsorption Refrigeration Cycle

The effect of the heat recovery process on the COP is shown in Figure 4.3(a). As seen from Figure 4.3(a), there is a discontinuity (at $\sim$ 90°C) in the graph. Up to this point only sensible heat of the isosteric cooling process is recovered, after this point heat of adsorption plus sensible heat is recovered.

Effect of the evaporator and condenser temperature on the COP of the silica gel-water heat recovery cycle is shown in Figure 4.3(b) and in Figure 4.3(c) respectively. T_{g2} and T_{ev} are kept constant at 110°C and 10°C respectively in condenser temperature analysis and T_{g2} and T_{cond} are kept constant at 110°C and 30°C respectively for evaporator temperature analysis.

4.2.3 Heat & Mass Recovery Adsorption Refrigeration Cycle

Lastly dependence of the COP of the heat & mass recovery cycle on the regeneration temperature is presented in Figure 4.4(a). Similar to the zeolite 4A-water pair, COP of the silica gel-water heat & mass recovery cycle is slightly higher than the heat recovery cycle.

The effect of the evaporator and condenser temperature on the COP of the silica gel-water heat & mass recovery cycle is shown in Figure 4.4(b) and in Figure 4.4(c) respectively. T_{g2} and T_{ev} are kept constant at 110°C and 10°C respectively in condenser temperature analysis and T_{g2} and T_{cond} are kept constant at 110°C and 30°C respectively for evaporator temperature analysis.

4.3 Activated Carbon-Methanol Pair

Finally activated carbon-methanol (AC-M) pair will be investigated. One major difference of the AC-M pair from the other pairs is it can be used for refrigeration purposes since freezing point of methanol (-97.68°C at 1 atm) is well below 0°C. Activated carbon is a hydrophobic adsorbent, so it is not appropriate to be used with water. All the equations used for the simulation of zeolite-water pair are also valid for the activated carbon-methanol pair, but the adsorption equilibrium and the heat of adsorption equations should be replaced. Several different adsorption equilibrium equations for various types of activated carbons are available in the literature Wang & Wang (2005); Pasos, Meunier & Gianola (1986); Pons et al. (1986). In addition, heat of adsorption for activated carbon-methanol is given by Sumathy et al. (2003). The heat of adsorption for methanol on activated carbon is taken as 1900 kJ/kg in the simulations. The heat of adsorption is assumed to be equal to the heat of desorption. In addition specific heats of activated carbon and methanol are assumed to be constant and taken as 840 J/kg·K and 2531 J/kg·K respectively.

The adsorption equilibrium equation which is used in the simulations is as follows (Pasos et al., 1986):

$$W = W_0 \exp\left[-D\left(T \ln \frac{P_s}{P}\right)^n\right] \tag{4.27}$$

where W_0 is the total volume of the micropores accessible to the vapor, W is the volume of adsorbate condensed in the micropores of the adsorbent at temperature T and relative pressure P/P_s. D and n are the structural constants of the adsorbent.

4.3.1 Intermittent Adsorption Refrigeration Cycle

T_{ev} and T_{cond} are kept constant and dependence of the COP of the intermittent adsorption refrigeration system on T_{g2} for the activated carbon-methanol pair is shown in Figure 4.2(a).

As seen from Figure 4.2(a), activated carbon-methanol pair has a much lower regeneration temperature ($\sim 100°C$) than zeolite 4A-water pair for the same operating conditions. Moreover activated carbon-methanol system has a slightly higher COP for low operating temperatures ($\sim 80°C$).

As expected as T_{cond} increases COP of the system decreases. Effect of the condenser temperature on the COP is shown in Figure 4.2(c).

Lastly, effect of the evaporator temperature on the COP is shown in Figure 4.2(b).

4.3.2 Heat Recovery Adsorption Refrigeration Cycle

The effect of the heat recovery process on the COP is shown in Figure 4.3(a). As seen from Figure 4.3(a), there is a discontinuity (at $\sim 75°C$) in the graph. Up to this point only sensible heat of the isosteric cooling process is recovered, after this point heat of adsorption plus sensible heat is recovered. As seen from Figure 4.3(a) regeneration temperature of the heat recovery cycle is lower for the activated carbon-methanol pair than the zeolite 4A-water pair.

The effect of the evaporator and condenser temperature on the COP of the activated carbon-methanol heat recovery cycle is shown in Figure 4.3(b) and in Figure 4.3(c) respectively. T_{g2} and T_{ev} are kept constant at 110°C and 10°C respectively in condenser temperature analysis and T_{g2} and T_{cond} are kept constant at 110°C and 30°C respectively for evaporator temperature analysis.

4.3.3 Heat & Mass Recovery Adsorption Refrigeration Cycle

Lastly dependence of the COP of the heat & mass recovery cycle on the regeneration temperature is presented in Figure 4.4(a) below. Similar to the silica gel-water pair, COP of the activated carbon-methanol heat & mass recovery cycle is slightly higher than the heat recovery cycle.

The effect of the evaporator and condenser temperature on the COP of the activated carbon-methanol heat & mass recovery cycle is shown in Figure 4.4(b) and in Figure 4.4(c) respectively. T_{g2} and T_{ev} are kept constant at 110°C and 10°C respectively in condenser temperature analysis and T_{g2} and T_{cond} are kept constant at 110°C and 30°C respectively for evaporator temperature analysis.

4.4 Other Pairs

Up to now three different pairs are investigated; zeolite 4A-water, silica gel-water and activated carbon-methanol. As seen from the preceding sections, selection of the appropriate working pairs and the performance of the adsorption refrigeration system of any type are strongly dependent on the environmental conditions (T_{cond}), desired operating temperature (T_{ev}) and available/attainable heat source temperature (T_{g2}). Although most popular working pairs are discussed in this study, other promising pairs available in the literature are given below. Adsorption equilibrium equations and heat of adsorption equations are presented. For further information, readers should refer to related references.

- Monolithic Carbon – Ammonia pair (Tamainot-Telto & Critoph, 2000):

  Adsorption equilibrium is given by modified Dubinin-Radushkevich (D-R)

equation,

$$w = w_0 \exp\left[-K\left(\frac{T}{T_{sat}} - 1\right)^n\right] \tag{4.28}$$

where $w_0 = 0.270$ kg/kg is the concentration under saturation conditions, T is the carbon temperature in Kelvin, T_{sat} is the saturation temperature in Kelvin corresponding to the gas pressure. $K = 4.3772$ and $n = 1.1935$ are constants. And the heat of adsorption is given by,

$$\Delta H = RA\frac{T}{T_{sat}} \tag{4.29}$$

where R is the gas constant ($R \cong 488$ J/kg·K) and A is a constant corresponding to the slope of saturation curve on Clasius-Clapeyron diagram ($A = 2823.4$).

- Activated Carbon Fiber – Ethanol pair (Saha, El-Sharkawy, Chakraborty & Koyama, 2007):

  Adsorption equilibrium is given by Dubinin-Radushkevich (D-R) equation,

$$w = w_0 \exp\left[-D\left(T \ln\frac{P_s}{P}\right)^2\right] \tag{4.30}$$

  where $w_0 = 0.797$ kg ethanol/kg ACF is the maximum uptake, P is the equilibrium pressure in Pa, P_s is the saturated pressure in Pa and D is the exponential constant ($D \cong 1.72 \cdot 10^{-6}$ K^{-2}).

  Moreover adsorption equilibrium equations for ACF – methanol and ACF – water are given by Hamamoto, Alam, Saha, Koyama, Akisawa & Kashiwagi (2006).

- Activated Carbon – Ammonia pair (Qu et al., 2002):

Adsorption equilibrium is given by Dubinin-Astakhov (D-A) equation,

$$w = w_0 \exp\left[-K\left(\frac{T_{sat}}{T} - 1\right)^n\right] \tag{4.31}$$

where $w_0 = 0.258$ kg/kg is the maximum uptake, $K = 3.655$ and $n = 1.325$ are constants. And the heat of adsorption is given by,

$$\Delta H = RA\frac{T}{T_{sat}} \tag{4.32}$$

where R is the universal gas constant and $A = 2132.5$ is a constant.

- Charcoal – Methanol pair (Khattab, 2006):

  Adsorption equilibrium is given by Dubinin-Radushkevitch (D-R) equation,

$$w = w_0 \exp\left[-D\left(T \ln\frac{P}{P_s}\right)^n\right] \tag{4.33}$$

  where $w_0 = 0.335$ kg/kg is the maximum quantity of methanol which would be adsorbed by the total volume of charcoal micropore system (at saturation). w is the amount of methanol adsorbed by charcoal at the adsorbing temperature T and pressure P. P_0 denotes the saturation pressure of methanol at temperature T. And $D = 0.9 \cdot 10^{-6}$ and $n = 2$ are the structural constants of the adsorbent.

$$\Delta H = RA\frac{T}{T_{sat}} \tag{4.34}$$

  where $R = 260$ J/kg·K is the gas constant and $A = 4666$ is a constant.

4.5 Discussion

In this chapter ideal thermodynamic models of the intermittent, heat recovery and heat & mass recovery adsorption refrigeration cycles along with the adsorption equilibrium equations for zeolite-water, silica gel-water and activated carbon-methanol pairs are presented. The effects of the operating conditions on the adsorption refrigeration cycle's COP is investigated and the results are presented in Figure 4.2, Figure 4.3 and Figure 4.4 for intermittent, heat recovery and heat & mass recovery cycles respectively.

4.5.1 Intermittent Cycle

As seen from Figure 4.2(a), for the conditions investigated for the intermittent cycle silica gel-water pair has a higher COP compared to zeolite-water and activated carbon-methanol pairs. The silica gel-water pair reaches its highest COP(0.68) at 80°C regeneration temperature, activated carbon-methanol pair reaches its highest COP(0.44) at 110°C regeneration temperature and zeolite-water pair reaches its highest COP(0.57) at 170°C regeneration temperature. On the other hand, as seen from Figure 4.2(b) and Figure 4.2(c) silica gel-water pair is more sensitive to condenser and evaporator temperatures compared to zeolite-water and activated carbon-methanol pairs.

When COP values of the three pairs are compared, silica gel-water pair seems to be the most appropriate pair for the intermittent cycle, but in intermittent cycle aim is usually obtaining the highest possible refrigerating effect per unit mass of adsorbent instead of achieving the highest COP. Therefore zeolite-water pair is usually preferred in intermittent cycles under conditions of typical solar applications (i.e., high condenser temperature[9] and low regeneration temperature), because the amount of adsorbed water vapor on zeolite is extremely nonlinear function of partial pressure as seen from Figure 2.11. On the other

[9]The condenser temperatures above 40°C favor zolite-water pair, condenser temperatures below 40°C favor silica gel-water pair.

hand, the amount of adsorbed water vapor on silica gel is almost linear function of partial pressure which accounts for the low refrigerating effect, hence makes silica gel-water pair unsuitable for intermittent cycle under the conditions explained above (Tchernev, 1978).

4.5.2 Heat Recovery Cycle

As seen from Figure 4.3(a), for the conditions investigated for the heat recovery cycle silica gel-water pair has higher COP compared to zeolite-water and activated carbon-methanol pairs. The silica gel-water pair reaches its highest COP(0.92) at 140°C regeneration temperature, activated carbon-methanol pair reaches its highest COP(0.71) at 155°C regeneration temperature and zeolite-water pair reaches its highest COP(0.88) at 150°C regeneration temperature. On the other hand, as seen from Figure 4.3(b) and Figure 4.3(c) silica gel-water pair is more sensitive to condenser and evaporator temperatures compared to zeolite-water and activated carbon-methanol pairs. In addition activated carbon-methanol pair is more sensitive to condenser and evaporator temperatures compared to zeolite-water pair.

4.5.3 Heat & Mass Recovery Cycle

As seen from Figure 4.4(a), for the conditions investigated for the heat & mass recovery cycle zeolite-water and silica gel-water pairs have significantly higher COP compared to activated carbon-methanol pair. The zeolite-water pair reaches its highest COP(0.94) at 140°C regeneration temperature, activated carbon-methanol pair reaches its highest COP(0.72) at 160°C regeneration temperature and silica gel-water pair reaches its highest COP(0.93) at 150°C regeneration temperature. On the other hand, as seen from Figure 4.4(b) and Figure 4.4(c) silica gel-water pair is more sensitive to condenser and evaporator temperatures compared to zeolite-water and activated carbon-methanol pairs. In addition activated carbon-methanol pair is more sensitive to condenser

and evaporator temperatures compared to zeolite-water pair.

In brief, the heat & mass recovery cycle has the highest COP and the intermittent cycle has the lowest COP for all pairs. Since the sensitivity of the zeolite-water pair to condenser and evaporator temperatures is the lowest, zeolite-water pair is the most suitable pair for high condenser (e.g., 40°C) and low evaporator temperatures (e.g., 5°C). The activated carbon-methanol pair has a lower COP compared to silica gel-water and zeolite-water pairs, but it can be used for evaporator temperatures below 0°C.

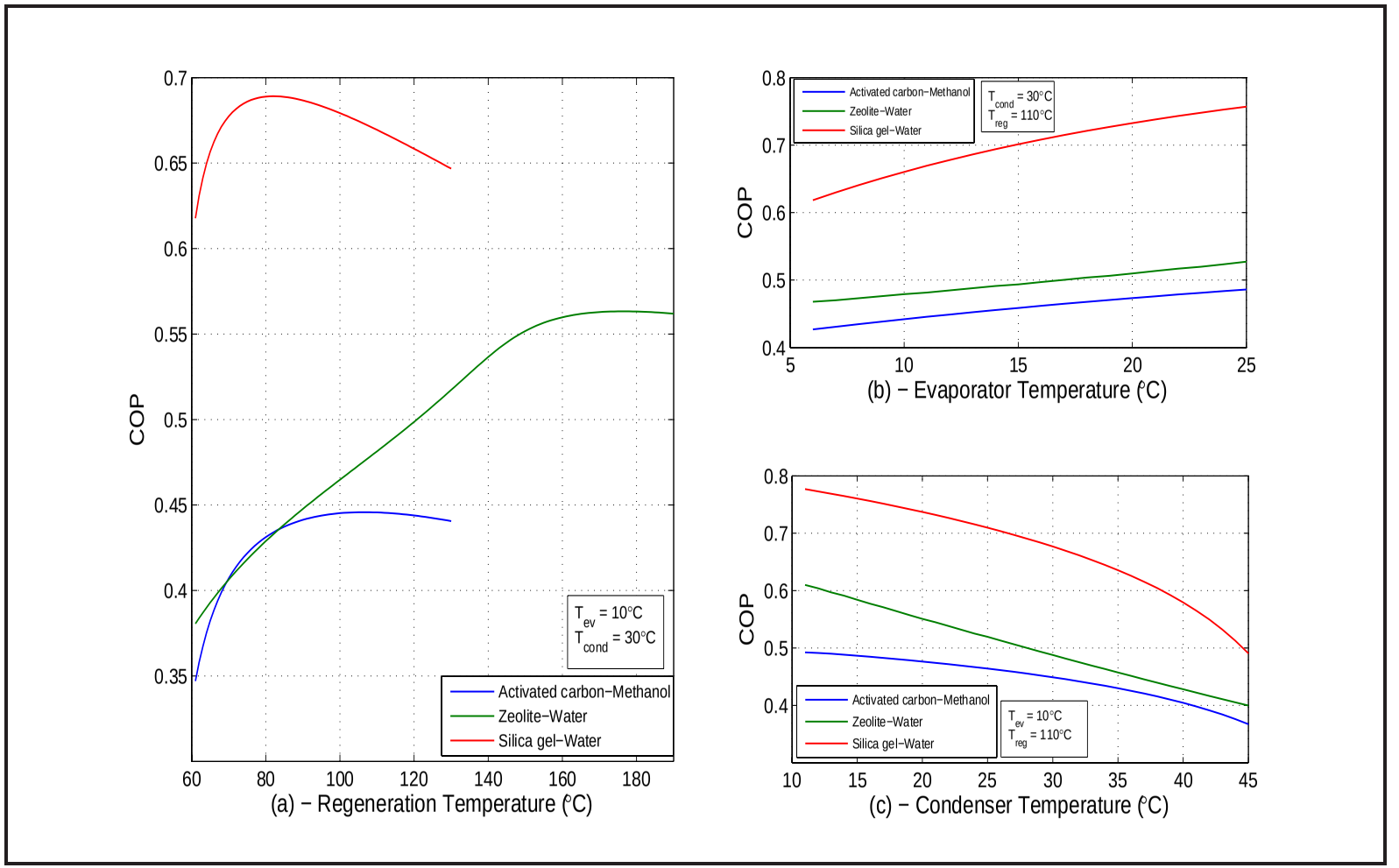

Figure 4.2: Influence of the regeneration temperature(T_{g2})**(a)**, evaporator temperature(T_{ev})**(b)** and condenser temperature(T_{cond})**(c)** on the COP of the intermittent cycle.

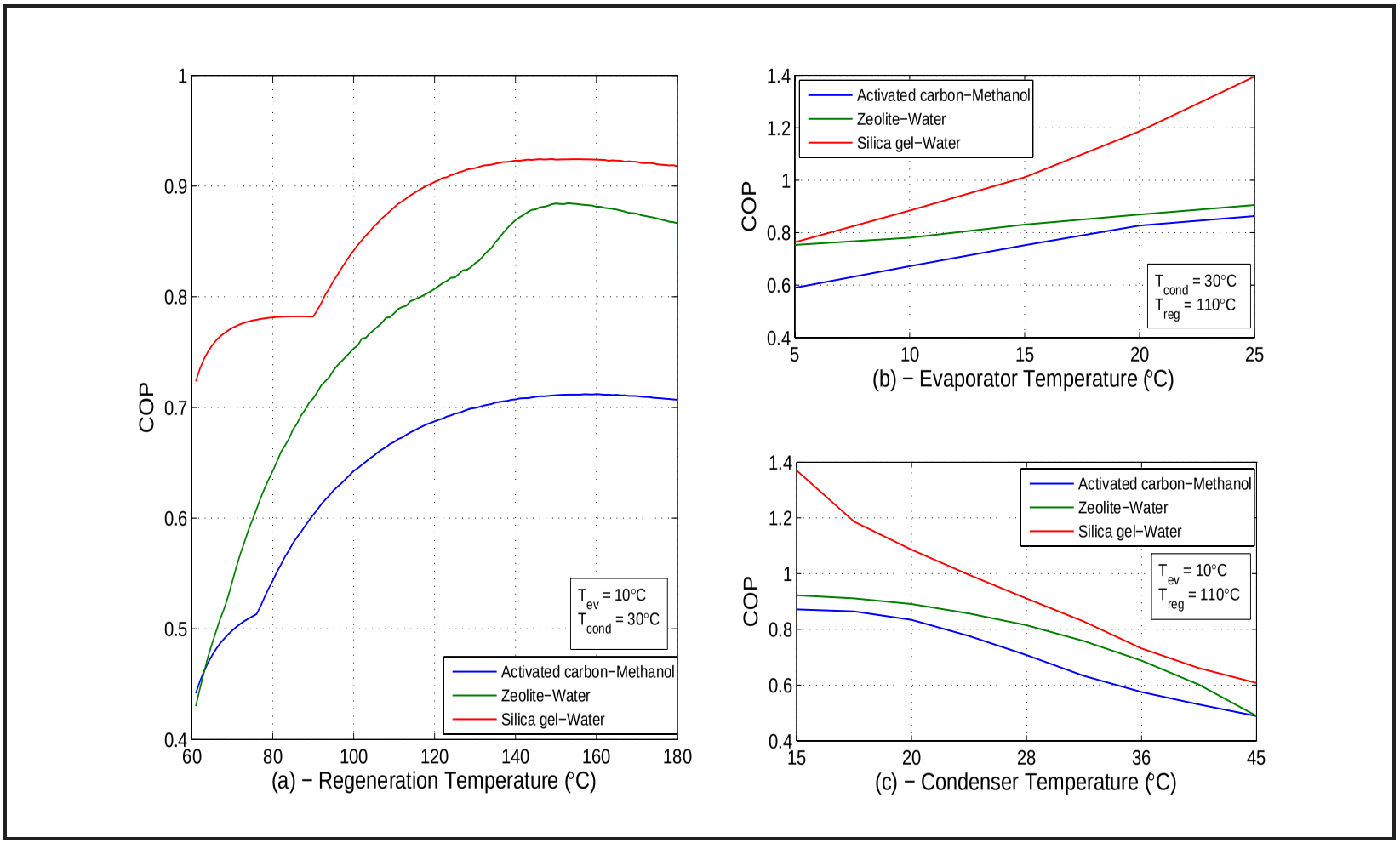

Figure 4.3: Influence of the regeneration temperature(T_{g2})**(a)**, evaporator temperature(T_{ev})**(b)** and condenser temperature(T_{cond})**(c)** on the COP of the heat recovery cycle.

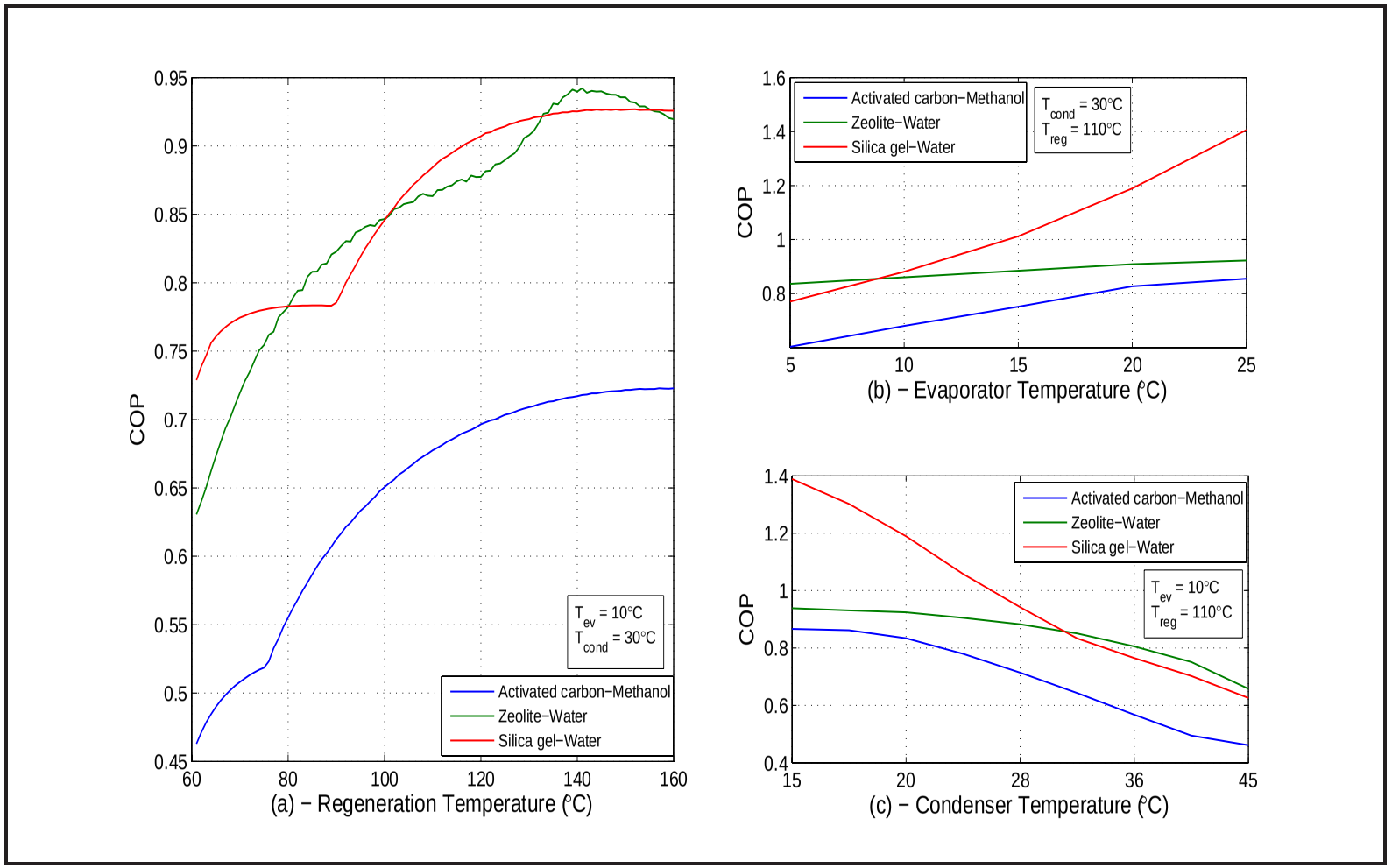

Figure 4.4: Influence of the regeneration temperature(T_{g2})**(a)**, evaporator temperature(T_{ev})**(b)** and condenser temperature(T_{cond})**(c)** on the COP of the heat & mass recovery cycle.

CHAPTER 5

ESTIMATION OF THE BUILDING COOLING LOAD

5.1 Description of the building

Calculation of the building cooling load is the first step in determining the overall performance of the adsorption cooling system. Selection of the building site, orientation, materials and plan are the rudiments of the building cooling load calculation. After determination of the above parameters, cooling load calculation methods can be utilized. However instead of starting from scratch, it is better to use available softwares for convenience and accuracy. There are various softwares available for hourly cooling load calculations [1]. One of the most widely used softwares is the TRNSYS [2]. TRNSYS is extensively used in academic and engineering community and it is continuously developed by the users worldwide. Since it is readily available in Middle East Technical University (METU) Mechanical Engineering Department, TRNSYS is preferred to be used for the building cooling load calculations.

Building which will be analyzed is decided to be in Antalya. The reasons for

[1] http://www.eere.energy.gov/buildings/tools_directory/
[2] for more information: http://sel.me.wisc.edu/trnsys/

this selection are as follows: Antalya is sunny during the most of the year so it is appropriate for solar cooling technologies; and Antalya is a hot and touristic city, so there is a large need for air conditioning during the summer months.

Selection of the building orientation is closely dependent on the building site. Since this study is not experimental, it is necessary to select the building orientation, materials and plan arbitrarily but depending on a rationale. According to Andersson, Place & Kammerud (1985), building cooling and heating loads are lower in northern hemisphere when the more extensively glazed facade is oriented to the south compared to the same building oriented to the east, west or north. Hence building's facade with more glazing will be taken as oriented to the south.

Selection of the building materials is a quite complex issue, because it depends on many criteria (i.e. available materials, insulation standards, budget, etc.). Regardless, application of Turkish standard TS 825 (Thermal Insulation Requirements for Buildings) is compulsory for building constructions in Turkey, so TS 825 can be used as a guideline for satisfying minimum insulation requirements. Here it should be noted that TS 825 is based on energy efficient insulation of buildings for space heating applications (i.e., TS 825 standard imposes limits of energy usage for space heating, not for space cooling applications). However, appropriately insulated buildings regarding space heating requirements mostly perform well in case of space cooling demand. Also one should note that, in practice usage of more insulation compared to TS 825 is suggested in order to reduce the operational costs. Clearly optimization is necessary between operational and investment costs. Wall types and the details of the layers of the walls are given in Table 5.1. Windows used in the building are type INS2_AR_1 which has a U value of 1.4 W/m^2K and a g value of 0.589[3]. Material types used in the layers and window type are selected from the TRNSYS library.

[3]g-value of a window is between 0 and 1 and determines how much of the heat from the sun is allowed to enter the building.

Table 5.1: Wall Construction

Assembly	**Layer**	**Thickness** (mm)	**U-Value** (W/m^2K)
External Wall	Wall board	6	0.286
	Mineral wool	102	
	Spruce pin	51	
	Plywood	6	
	Poly vinyl	13	
Internal Wall	Plstrgps20	20	2.551
	Airspace	-	
	Stucco20	25	
Ground Floor	Common leaf	15	0.275
	Plaster board	60	
	Extruded polystyrene	60	
	Light concrete	13	
Ceiling Wall	Wall board	125	0.844
	Wall board	125	
	Wall board	125	
Roof Wall	Plstrgps20	20	0.303
	Insul125	125	
	Airspace	-	
	Stucco20	25	

Lastly, the building plan is selected considering the summer houses in Antalya. These houses are usually detached two storey houses where entrance floor is used as a living room and kitchen and second floor has two or more rooms depending on the size of the house. Much bigger buildings like five star hotels or shopping centers may also be selected, but it is cumbersome to work with such detailed buildings within the scope of this thesis. As building size increases central heating/cooling system becomes advantageous and this system necessitates a complicated plumbing and/or a ducting system, sophisticated control system, and many auxiliary equipments. Obviously simulation of such a system is much more complicated than simulation of the simple heating/cooling system

of the summer house. In addition, the goal of this study is finding the performance of the adsorption cooling system under ideal conditions which means many factors like the effect of heat exchangers, pumps, etc. are not taken into consideration, so for large buildings results will be clearly less reliable.

One should keep in mind that the results obtained from this chapter are unique to the selected site, plan, materials and orientation of a specific building. In other words keeping all the properties of the building the same, but changing the orientation of the building will give different results. The plan and dimensions[4] of the selected two storey summer house is given in Figure 5.1 and the details of the windows are given in Table 5.2.

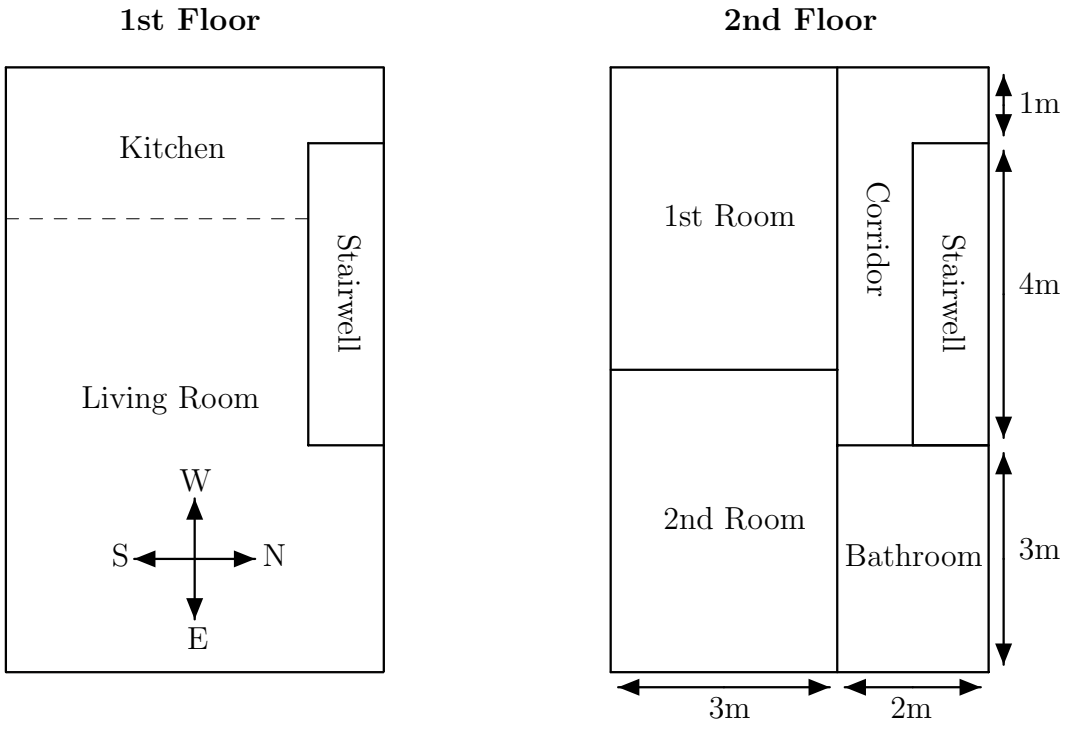

Figure 5.1: Floor plan of a two storey summer house.

[4]Floor height is 3m.
[5]Zones in Table 5.2 are defined in Section 5.2.

Table 5.2: Window areas on the building's facades.

Zones[5]	**Window Areas (m^2)**			
	North	**South**	**East**	**West**
1^{st} Zone	2	6	3	4
2^{nd} Zone	-	2	-	-
3^{rd} Zone	-	2	-	-

5.2 Calculation of the Building Cooling Load

The last step in determining the building cooling load is the specification of the indoor design conditions. Summer indoor design temperature of a comfort air conditioning is specified at 23.9 or 25.6°C with a tolerance of ± 1.1-1.7°C Wang (2001a). In this study summer indoor design temperature is set to 26°C.

As explained previously, TRNSYS is used for cooling load calculations. Building is modeled by TRNBuild[6] which is the visual interface of the multi-zone building model (Type 56) in TRNSYS. Cooling option[7] inside the TRNBuild is used in the determination of the cooling loads. Both sensible and latent loads are considered in cooling load calculations[8].

Two storey summer house is divided into five thermal zones as follows:

[6]TRNBuild creates .bui file which describes the building in all aspects and this file is necessary for the type 56 in TRNSYS. Another way for generating the .bui file is using Simcad software. For complex buildings it may be easier to use Simcad. For more information: http://software.cstb.fr

[7]This is not a cooling device, it only calculates the instantaneous cooling load depending on the various gains of the house. It is also possible to supply cooling from an external cooling device. This latter option will be utilized in the subsequent chapters to simulate the adsorption chiller.

[8]For conditioned spaces in the summer house, it is assumed that there is no mechanical ventilation, but infiltration is allowed (0.6 Air Changes per Hour [ACH]). Also there is human activity in the conditioned spaces. Hence latent loads are due to these components. One should note that latent loads in this study are defined approximately, so in real applications, latents loads should be defined more precisely.

- Zone 1 → Living Room + Kitchen + Stairwell + Corridor
- Zone 2 → 1st Room
- Zone 3 → 2nd Room
- Zone 4 → Bathroom
- Zone 5 → Attic (not shown in Figure 5.1)

Zones 1, 2 and 3 are air conditioned, but Zones 4 and 5 are not air conditioned. The sensible, latent and total cooling loads of zone 1 are given in Figures 5.3, 5.4 and 5.5 respectively. Since results for zone 2 and zone 3 are similar to zone 1, for brevity only total cooling loads of zone 2 and 3 are given in Figures 5.6 and 5.7 respectively.

The TRNSYS model used in the simulation is also given in Figure 5.2 below for brevity. In the subsequent chapters solar collector, storage and adsorption chiller models will be added to this model step by step. The building file (.bui) used in TRNSYS is given in Appendix B for reference.

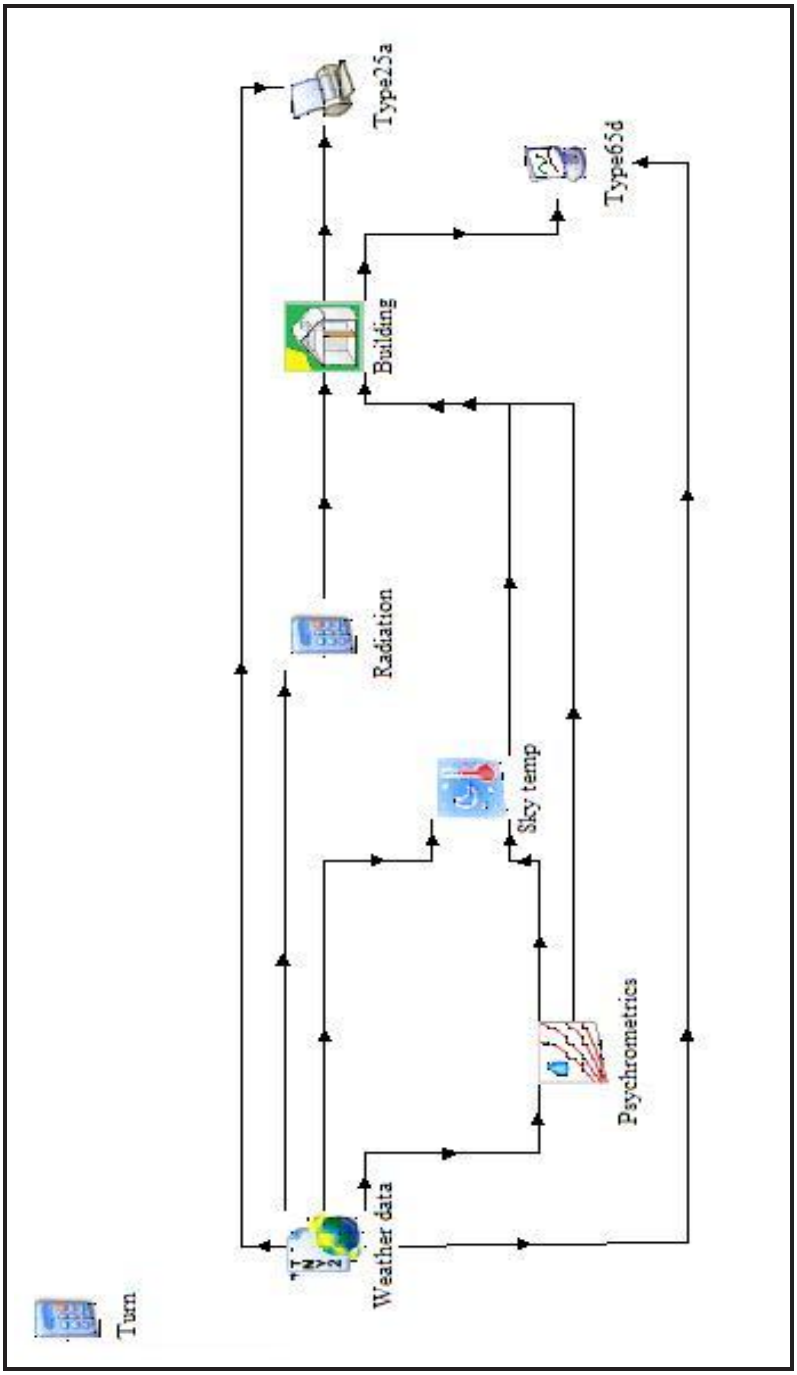

Figure 5.2: TRNSYS model for building cooling load calculation

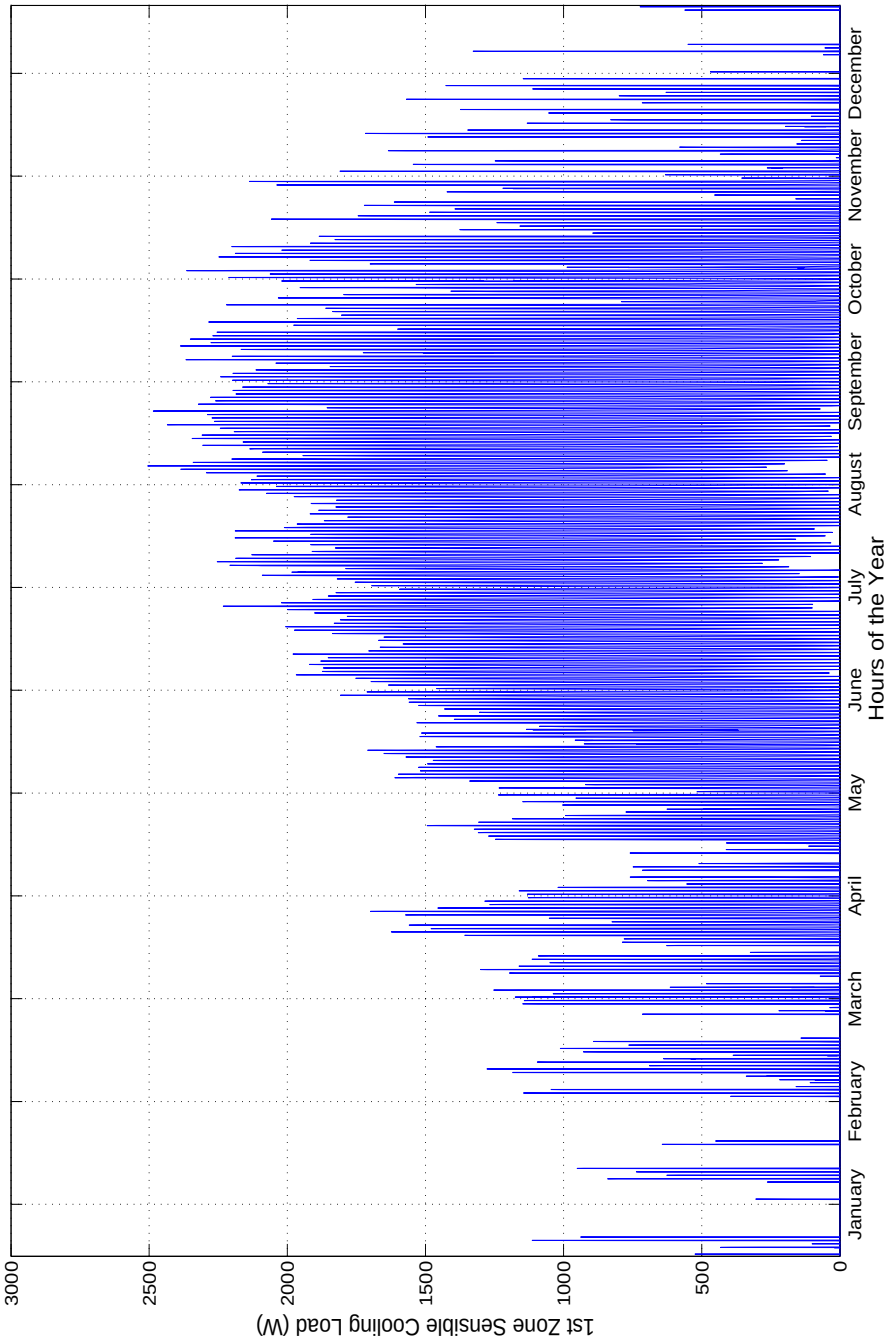

Figure 5.3: Sensible cooling load of the 1st zone

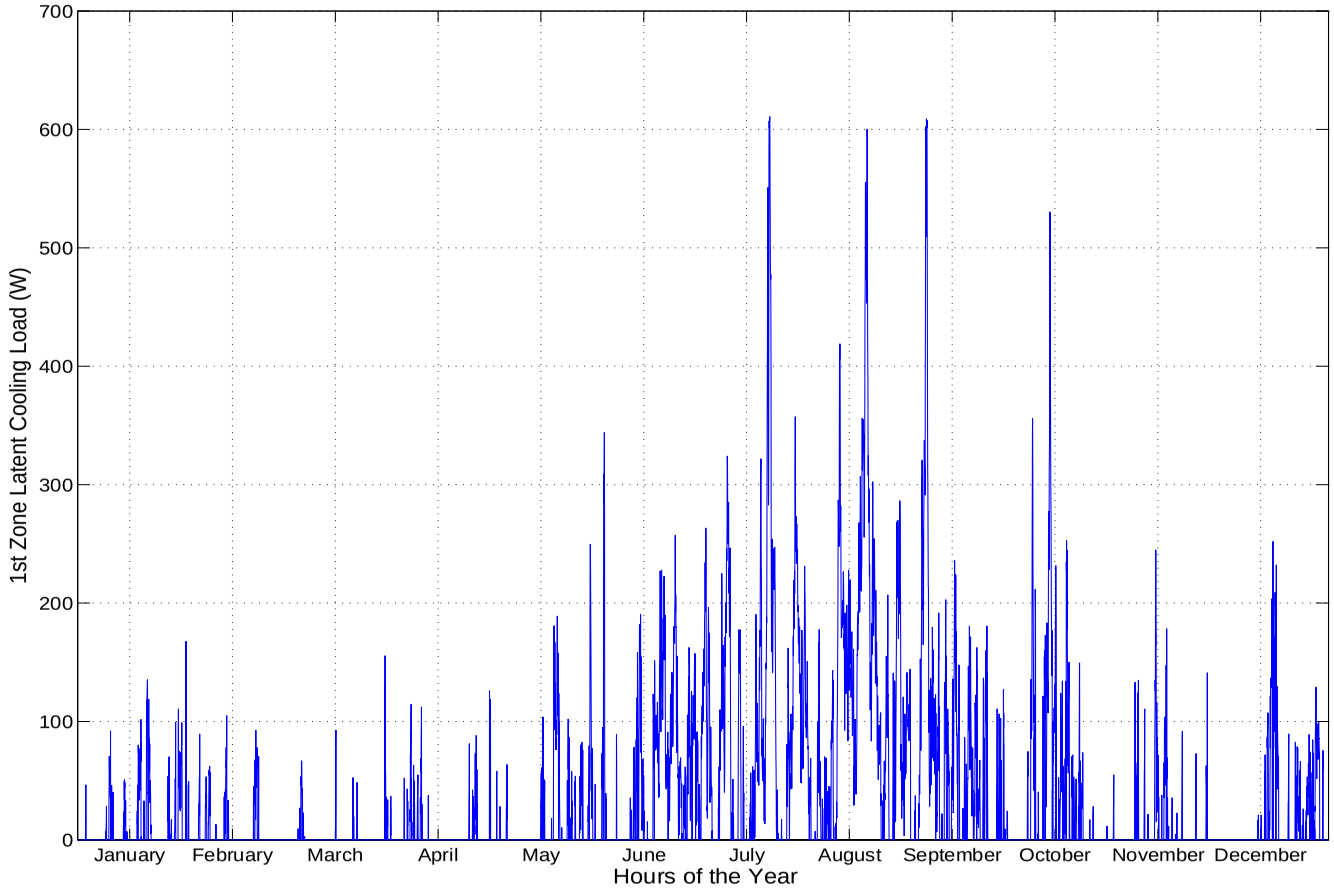

Figure 5.4: Latent cooling load of the 1st zone

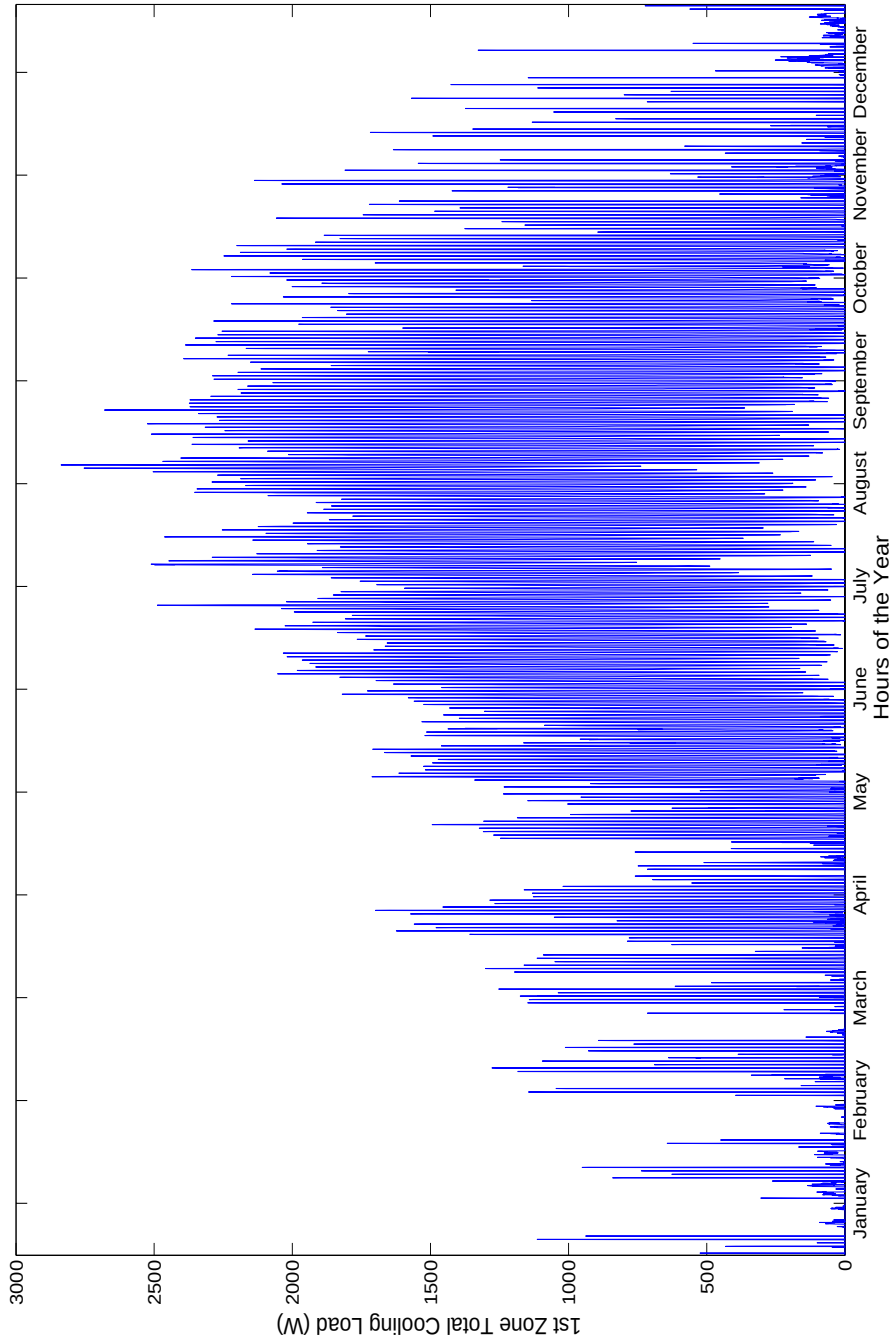

Figure 5.5: Total cooling load of the 1st zone

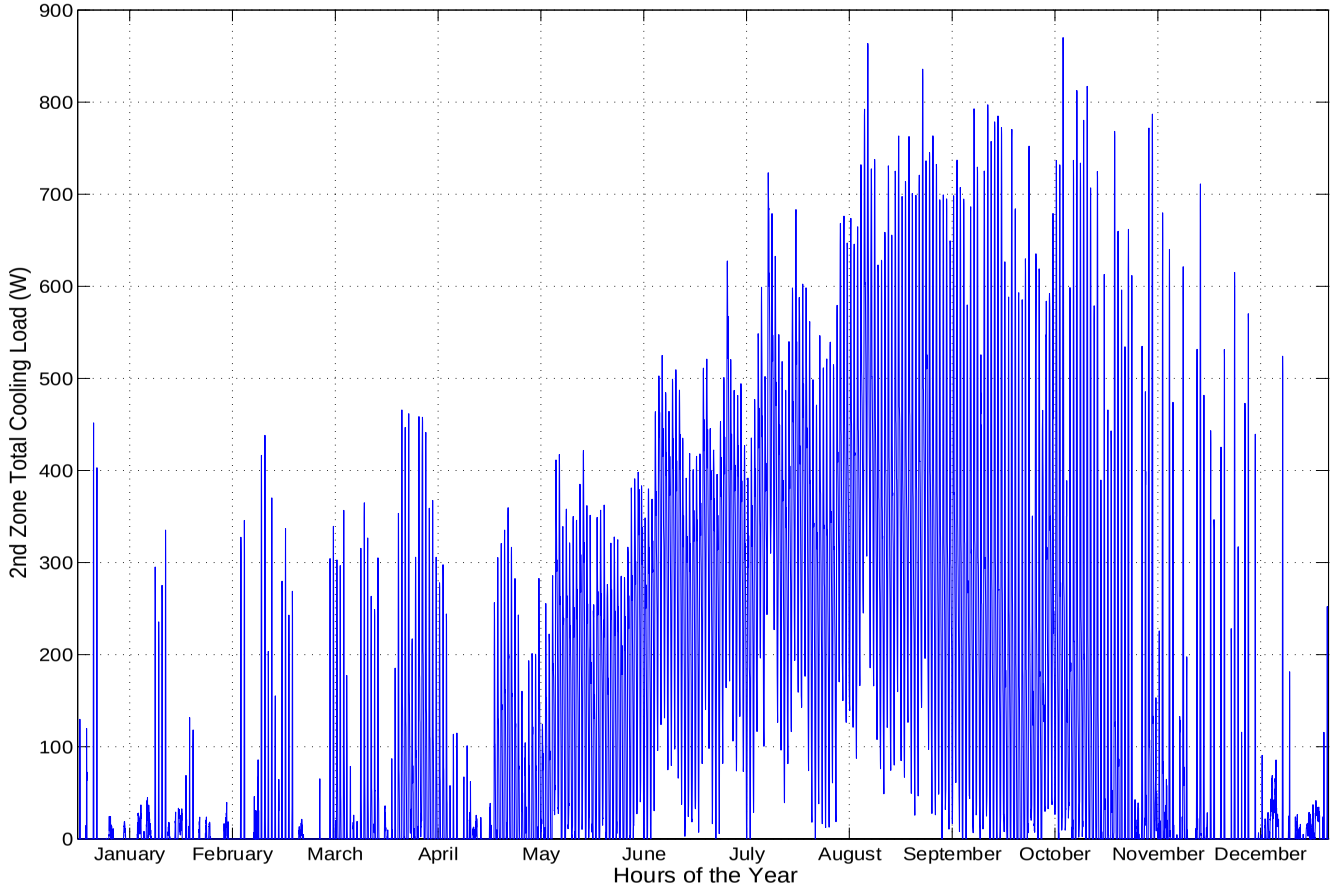

Figure 5.6: Total cooling load of the 2nd zone

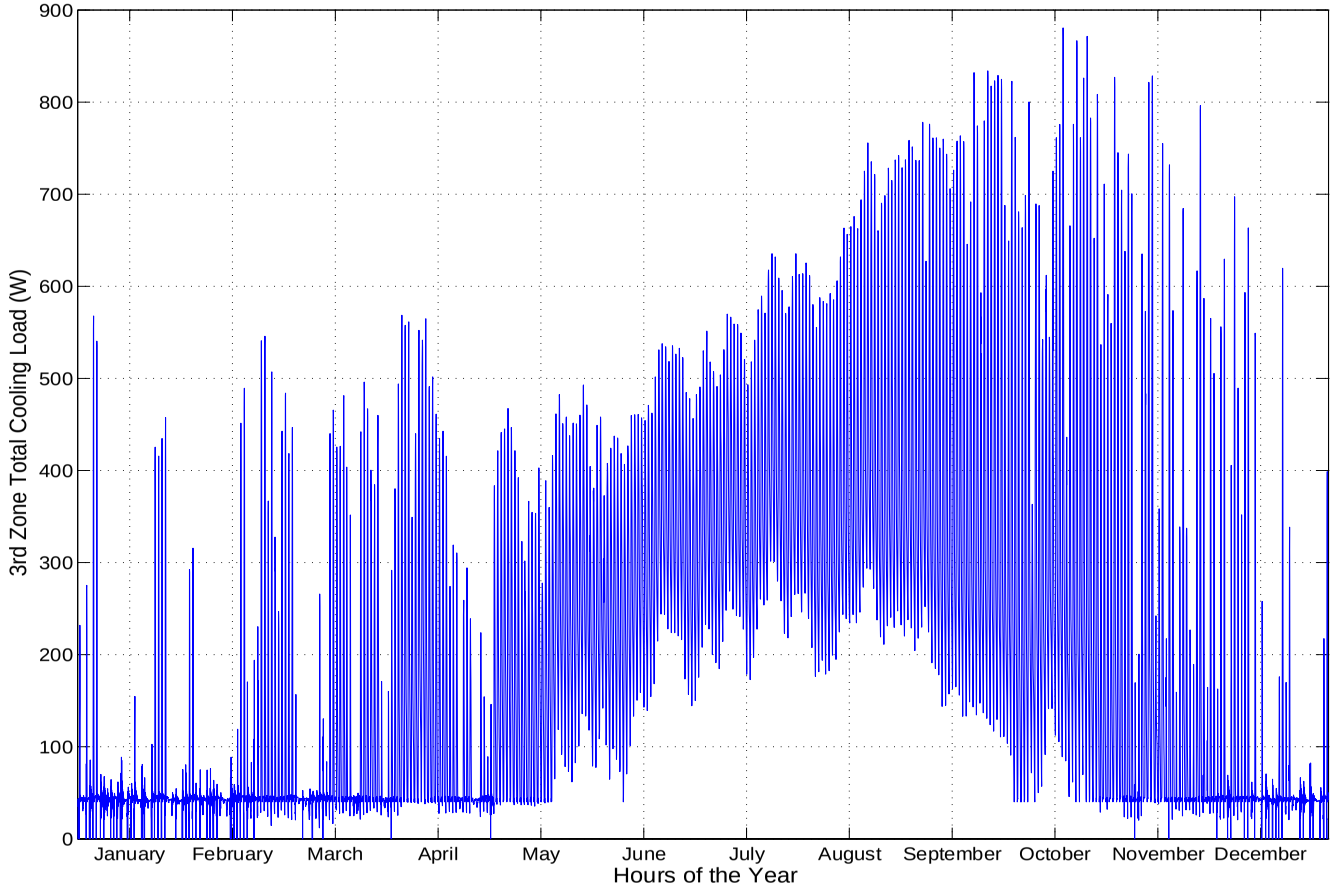

Figure 5.7: Total cooling load of the 3rd zone

5.3 Effect of the Building Thermal Mass on the Cooling Load

Building thermal mass is an important parameter which should be considered in detail in controlling building cooling load. Actually building thermal mass is an extensive subject which has effects on HVAC system controlling and operating strategies (i.e., precooling, night ventilation (Keeney & Braun, 1997)), HVAC system sizing, operational costs and overall cost of the building. In the scope of this study it is not possible to deal with all of these issues related to the building thermal mass, instead it is aimed to focus on the effects of building thermal mass on the cooling load and also investigate the swing in indoor temperatures.

Thermal mass refers to materials which have the capacity to store thermal energy for extended periods. Traditional types of thermal mass include water, rock, brick and concrete. There are also novel phase change materials which store energy while maintaining constant temperatures (Khudhair & Fair, 2004). Thermal mass can be used effectively to absorb daytime heat gains (reducing cooling load) and release the heat during the nighttime (reducing heat load). In addition thermal mass can be utilized to control the swing of the indoor temperature. These effects are shown in Figure 5.8.

As seen from Figure 5.8, fluctuation of the indoor temperature is not as much as the sol-air temperature[9] and there is a lag between the time of occurrence of the maximum indoor temperature and the sol-air temperature.

Effects of the building thermal mass is examined by using the building model explained in section 4.1. Two different types of external walls are used in the calculations. One is the heavy weight and the other one is light weight wall. These wall types are chosen from the TRNBuild library. Only the external

[9]Sol-air temperature is the fictitious temperature of the outdoor air which, in the absence of radiative exchanges on the outer surface of the roof or wall, would give the same rate of heat transfer through the wall or roof as the actual combined heat transfer mechanism between the sun, the surface of the roof or wall, the outdoor air and the surroundings.

wall layer of the wall structure explained in Figure 5.1 is replaced by heavy and light weight walls.

Effect of the heavy and light weight walls on the temperature fluctuation of the first zone can be clearly seen in Figure 5.9. During this analysis the cooling device in the multizone building model, type 56, is off. Hence it is possible to observe the temperature swing in the first zone if there is no cooling supplied. As expected temperature swing in light weight wall is greater than the heavy weight wall.

In Figure 5.10, effect of the heavy and light weight walls on the cooling load of the first zone throughout the year can be seen. Cooling load of the building with heavy weight wall is 12% less than the building with light weight wall on average during summer months. For brevity monthly cumulative cooling loads are presented.

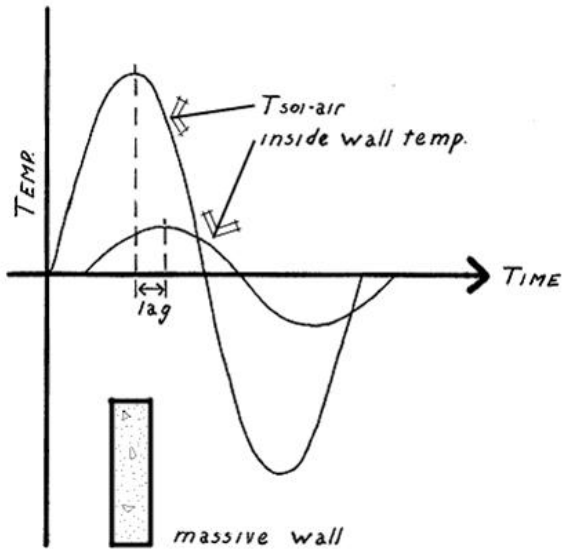

Figure 5.8: Temperature swing and lag inside building (McQuiston, Parker & Spitler, 2005)

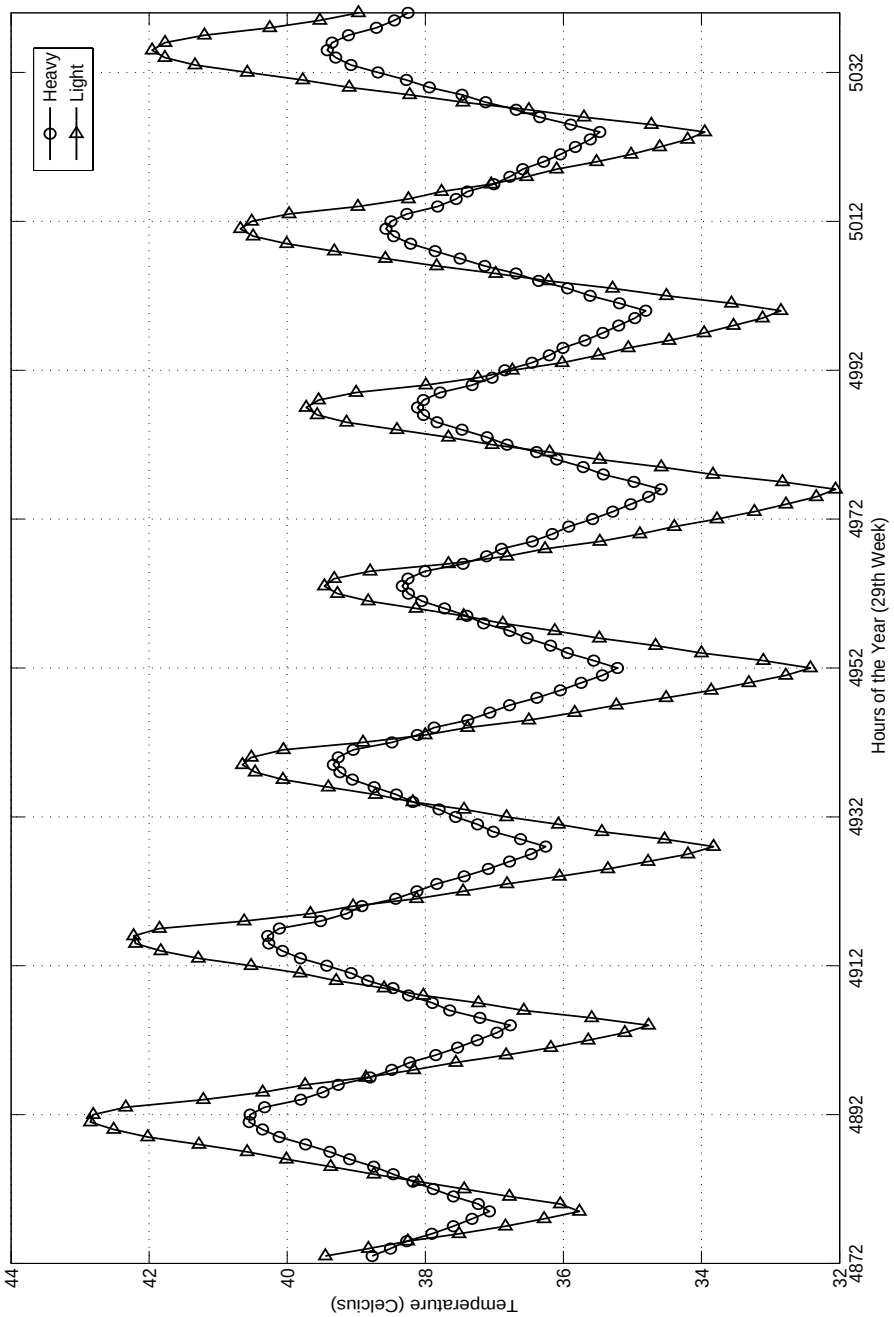

Figure 5.9: Temperature swing in the 1st zone

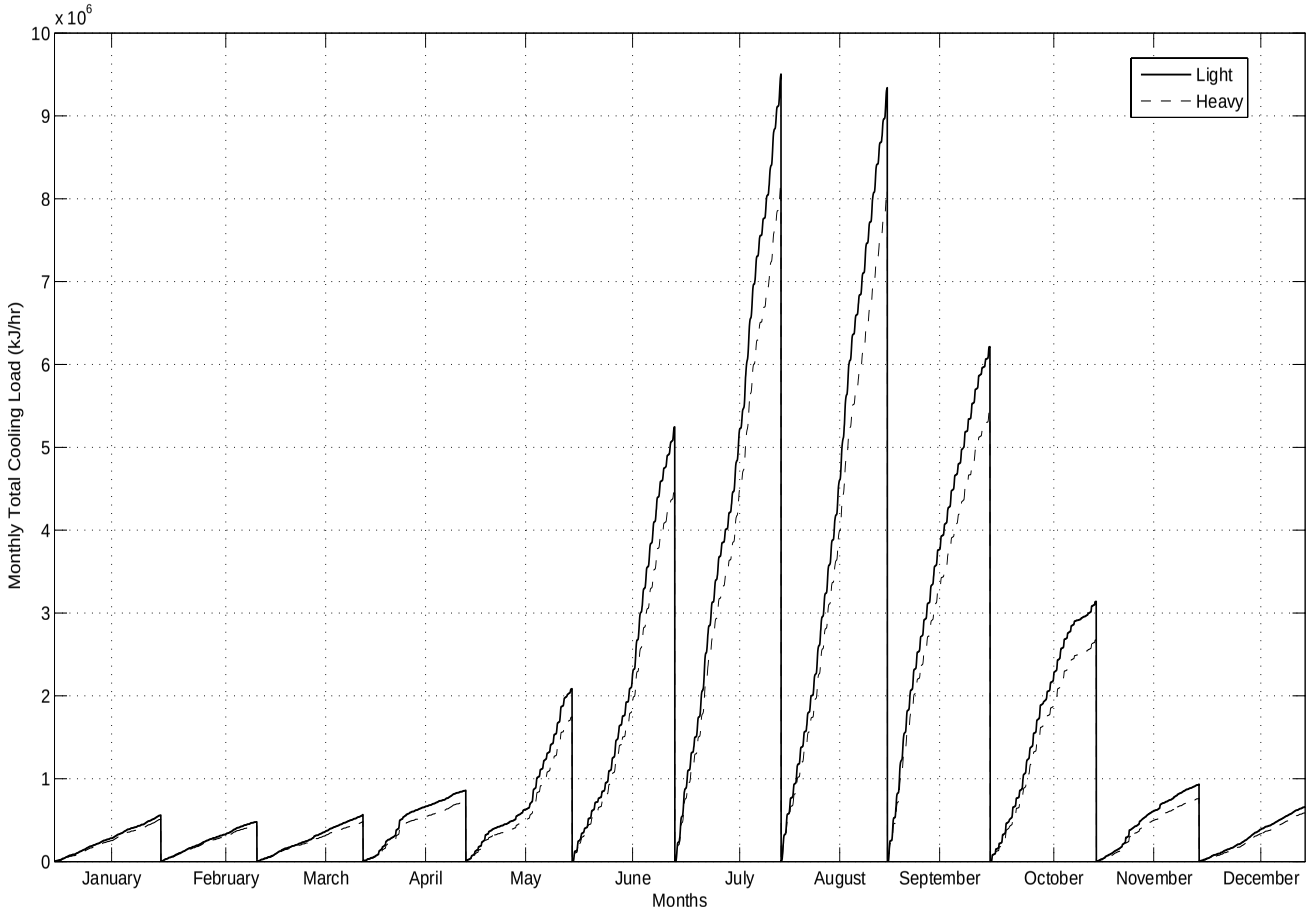

Figure 5.10: Cooling loads of the 1st zone for heavy & light weight walls

CHAPTER 6

DESIGN OF SOLAR THERMAL COOLING SYSTEM

In this chapter, design of an integrated model of the solar adsorption cooling system is investigated in detail. Actually there is a limited experience and knowledge in planning and designing solar cooling systems, and there is no standard or complete guideline available for whole system planning. Just recently some useful books are published (Henning, 2007); (German Solar Energy Society (DGS), 2005). These books are used as reference in integrated system modeling.

6.1 Solar-thermal Cooling System Concepts

Solar cooling system design starts with the fundamental decision which concerns the solar energy fraction, (Henning, 2007). Solar energy fraction, shortly solar fraction (SF) is the ratio of solar energy used in the whole system divided by the total energy requirement of the solar cooling plant. Basically there are two types of system design approaches:

- Solar-thermally autonomous systems
- Solar-assisted systems

Solar-thermally autonomous systems are self sufficient systems. In other words, all the required heat for a thermally driven cooling system is extracted from the sun[1]. This type of systems may not always satisfy the desired indoor conditions, and statistical analysis is used to evaluate how often indoor temperature and humidity will exceed certain comfort requirements. Also cooling loads and solar gains should be very well synchronised in these systems. Usually solar-thermally autonomous systems are reasonable when using a back-up system is not feasible[2] or recommended.

Solar-assisted systems are used to reduce conventional energy usage by using solar energy. These systems use back-up systems to provide the required amount of cooling under all circumstances. The back-up system may be a second heat source like a gas-fired boiler or a convential compression chiller for generating cooling power directly. In selection of the back-up system there is no silver bullet. Selection criteria closely dependent on the project itself.

In this study solar-assisted cooling system with a second back-up heat source system is emphasized. This configuration is the most widely used system among the solar heat driven chiller based systems (Henning, 2007). Economics and the performance of this system may be compared with other configurations in further studies.

[1]Solar cooling systems always need electricity to drive pumps, fans, etc. Electricity energy required for these systems are small compared to thermal energy used for cooling. Hence systems which use electricity from the grid can also be assumed as solar-thermally autonomous systems. Note, electricity required to drive auxiliary systems can be generated by PV cells, but this is usually economical only in remote areas

[2]For instance, accessing conventional energy sources (electricity, gas, etc.) in remote areas is difficult.

6.2 Subsystems of the Solar-thermal Cooling System

There are four major subsystems in a solar thermal cooling system (DGS, 2005). These are;

- Building (thermal insulation, intelligent skins, etc.)
- Air-conditioning system (fan-coils, air handling unit, chilled ceilings, etc.)
- Cold-supply circuit (chiller, cold storage tank, etc.)
- Heat-supply circuit (solar collectors, heat storage tank, auxiliary heater, etc.)

Depending on the requirements and climatic zone, some of these subsystems may not be used. For instance, if humidification/dehumidification is not so important in a building, an air-conditioning unit may not be installed. In the scope of this study the air-conditioning system is not considered, since this requires detailed design of the building. The other three subsystems are investigated in detail.

6.2.1 Building

Design of a low energy demand (low heating, cooling and lighting load) building is an extensive subject itself and requires interdisciplinary cooperation between architects and engineers. It is the first step to be considered for an economically rational solution in solar cooling system applications. Developed countries continuously improve the energy efficiency requirements of buildings by imposing strict limits on building energy usage. The most widely used standards related to the building energy performance are ISO 13790[3] and ASHRAE 90.2-2007[4].

[3]Energy performance of buildings - Calculation of energy use for space heating and cooling
[4]Energy-efficient design of low-rise residential buildings

By 2050, the aim is designing zero energy demand and/or zero carbon footprint buildings.

The building used in the simulations of this study is explained in detail in Chapter 5, so it will not be repeated here again. But the main points which should be considered in building design can be summarized as follows, (DGS, 2005);

- thermal insulation and thermal mass of the building
- integration of exterior sunshade systems to the building
- using intelligent skins in facade of the building, (Wigginton & Harris, 2002)
- reduction of internal loads (lighting and appliances)

6.2.2 Heat-supply Circuit

The heat-supply circuit is primarily comprised of the solar collector field and hot storage tank. Among these, the solar collector area and type has an important effect in terms of economics and performance of the solar cooling system. Selection of the collector type depends on the driving temperature of the chiller. Since collector efficiency should be at least 50-60% for any solar application, collector efficiency curves should be utilized when choosing appropirate collector type for a specific cooling technology (Henning, 2007). This is depicted in Figure 6.1 for different collector types and cooling technologies.

The driving temperature for the commercially available adsorption cooling systems is in the range 55°C to 90°C as seen from Figure 6.1. For this temperature range both flat plate and evacuated tube collectors can be used. Usually flat plate collectors are used in this temperature range, therefore flat plate collectors will be evaluated in terms of economics and performance of the solar cooling system.

Hot storage tank is the other key element in the heat-supply circuit. Since

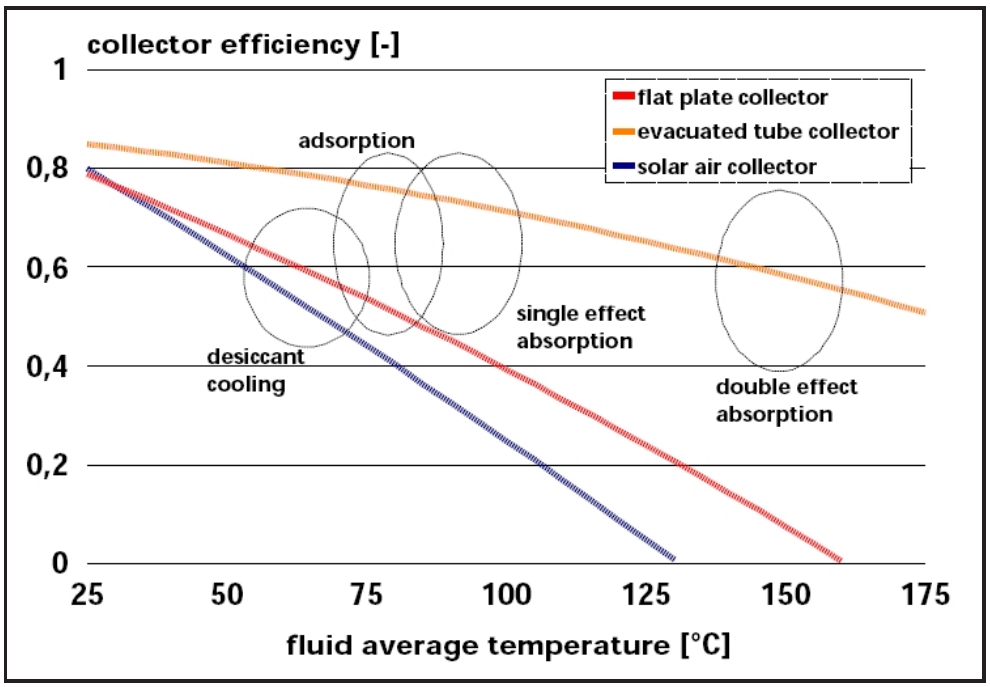

Figure 6.1: Operating range for solar cooling technologies, (Henning, 2007)

the heat supplied by the sun and the heat required for driving chiller is not usually in phase, excess solar heat generated by the collectors should be stored for later use. The main functions of the hot storage can be explained as follows (Henning, 2007);

- decouples the solar collector field (heat source) and chiller (heat sink)
- stores heat from fluctuating source for later use
- reduces exergy losses by stratification

6.2.3 Cold-supply Circuit

The cold-supply circuit is primarily comprised of solar-thermal driven chiller, cold storage tank and cooling tower.

Solar-thermal driven chillers are absorption, adsorption and desiccant systems which are discussed in Chapter 2 in detail. In this study adsorption chiller

is used and the adsorption chiller model will be described in the next section.

Cooling towers are necessary in order to transfer rejected heat from the refrigerant to the ambient. Mainly there are two types of systems: wet cooling towers and dry (closed-circuit) cooling towers. Wet cooling towers use evaporating water to cool a coolant. If the coolant is water this can be an open circuit or a closed circuit. If the coolant is not water this will be a closed circuit. Advantages of wet cooling tower are: it can cool to the ambients wet-bulb temperature and it has good heat transfer characteristics. On the other hand, the disadvantage of a wet cooling tower is that it requires water, which can be a problem in dry climates. Dry cooling towers only use air to do cooling and is always a closed circuit. Advantage of a dry cooling tower is that it does not require water and therefore is preferred in areas with limited water. On the other hand, disadvantages of dry cooling tower are that it can only cool to ambients dry bulb temperature and has worse heat transfer characteristics than wet cooling tower. Dry cooling towers are generally less preferable because of increased electricity consumption due to larger fans and higher investment costs compared to wet cooling towers except in areas with limited water (Henning, 2007).

Cold storage tank has similar functions as hot storage tank. For detailed information reader should refer to Henning (2007).

6.3 TRNSYS Model of the Solar-assisted Cooling System

Solar-assisted cooling system model is developed in TRNSYS. The integrated model is given in Figure 6.2 below. First, components used in the model will be explained shortly. Then system design parameters are discussed and the methodology used in the design of solar cooling system is explained.

6.3.1 TRNSYS Components Used in the Model

Following are the short descriptions of the important components used in TRNSYS model. Reader should refer to TRNSYS user's manual for detailed explanations (Klein et al., 2006).

Weather data, type109: This component reads weather data at regular time intervals from a data file[5], converting it to a desired system of units and processing the solar radiation data to obtain tilted surface radiation and angle of incidence for an arbitrary number of surfaces.

Psychrometrics, type33: This component takes as input the dry bulb temperature and dew point temperature of moist air and calls the TRNSYS Psychrometrics routine, returning the following corresponding moist air properties: dry bulb temperature, dew point temperature, wet bulb temperature, relative humidity, absolute humidity ratio, and enthalpy.

Sky temperature, type69: This component determines an effective sky temperature, which is used to calculate the long-wave radiation exchange between an arbitrary external surface and the atmosphere.

Controller, type2b: The on/off differential controller generates a control function which can have a value of 1 or 0.

Pump, type3b: This pump model computes a mass flow rate using a variable control function, which must have a value between 1 and 0, and a fixed (user-specified) maximum flow capacity.

Building, type56: This component models the thermal behaviour of a building having up to 25 thermal zones.

Flat plate collector, type1: This component models the thermal performance of a flat-plate solar collector. In this instance of type1, a second order quadratic function is used to compute the incidence angle modifier.

[5]TMY data file of Antalya.

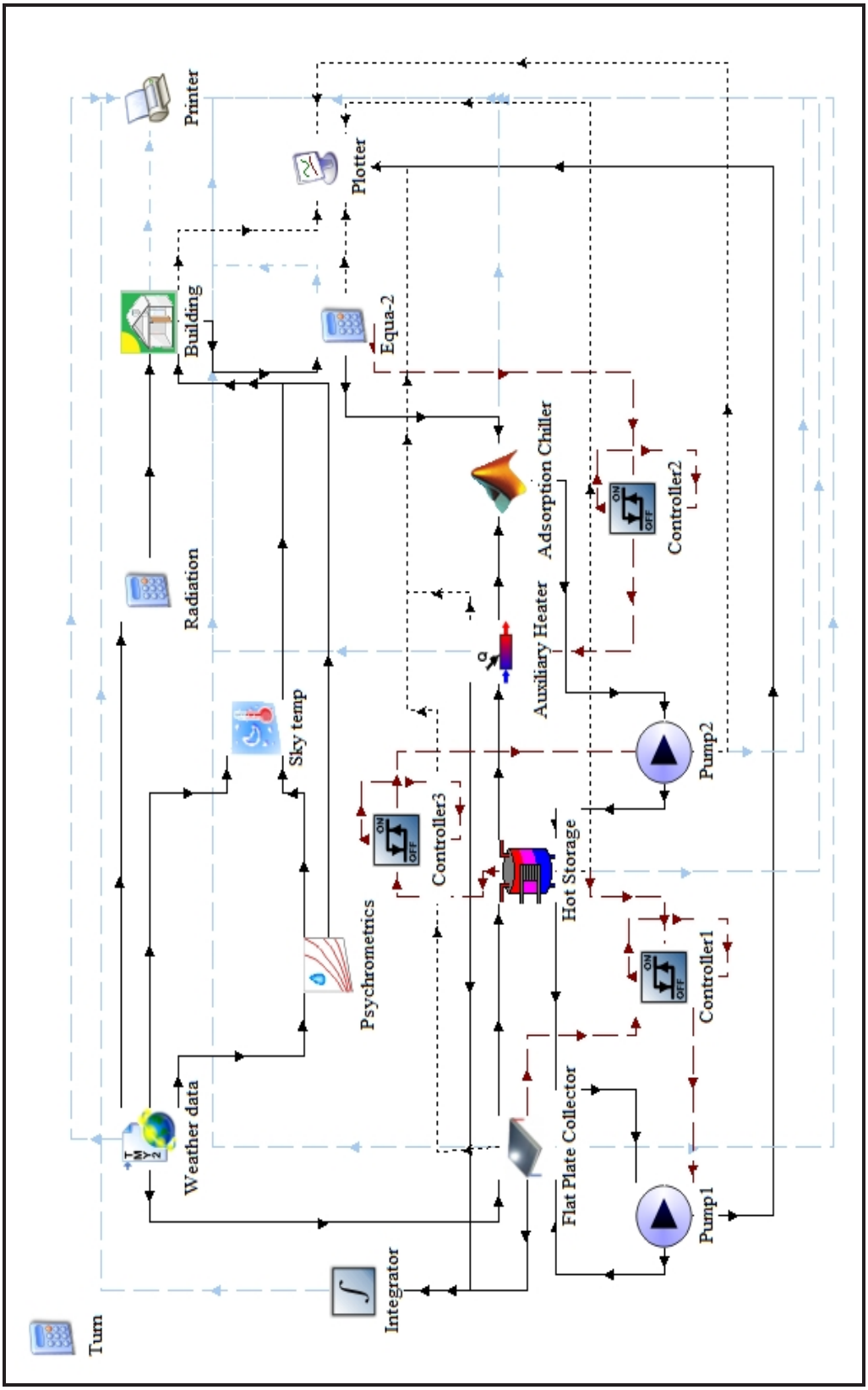

Figure 6.2: Integrated model developed in TRNSYS

Hot storage, type534: This component models a fluid-filled, constant volume storage tank with immersed heat exchangers. This component models a cylindrical tank with a vertical configuration. The user has the ability to specify one of four different immersed heat exchanger types (or no HX if desired); horizontal tube bank, vertical tube bank, serpentine tube, or coiled tube.

Auxiliary heater, type6: An auxiliary heater is modeled to elevate the temperature of a flowstream using either internal control, external control or a combination of both types of control. The heater is designed to add heat to the flowstream at a user-designated rate whenever the external control input is equal to one and the heater outlet temperature is less than a user-specified maximum.

Adsorption chiller, type155: This component calls Matlab from TRNSYS. Since there is no adsorption chiller model readily available in TRNSYS, this ideal adsorption chiller model is created in Matlab. Adsorption chiller component accesses the results of the ideal thermodynamic model.

Ideal thermodynamic models of the intermittent, heat recovery and heat & mass recovery adsorption refrigeration cycles are given for zeolite-water, silica gel-water and activated carbon-methanol pairs in Chapter 3. The ideal model explained in Chapter 3 for heat & mass recovery adsorption refrigeration cycle is used in the model and all three pairs are investigated. In this adsorption chiller model, cooling water (condenser) and chilled water (evaporator) temperatures are taken as constant at 30° and 10° respectively, but driving temperature of the chiller is taken as variable with a minimum value of 60°C. If the inlet hot temperature to the adsorption chiller is below 60°C, auxiliary heater is switched on. The COP values of the chiller for the corresponding driving temperatures are calculated by using the ideal model. On the other hand, cooling load of the building for each zone is calculated by using multi-zone building model (type56), then total cooling load of the building is calculated by summing cooling loads of each zone using the Equa-2 component in TRNSYS. Total cooling load of the building is given as an input to the adsorption chiller model and it is divided by the corresponding COP value. In this way, heat demand

of the chiller in order to provide just the required amount of cooling to the building is calculated. Dynamic coupling of the chiller to the integrated model is done as follows. Hot water inlet temperature of the chiller is already known, and by writing energy balance equation between load and supply side, hot water outlet temperature of the chiller is calculated as

$$\dot{m} \cdot C_{pw} \cdot (T_{hi} - T_{ho}) = \frac{Q_{tot}}{COP} \tag{6.1}$$

where $\dot{m}$ is the auxiliary heater circuit mass flow rate (kg/s), C_{pw} is the specific heat of water (kJ/kg·K), T_{hi} is the hot water inlet temperature to the chiller (°C), T_{ho} is the hot water outlet temperature from the chiller (°C) and Q_{tot} is the total cooling load of the building (kW).

6.3.2 Control Strategy

The schematic figure of the solar-assisted cooling system is given in Figure 6.3. Since the control strategy of the solar-assisted cooling system has an important effect on the overall system performance, it is important to discuss it here. Three on/off controllers are used in the system.

Controller 1 controls the collector circuit mass flow rate. Basically, it compares the hot storage tank outlet temperature with the collector outlet temperature. If hot storage tank outlet temperature is higher than the collector outlet temperature, controller 1 stops pump 1.

Controller 2 is implemented into the model to control the auxiliary heater in case of low cooling demand in order to increase the solar fraction of the solar cooling system. Controller 2 turns off the auxiliary heater if the cooling load of the building is below 100 kJ/hr. Therefore if the cooling load is below 100 kJ/hr, no cooling is provided to the building[6].

[6]Actually, cooling load is always above 100 kJ/hr during summer months (i.e., between days 150 and 300 of the year) as depicted in Chapter 5. Hence controller 2 is only functional during cooler days.

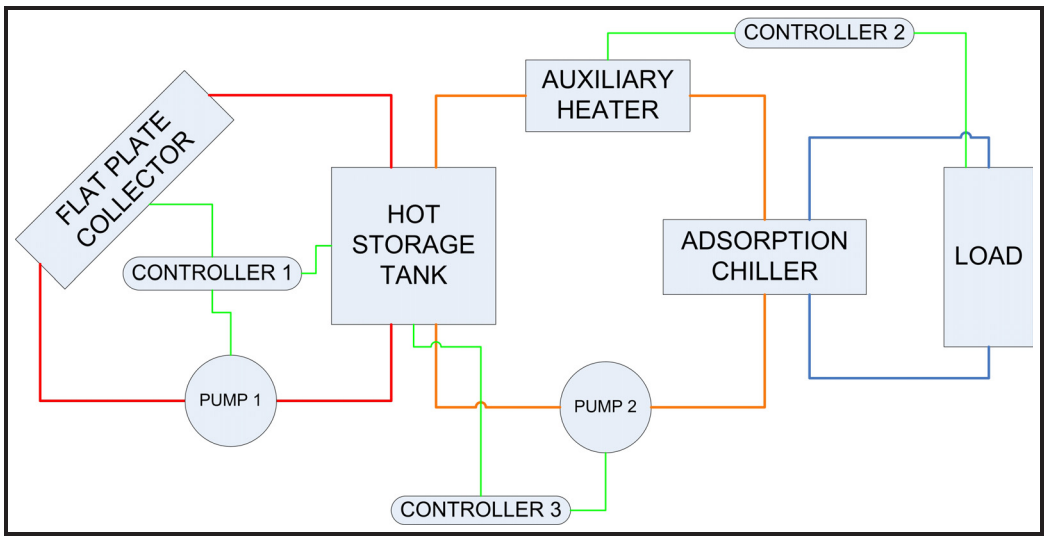

Figure 6.3: Schematic diagram of the solar-assisted cooling system

Controller 3 is also used to increase the solar fraction of the solar cooling system. Controller 3 controls the auxiliary heater circuit mass flow rate by comparing hot storage tank average temperature with the user specified value. If the average temperature of the hot storage tank is below 50°C, it stops pump 2 (Henning, 2007). In other words, if average hot storage tank temperature is below 50°C, no cooling is supplied to the building since pump 2 is off[7].

6.4 Solar-assisted Cooling System Design Methodology

The ultimate goal in the application of any solar-assisted cooling system is reducing fossil fuel usage compared to grid electricity powered conventional mechanically driven compression cooling systems[8]. So any system design should

[7]Controller 3 is functional early in the morning and late in the evening. Also it is functional during cloudy days when there is low solar radiation available.

[8]Appropriately designed solar-assisted cooling system should save primary energy compared to conventional cooling system, but saving primary energy does not always imply that

depend on primary energy reduction. Solar fraction is the key parameter to be considered during the decision making process of the solar-assisted cooling system design as mentioned at the beginning of this chapter. Other important parameters to be considered are the electricity generation efficiency from fossil fuels, COP of the mechanically driven chiller and the COP of thermally driven chiller. The relation among these parameters is depicted in Figure 6.4 which is valid for a primary energy conversion factor[9] of 0.58 for generating electricity from natural gas (kWh of electricity per kWh of primary energy). If other fossil fuels like coal is used for generating electricity, conversion factor will be in the range 0.3 to 0.45. Selecting conversion factor as 0.58, is a conservative approach. In addition, primary energy conversion factor for heat from fossil fuels is taken as 0.9 (kWh of heat per kWh of primary energy) in Figure 6.4[10] below.

The COP of the adsorption chillers in the market are approximately 0.6. The COP of the ideal model of the heat & mass recovery adsorption chiller used in this study is in the range 0.6 to 0.8 depending on the possible inlet hot water temperatures. Referring to Figure 6.4, in order to save primary energy with solar-assisted cooling system solar fraction should be at least 40%[11]. But it is recommended to design solar-assisted cooling system with a solar fraction of 70-80%, in order to save significant amount of primary energy (DGS, 2005).

Now the effect of the system design variables on the solar fraction of the solar-assisted cooling system will be investigated in the following part. Referring to Figure 6.2, there are mainly 4 variables to be considered. These are:

- collector area and collector circuit (primary loop) mass flow rate
- collector tilt angle and orientation
- auxiliary heater circuit (secondary loop) mass flow rate

solar-assisted cooling system installation is also economically feasible. This point will be explained in Chapter 6 in more detail.

[9] First law efficiency

[10] Primary energy source used in generating Figure 6.4 is only natural gas, not solar energy.

[11] In comparison with the compression chiller which has a COP of 2.5.

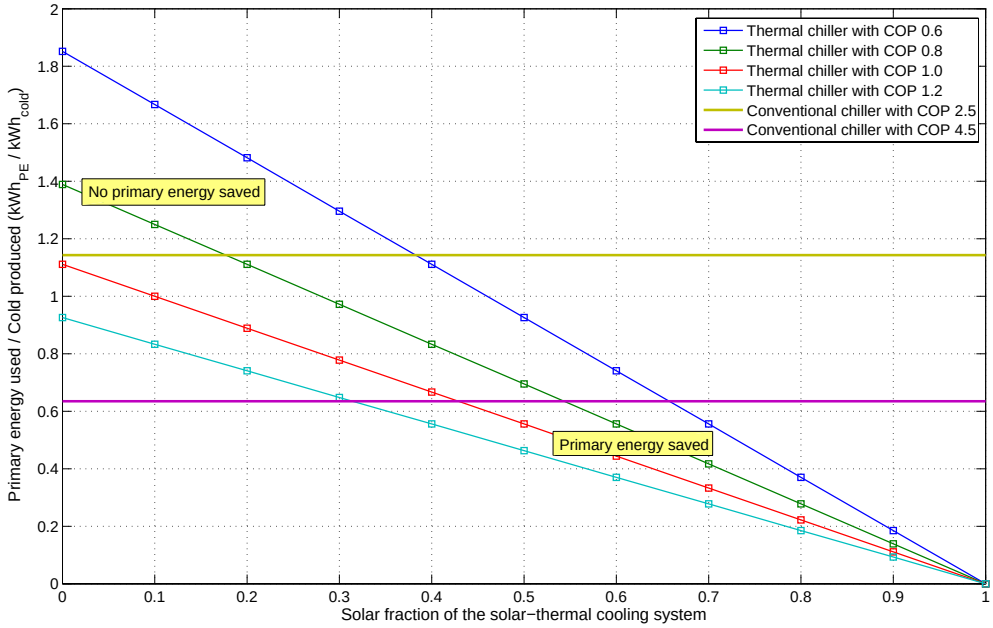

Figure 6.4: Primary energy consumption of solar-assisted cooling systems (thermal chiller) and conventional chiller as a function of the solar fraction for different COP values of the thermally driven chiller.

- hot storage tank volume

6.4.1 Collector Tilt Angle and Orientation

Collector tilt angle(β) and azimuth should be adjusted to maximize the solar radiation collection. In theory, collector tilt should be adjusted continuously to obtain maximum energy from the sun, but since these tracking mechanisms are costly and require maintenance they are not preferred. Also studies show that the solar radiation received using the annual average of the optimum tilt angle is only 6% less than adjusting the tilt angle every month, (Hartley, Martinez-Lozano, Utrillas, Tena & Pedros, 1999). Considering non-tracking collectors, the optimum orientation in northern hemisphere is due south and the optimum

tilt angle is equal to the latitude(ϕ) of the location for systems used throughout the year. For systems used during summer $\beta_{opt} = \phi + 15°$ and during winter $\beta_{opt} = \phi - 15°$, (Günerhan & Hepbaşlı, 2007). Since solar cooling system is located in Antalya, which has a latitude of $36°52'$, and planned to be used for cooling in summer months, the tilt of the solar collectors are taken as $45°$.

6.4.2 Collector Area and Primary Loop Mass Flow Rate

There is a close relationship between the collector area and the collector mass flow rate. The optimum mass flow rate through a flat plate collector is researched extensively, (Hewitt & Griggs, 1976), (Duffie et al., 2003), (Saha & Mahanta, 2001). The optimum mass flow rate through flat plate collectors is in the range between 0.01 to 0.05 kg/s·m^2. Effect of the collector mass flow rate on the solar fraction will be investigated below.

As a starting point[12], collector area can be calculated by using the following equation, (Henning, 2007):

$$A_{coll} = \frac{Q_{tot}}{G_{\perp} \cdot \eta_{collector} \cdot COP_{chiller}} \tag{6.2}$$

where A_{coll} is the collector area, Q_{tot} is the nominal cooling capacity, $G_{\perp}$ is the total solar normal radiation incident on the collector and $COP_{chiller}$ is the coefficient of performance of the solar thermal chiller.

From equation 6.2, collector area is found to be $\cong 18m^2$ for $Q_{cooling} = 5kW$, $G_{\perp} = 0.8kW/m^2$, $\eta_{collector} = 0.5$ and $COP_{chiller} = 0.7$. Thus specific collector area, A_{spec}[13], is:

$$A_{spec} = \frac{18m^2}{5kW} = 3.6m^2/kW \tag{6.3}$$

[12]Here, the collector area is calculated in order to determine a reasonable starting point for the simulations. In other words, solar thermal cooling system simulations are performed around this reference collector area.

[13]Specific collector area is the collector are required per kW of cooling capacity.

Available information from the actual installations show that specific collector area varies between 1 to $6m^2/kW$, (Henning, 2007). Effect of the collector area on the solar fraction is also presented below.

In TRNSYS simulations, collector area is taken as $20m^2$ and the effect of the primary loop mass flow rate on the solar fraction is investigated. Solar fraction (SF) is calculated as follows;

$$SF = \frac{Q_{coll}}{Q_{coll} + Q_{aux}} \tag{6.4}$$

where Q_{coll} is the useful energy gain of the flat plate collectors and Q_{aux} is the rate of energy delivered to the secondary loop fluid stream. Useful energy gain of the collector and the energy delivered to the fluid stream by the auxiliary heater are integrated daily and daily average solar fractions of four different primary loop mass flow rates for zeolite-water pair during summer months are given in Figure 6.5.

As seen from Figure 6.5, as collector mass flow rate increases up to 3600 kg/hr, solar fraction increases. This is because, as the mass flow rate through the collector increases, the temperature rise through the collector decreases. This causes lower losses since the average collector temperature is lower and there is a corresponding increase in the useful energy gain of the collector[14]. Increasing primary mass flow rate above 3600 kg/hr decreases solar fraction. This can be explained with the help of Figure 6.6. As seen from Figure 6.6, as $\dot{m}_{pl}$ increases collector outlet temperature decreases, and storage tank outlet temperature is the highest for 3600 kg/hr $\dot{m}_{pl}$. These results show that there is an optimum $\dot{m}_{pl}$ value for the effective heat transfer between primary and secondary loop[15].

Solar fractions of three different primary loop mass flow rates for activated

[14]Although solar fraction of 5040 kg/hr $\dot{m}_{pl}$ is lower than 3600 kg/hr $\dot{m}_{pl}$, useful energy gain from the collectors is higher for 5040 kg/hr $\dot{m}_{pl}$ compared to 3600 kg/hr $\dot{m}_{pl}$.

[15]In order to describe this phenomena thoroughly, TRNSYS built-in storage tank model and the heat exchanger model utilized in this model should be investigated in detail.

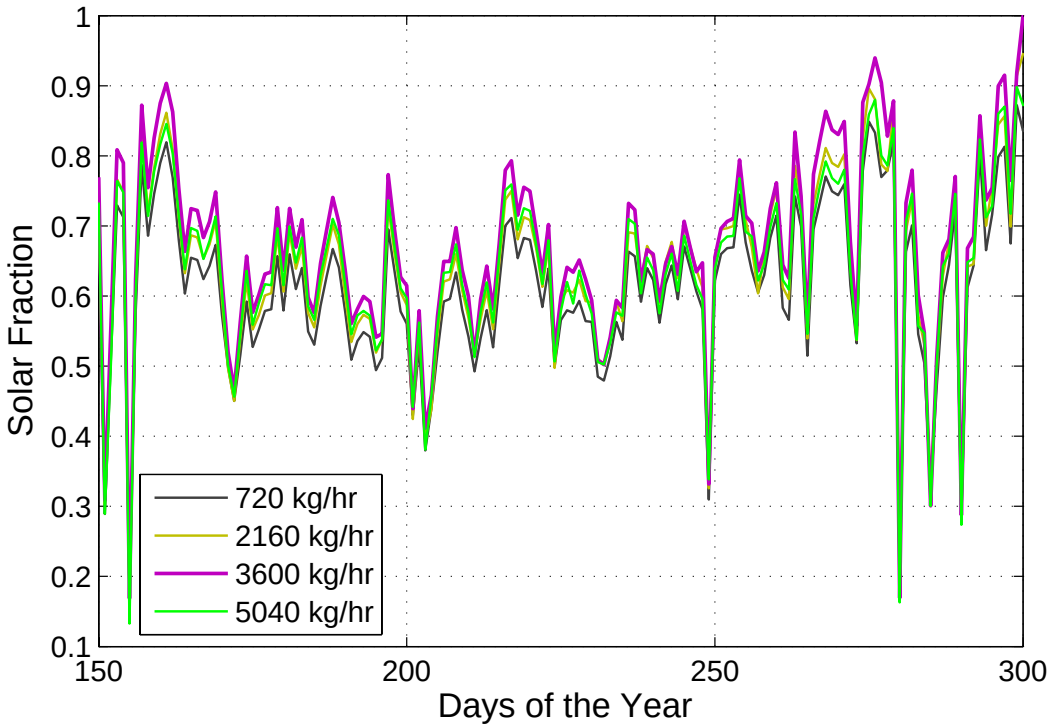

Figure 6.5: Solar fractions of four different primary loop mass flow rates during summer months. (Zeolite-Water pair, $A_{coll} = 20m^2$, $V_{tank} = 1m^3$, $\dot{m}_{sl} = 1000kg/hr$)

carbon-methanol, silica gel-water and zeolite-water pairs during summer months are also given in Figure 6.7 for reference. The COP of the silica gel-water pair is the highest and the COP of the activated carbon-methanol pair is the lowest for operating temperatures between 60°C and 80°C referring to Figure 4.4(a). Auxiliary heater outlet temperatures fluctuate between 60°C and 80°C for all three pairs as depicted in Figure 6.8.

The effect of the collector area on the solar fraction is given in Figure 6.9. As expected, as collector area increases, solar fraction increases. Economics of the collector area and the solar fraction will be investigated in the next chapter

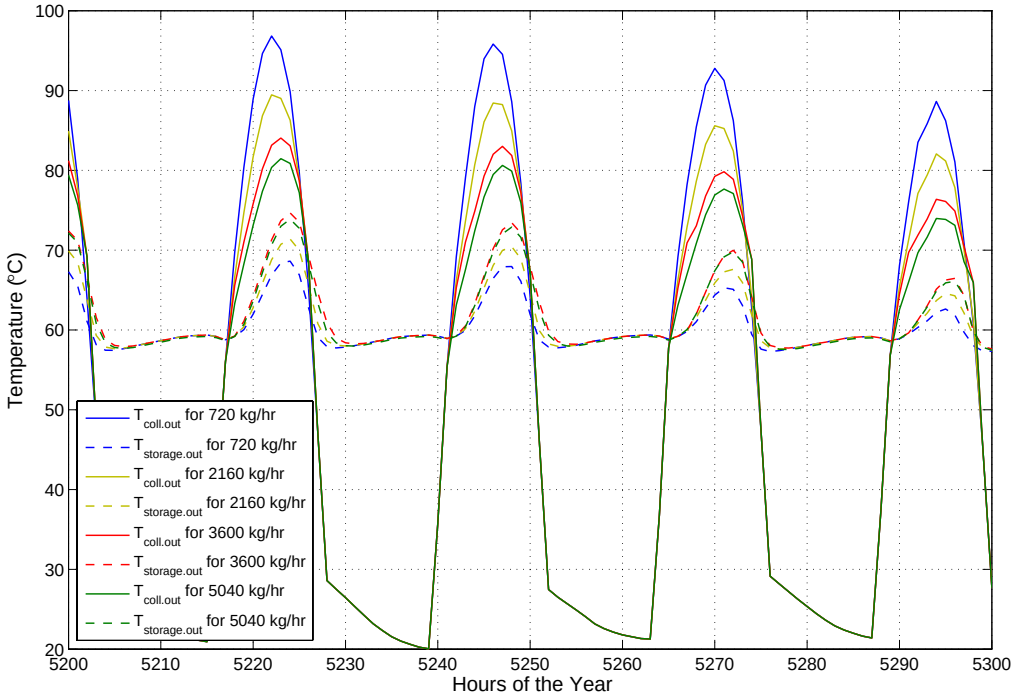

Figure 6.6: Variation of the collector outlet temperature and the hot storage tank outlet temperature for four different primary mass flow rates. (Zeolite-Water pair, $A_{coll} = 20m^2$, $V_{tank} = 1m^3$, $\dot{m}_{sl} = 1000kg/hr$)

based on the investment and operational costs of the solar cooling system.

6.4.3 Secondary Loop Mass Flow Rate

Secondary loop is controlled by two controllers, controller2 and controller3, as seen from Figure 6.2 and control strategy is explained in Section 6.3.2 in detail. For brevity, the effect of the secondary loop mass flow rate($\dot{m}_{sl}$) is investigated considering zeolite-water pair since the other pairs will also show the similar behavior. The effect of the secondary loop mass flow rate on the solar fraction is given in Figure 6.10. As seen from Figure 6.10 as $\dot{m}_{sl}$ decreases solar fraction

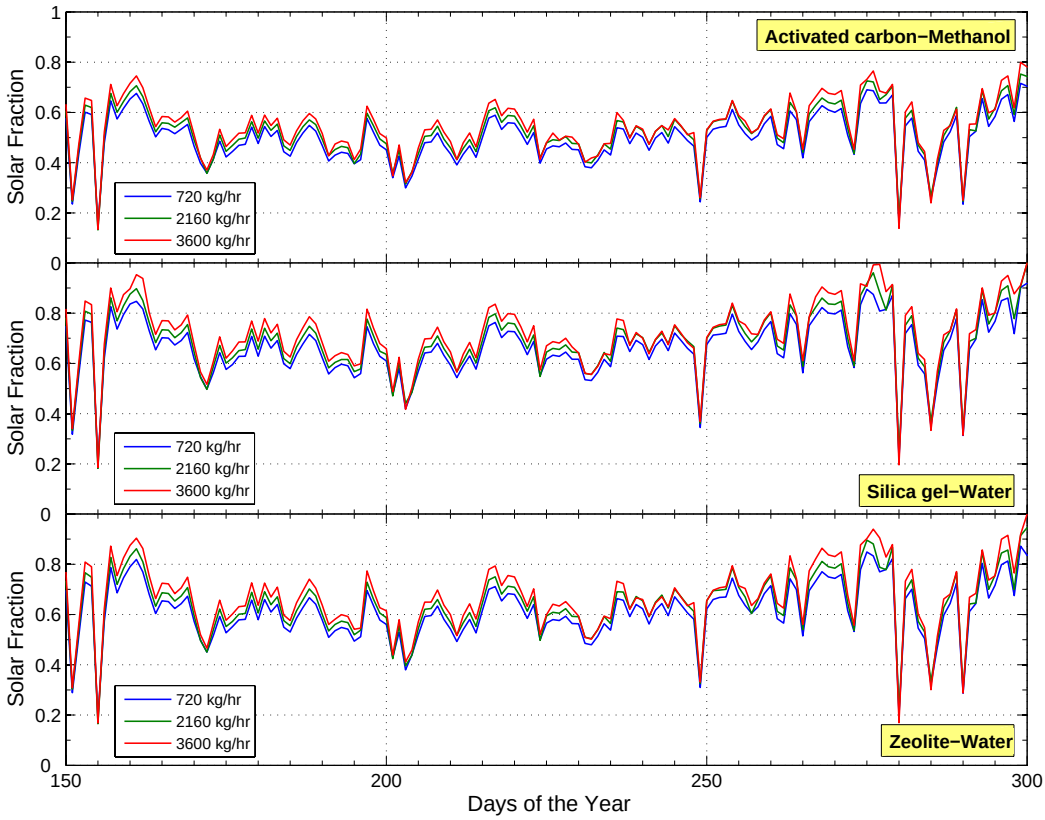

Figure 6.7: Solar fractions of three different primary loop mass flow rates during summer months. ($A_{coll} = 20m^2$, $V_{tank} = 1m^3$, $\dot{m}_{sl} = 1000kg/hr$)

increases. This is because, as $\dot{m}_{sl}$ decreases temperature difference between inlet and outlet of the hot storage tank of the secondary flow increases. In other words, secondary flow outlet temperature from the hot storage tank becomes higher which lowers the auxiliary heater energy demand. Hence solar fraction increases.

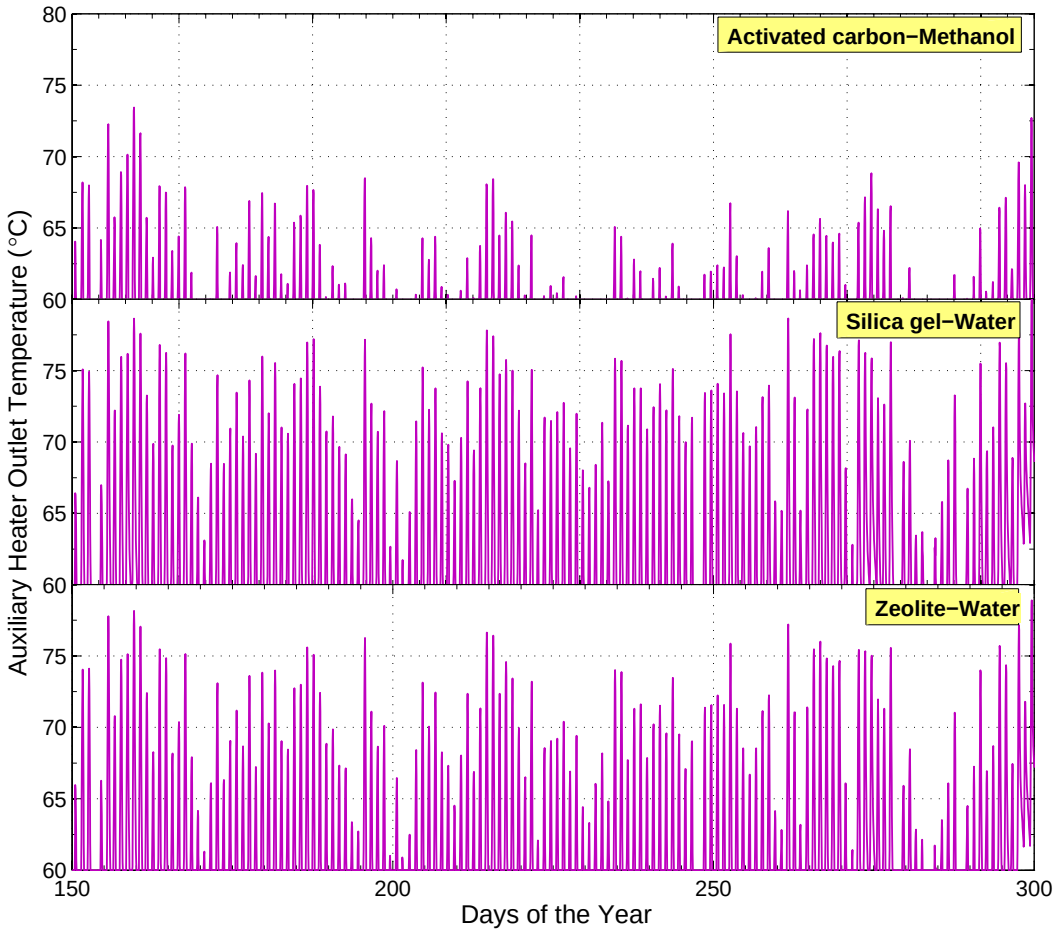

Figure 6.8: Auxiliary heater outlet temperatures during summer months. ($A_{coll} = 20m^2$, $V_{tank} = 1m^3$, $\dot{m}_{pl} = 3600kg/hr$, $\dot{m}_{sl} = 1000kg/hr$)

6.4.4 Hot Storage Tank Volume

Hot storage tank volume is also important on the system performance. For brevity, the effect of the hot storage tank volume is investigated considering zeolite-water pair since the other pairs will also show the similar behavior. Volume of the tank should not be so big since the thermal inertia of the system increases as the storage tank volume increases. On the other hand tank volume should not be too small, because tank should store enough energy for the times when there is not enough solar radiation for operating the thermal chiller.

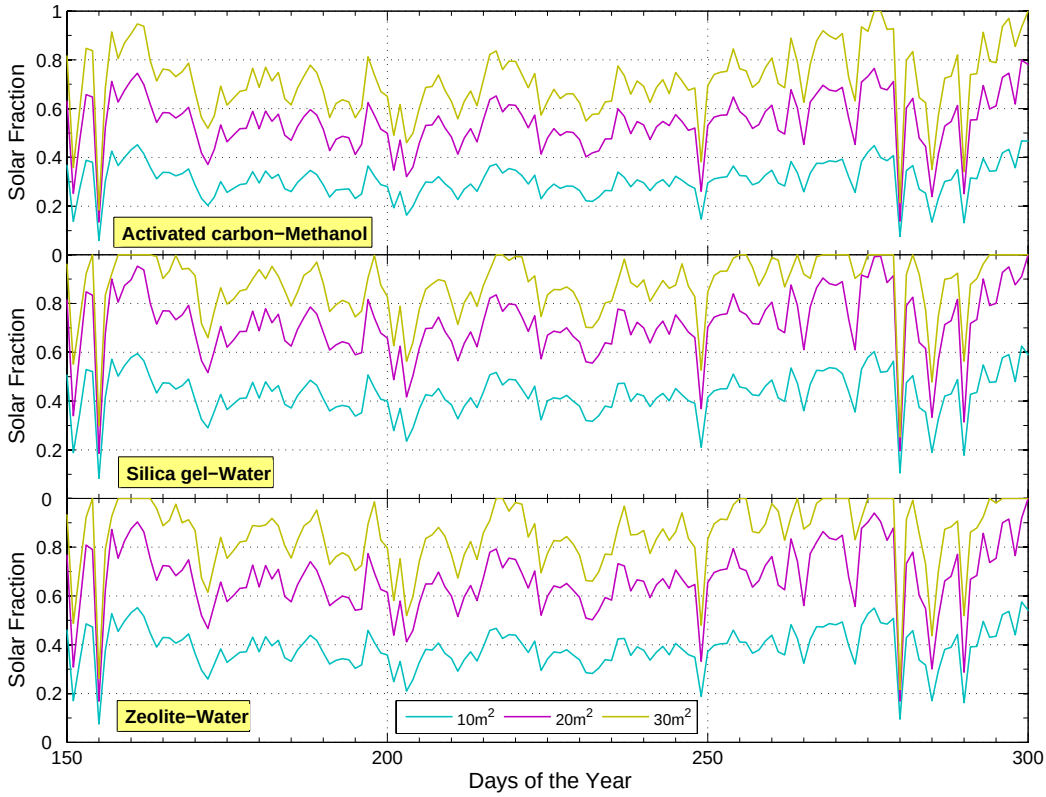

Figure 6.9: Solar fractions of three different collector areas during summer months. ($\dot{m}_{pl} = 0.05kg/s \cdot m^2$, $V_{tank} = 1m^3$, $\dot{m}_{sl} = 1000kg/hr$)

Since the hot storage tank volume is closely related to solar collector area, hot storage tank volume is investigated for $10m^2$, $20m^2$ and $30m^2$ collector areas. Effect of the hot storage tank volume on the solar fraction is given in Figure 6.11. As seen from Figure 6.11, for a $10m^2$ collector area $1m^3$, for a $20m^2$ collector area $3m^3$ and for a $30m^2$ collector area $3m^3/4m^3$ tank volumes are optimal. Figure 6.11 implies that as solar collector area increases required hot storage tank volume in order to maximize the solar fraction is also increases because as the collector area increases useful energy gain from the collector array increases and this excess useful energy gain resulting from the increase in collector area should be stored for later use. If hot storage tank volume is smaller than the optimum value, excess useful energy gain will be lost to the

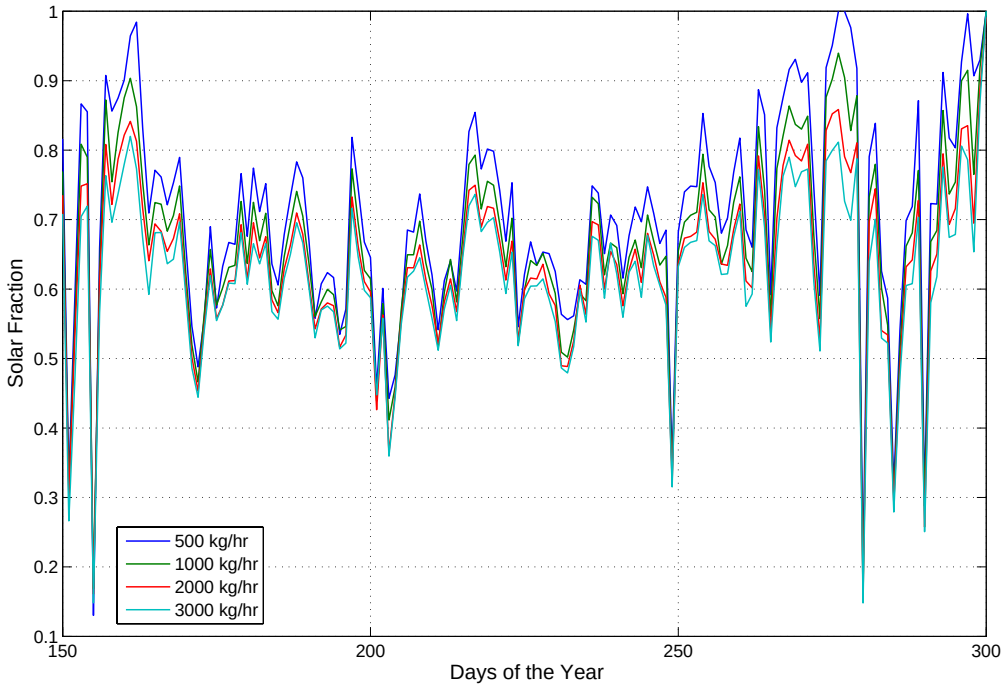

Figure 6.10: Solar fractions of different auxiliary heater mass flow rates during summer months. (Zeolite-Water pair, $A_{coll} = 20m^2$, $\dot{m}_{pl} = 3600kg/hr$, $V_{tank} = 1m^3$)

environment instead of stored.

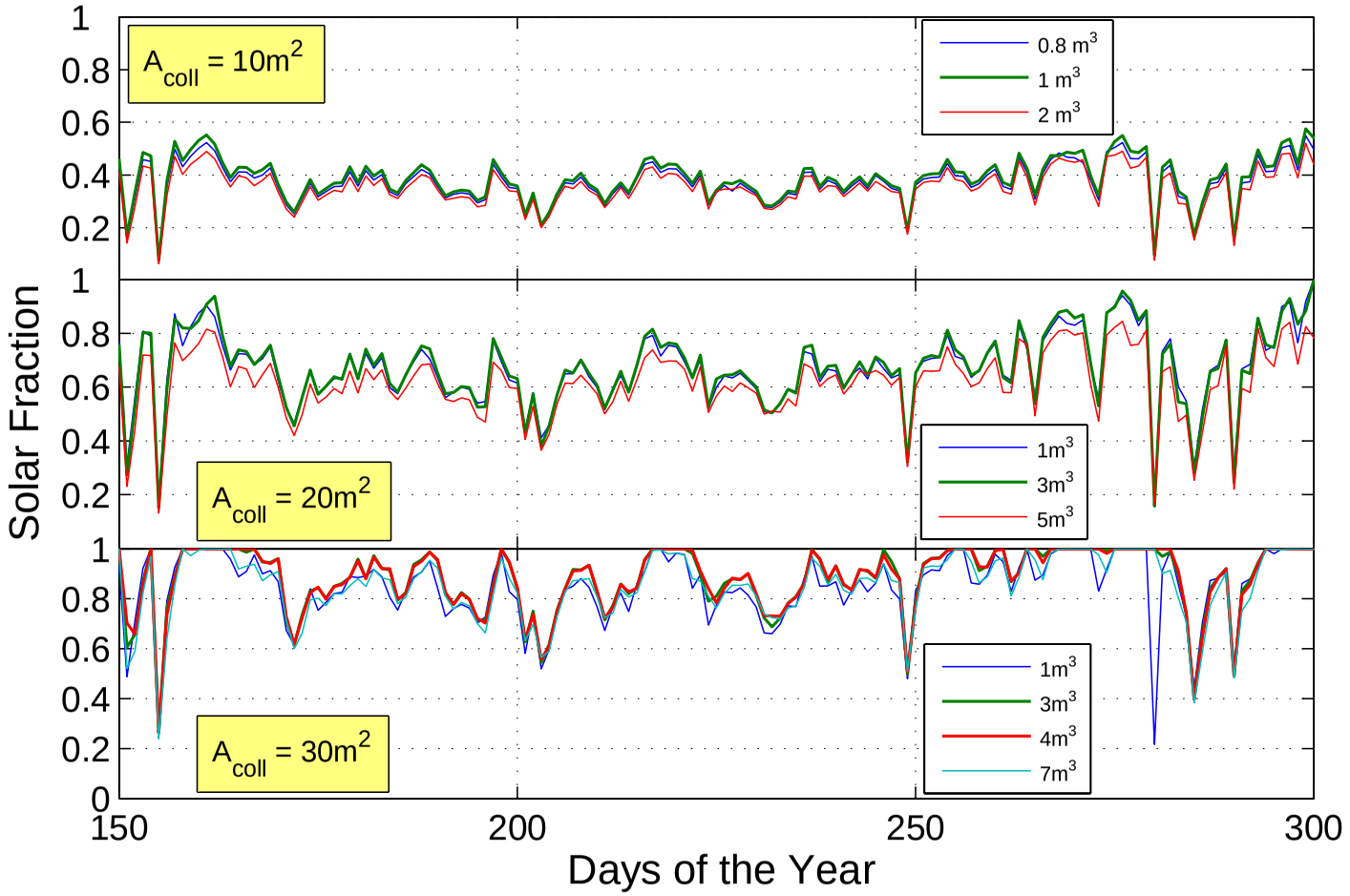

Figure 6.11: Solar fractions of different hot storage tank volumes during summer months. (Zeolite-Water pair, $\dot{m}_{pl} = 0.05kg/s \cdot m^2$, $\dot{m}_{sl} = 1000kg/hr$)

6.5 Results and Discussion

In this chapter a general overview of solar cooling systems is given. Solar-autonomous and solar-assisted systems are explained. In addition the TRNSYS model of the solar-assisted cooling system which uses newly generated ideal adsorption chiller model is presented. Details of the integrated model and the ideal adsorption chiller model is explained in detail in the preceding sections. The main factor to be considered in solar-assisted cooling system design is the solar fraction, so system parameters are investigated over a fixed range in order to find the values of the parameters which maximize the solar fraction of the solar-assisted cooling system. Therefore the collector orientation and tilt angle, collector area, collector mass flow rate, secondary loop mass rate and hot storage tank volume are investigated for different values using TRNSYS and the values which maximize the solar fraction of the solar-assisted cooling system for the conditions explored are given in Figures 6.7, 6.5, 6.9, 6.10 and 6.11.

In brief, variables for a solar-assisted cooling system model described in Figure 6.2, which is used to cool a two-storey summer house in Antalya should be selected as follows in order to maximize the solar fraction of the solar-assisted cooling system for the conditions explored:

- collector orientation $\Rightarrow$ south
- collector tilt angle $\Rightarrow 45^{\circ}$
- collector area[16] $\Rightarrow 20\text{m}^2$ or 30m^2
- collector circuit (primary loop) mass flow rate $\Rightarrow 0.05$ kg/s$\cdot$m^2
- auxiliary heater circuit (secondary loop) mass flow rate $\Rightarrow 500$ kg/hr

[16]The collector area should be selected at least 20m^2 in order to obtain solar fraction of **70-80%** depending on the working pairs (Henning, 2007). For decision making process in the selection of a collector area above 20m^2, economics and primary energy analysis, which are explained in Chapter 7, should be performed.

- hot storage tank volume $\Rightarrow$ $1m^3$ for $10m^2$, $3m^3$ for $20m^2$ and $3m^3/4m^3$ for $30m^2$ solar collector area.

Solar-assisted cooling system with the values given above, has a solar fraction between 0.5 to 0.8 depending on the working pair in summer months in Antalya. The silica gel-water pair has the highest solar fraction and the activated carbon-methanol pair has the lowest solar fraction, since the COP of the silica gel-water pair is the highest and the COP of the activated carbon-methanol pair is the lowest. A 9th degree polynomial curve fit to the yearly solar fraction is given in Figure 6.12 for the zeolite-water solar cooling system. In addition one should note that, solar fraction of the solar-assisted cooling system is closely dependent on the control system strategy, especially for complicated systems.

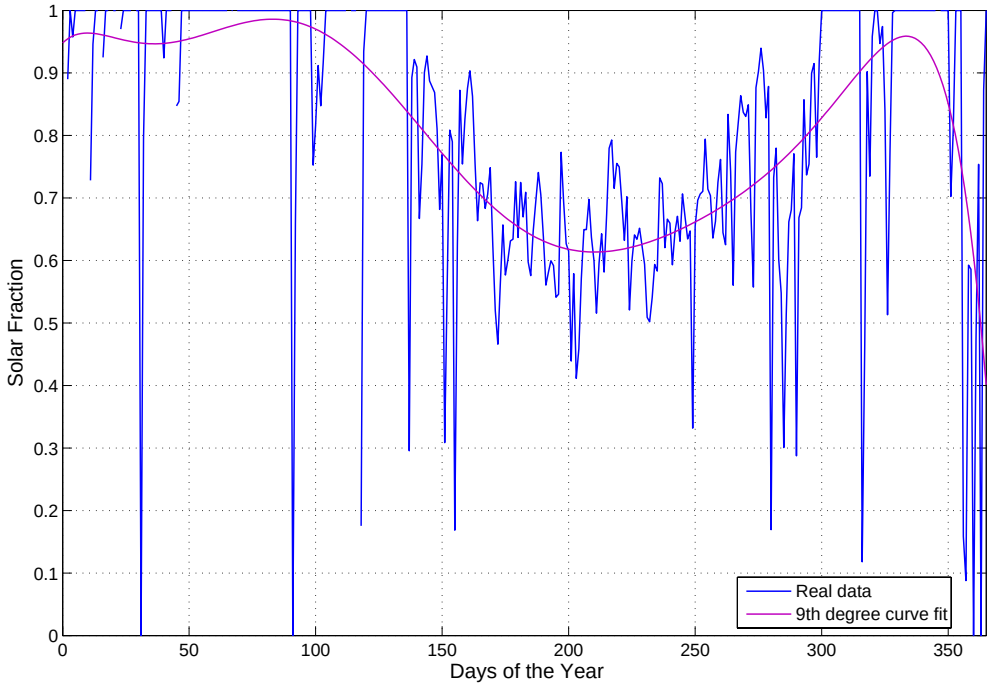

Figure 6.12: Yearly solar fraction of the solar-assisted cooling system. (Zeolite-Water pair, $A_{coll} = 20m^2$, $\dot{m}_{pl} = 3600kg/hr$, $\dot{m}_{sl} = 1000kg/hr$, $V_{tank} = 1m^3$)

CHAPTER 7

ECONOMIC ANALYSIS

The main competitors of the solar-thermal cooling systems are the conventional[1,2] vapor compression cooling systems. Nowadays it is commonly accepted that none of the solar-thermal powered cooling plants are cost competitive with conventional vapor compression cooling plants, because the main capital cost in solar-thermal cooling plants is the solar energy collection and conversion equipments' cost (i.e., solar collectors cost) (Syed, Maidment, Tozer & Missenden, 2002). In a solar-assisted cooling system, solar collector cost is between 50 to 80% of the overall system cost and is strongly dependent on the operating temperature of the solar-thermal driven chiller. Cooling systems with chillers which are driven at lower operating temperatures are more economical (Syed et al., 2002). However increasing fossil prices, decreasing solar collector prices and technical improvements in solar collectors favor the proliferation of solar-thermal cooling plant installations in near future. Additionally, there are also indirect benefits of the solar-thermal cooling plant installations like electricity peak demand reduction and greenhouse gas emission mitigation. Certainly these indirect benefits also have an economical value, but for now they do not have a direct effect on solar-thermal cooling plant users in

[1]By conventional, author imply that vapor compression chiller is driven with grid electricity.

[2]Unconventional vapor compression cooling systems (i.e., PV powered vapor compression cooling systems) are not within the scope of this study.

most of the countries. Some governments in the world, especially in developed countries, support installation of solar-thermal cooling plants through incentives and subsidies. The Kyoto protocol is the main driving force which put governments in action in supporting solar-thermal technologies.

In the literature there are many studies related to the economics and feasibility of the solar-thermal cooling technologies in which solar-thermal cooling technologies are compared with each other and with conventional vapor compression technology: (Syed et al., 2002), (Elsafty & Al-Daini, 2001), (Tsoutsos, Anagnostou, Pritchard, Karagiorgas & Agoris, 2003) and (Casals, 2006).

In this chapter, investment and operational costs of solar thermal and conventional cooling systems are compared. Solar thermal cooling system used in the economic and primary energy analysis is the heat & mass recovery zeolite-water system with the system parameters selected as follows: $\dot{m}_{pl} = 0.05$ kg/s $\cdot$ m^2, $\dot{m}_{sl}$=1000 kg/hr and V_{tank}=1m^3. Moreover, effect of the solar fraction on the economics of the solar-thermal cooling plants is investigated. Therefore the reader will have an idea on the investment and operational costs of the solar-thermal and conventional cooling plants. In addition, primary energy analysis of solar-thermal and conventional cooling systems is done.

7.1 Effect of the Solar Fraction on Costs

In the previous chapter, it is emphasized that for a reasonable solar-assisted cooling system installation the annual solar fraction of the system should be at least 70-80%. In Figure 7.1 below, useful energy gain of the solar collector array and the energy consumed by the auxiliary heater during summer months are given for 10, 20, 30, 40 and 50m^2 flat plate collector areas.

The average solar fractions of different collector areas are also given in Table

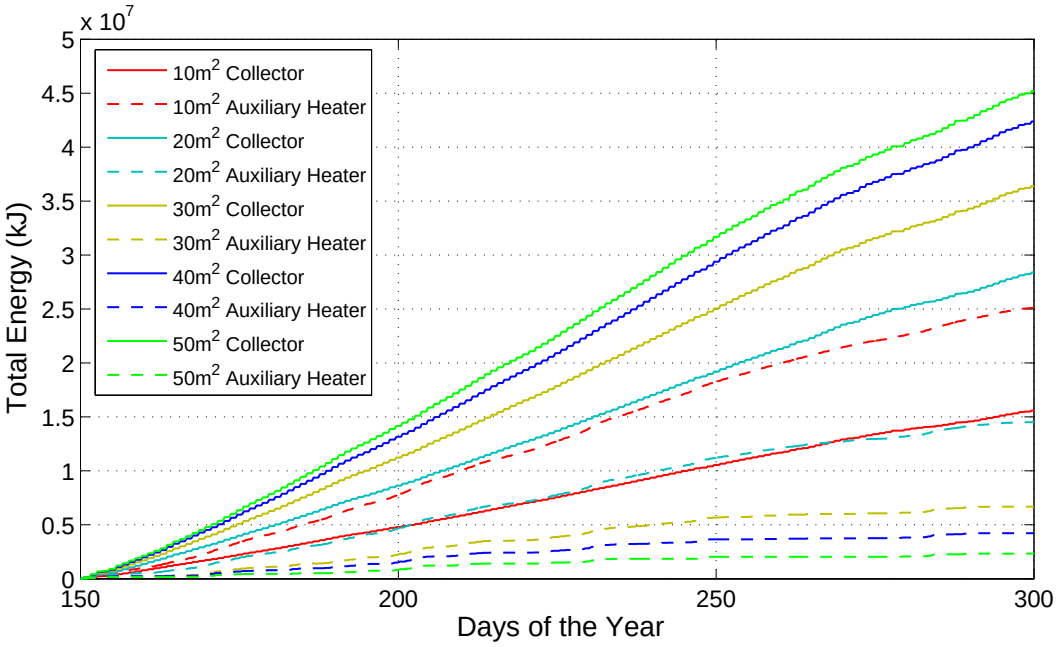

Figure 7.1: Energy consumption of the auxiliary heater and the useful energy gain of the collector array for different collector areas during summer months.

7.1[3,4] considering summer months. As expected, as collector area increases solar fraction of the cooling system also increases, but rate of increase in solar fraction decreases. Costs of the cooling systems can be investigated in the two categories, investment and operational costs which are described below.

[3]The solar fractions presented in Table 7.1 are calculated as follows: yearly total useful energy gain of the collector is divided by the yearly total useful energy gain of the collector plus yearly total energy consumption of the auxiliary heater for the corresponding collector areas.

[4]Solar fraction is calculated as follows: SF = (Qchil - Qaux) / Qchil, where Qchil is the total energy supplied to the solar thermal chiller and Qaux is the total energy added to the secondary flow from the auxiliary heater. By this way more realistic solar fraction values can be obtained because when there is no or low cooling demand, some part of the useful energy obtained from the solar collectors are lost to the environment eventually.

Table 7.1: Annual average solar fractions of different collector areas

Collector Area (m^2)	Solar Fraction
10	0.203
20	0.515
30	0.757
40	0.839
50	0.908

7.1.1 Investment Costs

Investment costs include the delivered price of solar energy equipments such as collectors, chiller, storage tank, pumps, fans, ducts, pipes, heat exchangers, controls and etc. related to the solar-thermal cooling system installation. Also cost of installing this equipment (i.e., labor) must also be taken into account. Hence the investment costs of the solar installation can be shown as follows, (Duffie et al., 2003):

$$C_S = C_A A_c + C_E \tag{7.1}$$

where C_S is the total cost of installed solar energy equipment (YTL), C_A is the total area-dependent cost (YTL/m^2), A_c is the collector area (m^2) and C_E is the total cost of equipment which is independent of collector area (YTL).

Certainly equipments and system components for a solar-thermal cooling system with $10m^2$ and $50m^2$ collector area are different. System with bigger collector area will be more costly than the system with smaller collector area, because as collector area increases system requires more piping and insulation, bigger pumps and storage tank and more labor work for the installation. However it is hard to evaluate the difference in investment costs precisely for different system sizes. Therefore in the scope of this study C_E is assumed to

be same for all systems (i.e., same solar-thermal chiller, storage tank, pumps and etc. are used in all systems). Accordingly C_E is not considered in the economic analysis. As a result, investment costs are simply calculated by multiplying collector area by the unit price of the flat plate solar collector. The unit price of the flat plate solar collector is taken as 400(YTL/m^2), (Tsoutsos et al., 2003).

Investment costs, C_{conv}, of a conventional vapor compression cooling system is the total cost of the installed equipment (e.g., conventional chiller, piping, pumps, controllers, etc.). C_{conv} is assumed to be equal to the collector area independent investment costs, C_E, of the solar-thermal cooling system. Since C_E is not considered in the economic analysis, C_{conv} is also not considered in the economic analysis. Investment costs for all systems are given in Table 7.2.

7.1.2 Operational Costs

7.1.2.1 Operational Costs of the Solar-thermal Cooling System

Operational costs are the continuing costs throughout the lifetime of the solar cooling system. Operational costs include the cost of auxiliary energy, cost of energy for the operation of fans, pumps and controllers (i.e., parasitic energy), maintenance and insurance costs, taxes and interest charges on any funds borrowed to purchase the solar equipment. In equation form, annual operational costs can be expressed as, (Duffie et al., 2003):

$$\begin{aligned} \textbf{Yearly Cost} &= \textit{fuel expense} + \textit{mortgage payment} \\ &+ \textit{maintenance and insurance cost} + \textit{parasitic energy cost} \\ &+ \textit{property taxes} - \textit{income tax savings} \end{aligned} \tag{7.2}$$

Proper calculation of the operational costs is laborious and closely dependent on the project itself [5]. In the scope of this study, only fuel expenses are taken into consideration. In other words, energy consumption of the auxiliary heater is only accounted for the operational costs and the remaining operational costs expressed in Equation 7.3 are assumed to be the same for all the systems.

Auxiliary heater is assumed to be driven with natural gas. Today in Turkey, cost of the natural gas is 0.83(YTL/m^3) for home users and the energy value of 1m^3 natural gas is 38305(kJ/m^3).

Operational cost is calculated as follows. Yearly total energy consumption of the auxiliary heater is calculated by using TRNSYS and presented in Figure 7.1. Yearly total energy consumption is divided by the energy value of a 1m^3 natural gas. Hence the volume of the yearly consumed natural gas is calculated. Finally, operational cost is simply calculated by multiplying the natural gas consumption with the unit price of the natural gas. Calculation of the operational cost is also presented in equation 7.3. Results are summarized in Table 7.2 for five different collector areas.

$$M_{tot,sol} = \frac{E_{aux}}{e_{ng}} \cdot ng_u \tag{7.3}$$

where $M_{tot,sol}$ is the yearly electricity bill of the solar assisted cooling system in YTL, E_{aux} is the yearly total energy consumption of the auxiliary heater in kJ, e_{ng} is the energy value of 1m^3 natural gas in kJ/m^3 and ng_u is the unit price of the natural gas in YTL/m^3.

7.1.2.2 Operational Costs of the Conventional Cooling System

As for the solar-thermal cooling system, only fuel expenses are taken as the operational costs of the conventional vapor compression cooling system. Conventional cooling system is powered by grid electricity, so yearly electricity

[5] Operational costs are dependent on the tax law of the country and the subsidies and incentives available for solar-thermal applications in the country.

energy consumption of the conventional chiller should be calculated. The COP of the conventional chiller is taken as 2.5. Yearly cooling load of the building, which should be supplied by the conventional chiller, is calculated by using TRNSYS. Yearly total cooling load, E_{cool}, of the building is $2.57 \cdot 10^7$ kJ. The unit price of the electricity, $elec_u$, is taken as 0.13(YTL/kWh)[6]. Conversion factor from kWh to kJ is 3600(kJ/kWh). The yearly electricity bill, $M_{tot,conv}$, of the conventional cooling system can be calculated by using Equation 7.4 below:

$$M_{tot,conv} = \frac{E_{cool} \cdot elec_u}{3600 \cdot COP} \tag{7.4}$$

from Equation 7.4, $M_{tot,conv}$ is calculated to be $\cong$ 372 YTL. Investment and operational costs of both solar-thermal and conventional cooling system are presented in Table 7.2 below.

Table 7.2: Investment and operational costs of the solar-assisted and conventional cooling system

Collector Area (m^2)	**Investment Cost** (YTL)	**Operational Cost** ($YTL/year$)
10	4000	678
20	8000	341
30	12000	151
40	16000	107
50	20000	60
Conventional chiller	-	372

[6]www.tedas.gov.tr, accessed on 28th August, 2008.

7.2 Economic Analysis

Various economic comparison methodologies are available for optimizing and evaluating solar energy systems, but there is no silver bullet on making decision on which methodology is the best. Some of these methods are Life-cycle cost (LCC), Annual life-cycle cost (ALCC), Payback time (PB) and Return on investment (ROI), (Duffie et al., 2003). LCC and PB are the mostly used methods in solar energy system's economic analysis.

In this study LCC method is employed. In this method all the costs, investment and operational, associated with the cooling system over its lifetime are summed. In addition, this method takes into account the time value of money[7].

Future value of money is expressed by, (Bejan, Tsatsaronis & Moran, 1996):

$$F = Pr(1+i)^n \tag{7.5}$$

where Pr is the present value of money (YTL), F is the future value of money (YTL), i is the percent interest per time period, and n is the time period.

Lifetime of the solar-thermal and conventional cooling system is taken as 15 years and energy inflation rate is taken as 15% annualy. Annual inflation rate in Turkey is taken as 14%, (TUİK, 2008). Using investment and operational costs given in Table 7.2, life-cycle cost of the solar-thermal and conventional cooling system can be calculated by using Equation 7.6 below.

$$F_t = Pr_i(1+i_i)^n + \sum_{i=0}^{n-1}[(Pr_{oi}(1+i_e)^n)(1+i_i)^n] \tag{7.6}$$

where F_t is the total future cost (YTL), Pr_i is the investment costs (YTL), Pr_{oi} is the initial operational costs (YTL), i_i is the inflation rate in decimal (e.g., 0.14 instead of 14%), i_e is the energy inflation rate in decimal, n is the

[7] *A money in hand today is worth more than a money received one year from now because the money in hand now can be invested for the year*, (Bejan et al., 1996).

lifetime of the solar-thermal cooling system in years. Life-cycle costs for all systems are given in Table 7.3 below.

Table 7.3: Life-cycle cost of the conventional cooling system and the solar-thermal cooling system for different collector areas

Lifetime (years)	**Life-cycle Cost (YTL)**					
	10m^2	**20m^2**	**30m^2**	**40m^2**	**50m^2**	**Conventional**
1	5449	9567	13880	18380	22880	488
2	7253	11430	16050	21120	26170	1127
3	9508	13650	18580	24270	29950	1965
4	12340	16320	21510	27900	34270	3064
5	15910	19530	24930	32100	39230	4505
6	20430	23420	28930	36960	44930	6393
7	26170	28150	33630	42590	51480	8870
8	33490	33930	39150	49130	59010	12120
9	42850	41020	45670	56740	67680	16370
10	54840	49780	53400	65630	77680	21950
11	70240	60640	62590	76040	89240	29260
12	90090	74160	73590	88260	102600	38850
13	115700	91080	86780	102700	118100	51430
14	148800	112300	102700	119700	136200	67910
15	191700	139200	122000	140000	157200	89510

As clearly seen from Table 7.3, LCC of the solar-thermal cooling system decreases up to 30m^2 collector area, then LCC of the solar-thermal cooling system increases as collector area increases. Therefore optimum collector area is around 30m^2 regarding life-cycle cost analysis. The relation between the collector area and the LCC of the solar-thermal cooling system and the LCC of the conventional cooling system is also depicted graphically in Figure 7.2 below.

As mentioned at the beginning of this chapter, solar-thermal cooling systems are not economically competitive with the grid powered conventional cooling

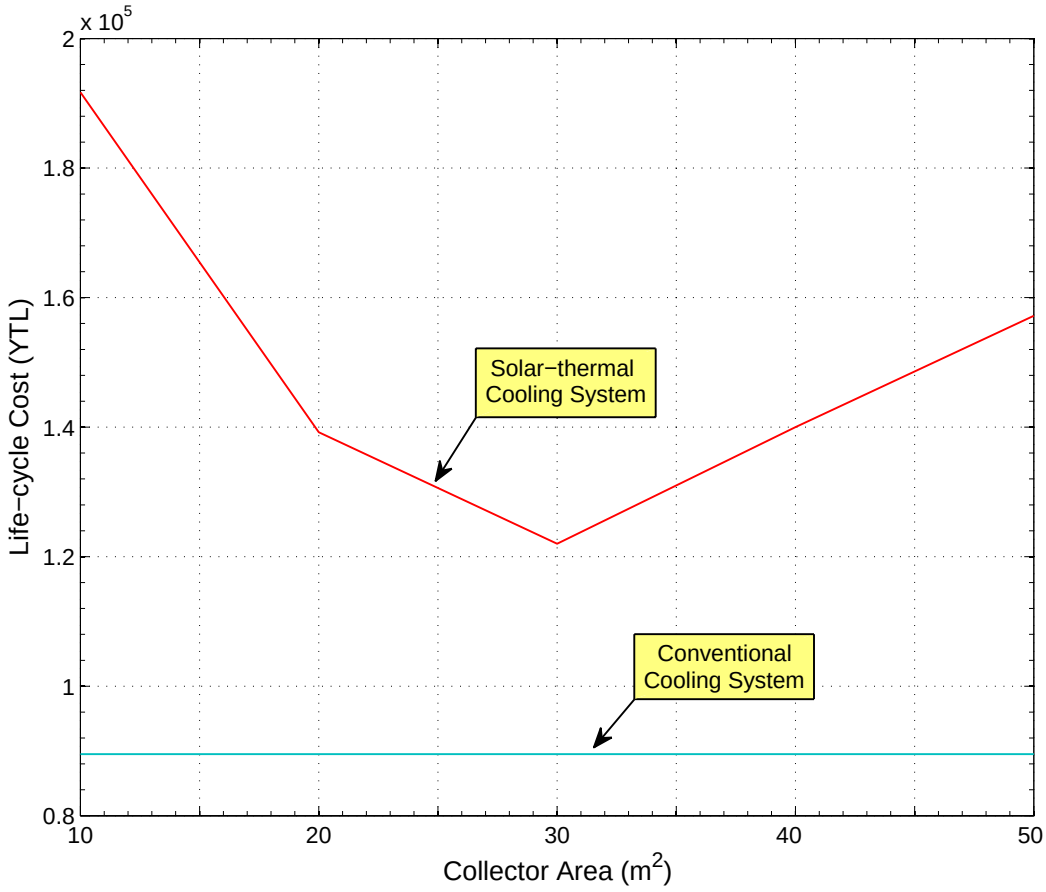

Figure 7.2: Variation of LCC of the solar-thermal cooling system with the collector area and the LCC of the conventional cooling system considering 15 years lifetime.

systems. But one should note that, the solar-thermal cooling system may be economically favorable if subsidies and incentives are available in the country where the cooling system will be installed. In addition, continually increasing fossil fuel prices and reducing collector prices will make solar-thermal cooling system attractive in the near future.

7.3 Primary Energy Analysis

Comparison of the primary energy consumptions of the cooling systems is an important factor which should be considered carefully. Solar-thermal cooling system use back-up heat which is supplied from fossil fuels. More specifically, back-up heat is assumed to be supplied by natural gas. On the other hand, conventional vapor compression cooling system is powered with grid electricity which is a secondary energy source. However in order to make comparison between the two systems, grid electricity is assumed to be generated by natural gas plant[8]. Efficiency of the natural gas plant, η_{ng}, is taken as 58%, COP of the conventional chiller is taken as 2.5 and the energy value, e_{ng}, of 1m^3 natural gas is taken as 38305 kJ/m^3. Yearly natural gas consumption of the conventional chiller can be calculated by using Equation 7.7 below:

$$NG_{conv} = \frac{E_{cool}}{\eta_{ng} \cdot COP \cdot e_{ng}} \tag{7.7}$$

where NG_{conv}(m^3) is the yearly natural gas consumption of the conventional cooling system.

Natural gas consumption of the solar-thermal cooling system is simply calculated by dividing yearly energy demand of the auxiliary heater, E_{aux}, by the energy value of the natural gas. This relation is also given in Equation 7.8 below:

$$NG_{sol} = \frac{E_{aux}}{e_{ng}} \tag{7.8}$$

where NG_{sol}(m^3) is the yearly natural gas consumption of the solar-thermal cooling system.

Yearly natural gas consumption of the solar-thermal and the conventional cool-

[8]Almost 50% of Turkey's total electricity supply is generated by natural gas plants, so this is a reasonable assumption.

ing systems is given in Table 7.4 and also depicted in Figure 7.3. As clearly seen from Figure 7.3, primary energy saving is possible if the solar collector area is over 18m^2. It is not reasonable to install solar-thermal cooling system with collector area below 18m^2, considering primary energy saving.

Table 7.4: Yearly natural gas consumption of the solar-thermal and conventional cooling system.

Collector Area (m^2)	**Natural gas consumption**(m^3)
10	817
20	411
30	182
40	128
50	73
Conventional chiller	463

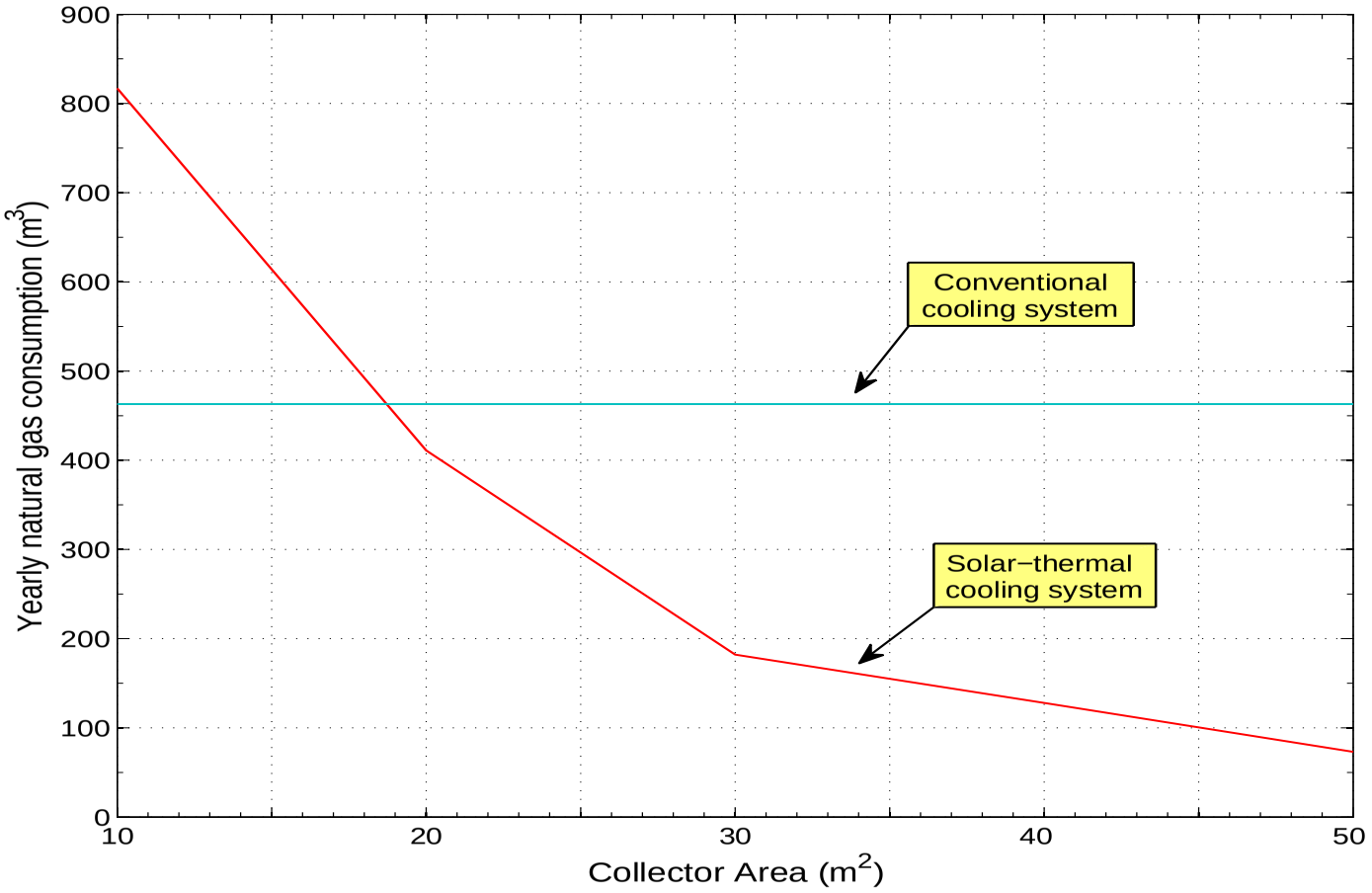

Figure 7.3: Yearly natural gas consumption of the solar-thermal and conventional cooling systems. (Conventional system assumes 58% conversion efficiency of natural gas to electricity and 2.5 COP)

CHAPTER 8

CONCLUSION

8.1 Discussion

Solar cooling technologies arouse more interest day by day. Among many solar cooling technologies, solar-thermal powered adsorption cooling seems to be a viable option. In this thesis, yearly performance of the solar adsorption cooling system is investigated in detail. In addition, system parameters effecting the performance of the adsorption chiller are analyzed and results are presented. Moreover, load side (i.e., building) of the system is modeled and parameters that should be considered in building design are presented. Finally, economic analysis is done in order to understand the economic feasibility of the solar-thermal cooling systems compared to conventional cooling systems. TRNSYS is used for the simulations. An integrated model of the overall system is developed in TRNSYS. The integrated model is composed of many components, but the solar collector, building, weather data and the adsorption chiller models are the key components. Below, main outcomes of this study are discussed and explained in detail.

In Chapter 3, typical meteorological year (TMY) for Antalya is generated by using 23 years weather data between 1983 and 2005.

In Chapter 4, ideal thermodynamic models of intermittent, heat recovery and heat & mass recovery adsorption refrigeration cycles for zeolite-water, silica gel-water and activated carbon-methanol pairs are presented. Adsorption characteristics of these pairs and some other ones are also presented. The COP of the heat & mass recovery cycle is the highest and the COP of the intermittent cycle is the lowest for all pairs. The COP values of the heat recovery and the heat & mass recovery cycles are almost same for silica gel-water and activated carbon-methanol pairs, but the COP of the heat & mass recovery cycle is ≅10% higher than the heat recovery cycle for zeolite-water pair. Therefore considering COP, mass recovery process is not very effective for silica gel-water and activated carbon-methanol pairs compared to zeolite-water pair. For operating temperatures between 60°C and 80°C heat recovery cycle with silica gel-water pair can be selected and for operating temperatures between 80°C and 100°C heat & mass recovery cycle with zeolite-water pair can be selected. Temperatures beyond 100°C is not favorable for solar-thermal powered adsorption cooling system applications and the commercially available adsorption cooling systems are usually operating between 60°C and 90°C.

Effects of the condenser and evaporator temperatures on the COP are also investigated. As expected, as evaporator temperature increases COP of the cycle also increases for all pairs. On the other hand, as condenser temperature increases COP of the cycle decreases for all pairs. The sensitivity of the zeolite-water pair to condenser and evaporator temperatures is the lowest, and the zeolite-water pair is the most suitable pair for high condenser (e.g., 40°C) and low evaporator temperatures (e.g., 5°C).

The activated carbon-methanol pair has a lower COP compared to silica gel-water and zeolite-water pairs, but it can be used for evaporator temperatures below 0°C.

In Chapter 5, cooling load of the building in Antalya is calculated by using TRNSYS. Important parameters in building design are explained and building is designed accordingly. In addition, effect of the thermal mass on the building cooling load is analyzed. Simulation results show that the building with heavy

external walls has lower cooling demand and the indoor temperature fluctuation during the day is narrower compared to building with light weight external walls.

In Chapter 6, design methodology for solar-thermal cooling system is presented. Importance of the solar fraction in the design is emphasized. Integrated model developed in TRNSYS is explained in detail and parametric studies are conducted to analyze the key system variables for maximum solar fraction for zeolite-water, silica gel-water and activated carbon-methanol pairs. The effects of varying collector area, collector circuit mass flow rate, auxiliary heater circuit mass flow rate and the hot storage tank volume are explored and the results are presented. According to the conditions examined, collector circuit mass flow rate should be selected as 0.05 kg/s·m^2 and the auxiliary heater circuit mass flow rate should be selected as 500 kg/hr. Selection of the hot storage tank volume is closely related to the collector area used in the solar-thermal cooling system. Simulation results imply that optimum hot storage tank volume increases with increasing collector area. For 10m^2, 20m^2 and 30m^2 collector area 1m^3, 3m^3 and 3 or 4m^3 hot storage tank volume should be selected respectively. It is shown that during summer months with a 20m^2 collector area, it is possible to obtain $\cong$ 0.5, $\cong$ 0.6 and $\cong$ 0.7 solar fraction on average for activated carbon-methanol, zeolite-water and silica gel-water pairs respectively.

In Chapter 7, economic analysis of the solar-thermal and conventional cooling systems is done. Investment and operational costs of these systems are calculated and compared. Usually solar cooling systems are characterized with high investment and low operational costs. This relation is also verified. As investment costs increase operational costs of solar-thermal cooling systems decrease. Moreover, life-cycle cost (LCC) analysis is done to compare the solar cooling system with different collector areas and to a conventional cooling system. As a result of LCC analysis, it is shown that solar-thermal cooling systems are not yet economically competitive with grid powered conventional vapor compression cooling systems. In addition a primary energy analysis is performed and it is shown that in order to save primary energy compared to a

conventional cooling system, the solar-thermal cooling system should have at least 18m^2 collector area.

8.2 Limitations

In this section major assumptions made in the thesis are discussed. One of the assumptions is assuming the adsorption cycle is ideal. Ideal cycle provides a performance limit for the adsorption cooling systems. The difference between the ideal performance limit and the actual performance is an indication of the potential for improvement of the thermodynamic performance. Real adsorption cooling systems certainly exhibit lower performances compared to ideal adsorption cycle results presented in Chapter 3, because of entropy generated from heat transfer, fluid friction and mass transfer resistances.

Another assumption made is related to heat transfer to the adsorption chiller in the integrated model presented in Chapter 5. It is assumed that all the thermal energy is delivered to the adsorption chiller is at hot water inlet temperature to the adsorption chiller. However this is not the case, since the outlet temperature from the adsorption chiller is lower than the hot water inlet temperature depending on the cooling load of the building. Therefore thermal energy is delivered to the adsorption chiller over a range of temperatures between hot water inlet and outlet temperature.

In the economic analysis chapter conversion factor from fossil fuels to electricity is assumed to be 58% which is an optimistic asumption for Turkey. When transmission losses and the average power plant efficiency in Turkey are taken into account conversion factor will be much lower (e.g., $\eta \cong 0.35$). The reason for selecting conversion factor as 0.58 is to be on the safe side during calculation of the primary energy consumed by the grid electricity powered conventional chiller. For conversion factors lower than 0.58, solar-thermal cooling systems will be more favorable. For instance, for conversion factors lower than 0.58 it is possible to save primary energy using solar-assisted cooling system with a

collector area lower than $18m^2$.

Another assumption is the dead mass (i.e., mass of metal parts) of the adsorption cooling system is neglected in the thermodynamic analysis. Therefore performance of the real adsorption cooling system will be lower than the ideal one presented here.

Finally, driving temperature for the ideal adsorption cooling system is between 60°C and 80°C as seen from Figure 6.8. For zeolite-water system, a regeneration temperature between 60°C and 80°C will cause small change in the adsorbed amount of water (Δw) on zeolite. Therefore in order to obtain the same cooling effect, large mass of zeolite will be required which will make the adsorption cooling system heavier and bulkier.

8.3 Future Work & Recommendations

In this thesis, the author did his best within the scope of this study. However due to complexity of the subject and the available resources there is still plenty of room for improvement. Recommendations and future work are grouped into three and explained below.

8.3.1 Adsorption Cooling Model

Adsorption cooling model is in the heart of this study and the conclusive goal of this study is to evaluate the performance of the adsorption cooling system for a residential house in Antalya throughout the year. For this reason, ideal thermodynamic model of the adsorption cooling cycle is implemented into TRNSYS to perform yearly simulations. Since the model used is ideal, results can be considered as the best case scenario. The aim using ideal model is to see how adsorption cooling system performs for the ideal case. However actual performance of the adsorption chiller is also important for realistic system simulations. For instance, it is not possible to see the real time effects of variations

in the cooling(T_{cond}) and chilled(T_{ev}) water temperatures on the performance of the adsorption chiller by using ideal model. In other words, it is possible to make simulations for different cooling and chilled water temperatures, but they remain constant during the simulation. As a result of this limitation, it also not possible to investigate the effects of the cooling tower on the performance of the overall system. Therefore adsorption chiller model should be improved for realistic simulations. There are two ways of doing this. First one is the method used in the absorption chiller model available in TRNSYS. TRNSYS make use of catalog data look up approach to estimate the COP of the absorption chiller. In this method, operating parameters (i.e., inlet hot water, chilled water and cooling water temperatures and the resulting COP of the chiller) of the chiller are obtained from the manufacturer and these are given as an input to the absorption chiller model in TRNSYS in a separate file. Second one is developing detailed theoretical adsorption chiller model in order to be used in TRNSYS. Developing such a model requires detailed bed design, consideration of heat and mass transfer limitations, estimation of the adsorption characteristics of the adsorbent/adsorbate pair, material selection, etc. This second option can be a long-term goal, since the theoretical design process will be laborious. In addition, developed model of the adsorption chiller should also be validated by experimental work. For future work, developing such a model is essential and mandatory to better understand the parameters effecting the performance of the adsorption chiller. Also such a model may be a milestone for developing novel adsorption cooling technologies.

8.3.2 Building Design, Thermal Mass & Standards

As previously mentioned, the first step in the design of any building should be reducing energy demand (i.e., heating/cooling & lighting demand) as much as possible. In this study cooling is emphasized, but designing buildings with low cooling demand is not a distinct process and it is associated with designing buildings with low heating and lighting demand. Therefore in building design, overall energy demand of the building should be considered. All the measures

taken to reduce the building energy demand are passive techniques and should be considered first. Passive design is an interdisciplinary process and, engineers and architects should collaborate during this phase. Building architectural design, site and orientation, shading devices, natural ventilation, keeping internal loads as low as possible (i.e, using appliances with A^+ certificate) and etc. can be considered as passive techniques. Only after passive design techniques are applied properly will active techniques be reasonable. Otherwise applying active techniques to a badly designed building (i.e., building with high energy demand) will be lesser of two evils.

Thermal mass of the building is a parameter which should be considered during building design. Effects of the thermal mass on the cooling load and indoor temperature is investigated in Chapter 5, but effects of thermal mass on the overall energy performance (i.e., heating load) of the building is not investigated and should be taken into account during absolute building design. Thermal mass is investigated by using light and heavy external walls. For future work, thermal mass can be investigated for different wall types and layers. Parametric studies should be conducted to find the optimum thermal mass of the building for a specific location.

Standards related to the building energy performance give guidelines and evaluation criteria for assessing the buildings' design. Many standards are available in developed countries and these standards are continually updated in order to reduce buildings' energy demand. Today in Turkey, TS 825[1] is in effect and mandatory to be applied for any building. However, TS 825 only impose limits on heating demand, not on cooling demand. Hence TS 825 should be updated properly to include limits on cooling demand and on lighting demand. In addition, there is no standard available related to passive techniques in Turkey. Such a standard will be definitely beneficial for further reducing buildings' energy demand.

[1]Thermal insulation requirements for buildings.

8.3.3 Economics of Solar-thermal Cooling

In Chapter 6, it is showed that solar-thermal cooling systems are still not competitive with the conventional vapor compression cooling systems. This result is also in accordance with the results found in the literature. However during economic analysis many assumptions are made in calculating the operational and investment costs of both systems. For complete economic analysis, parameters which are explained in Chapter 6, effecting the overall costs of the solar-thermal and conventional cooling systems should be determined precisely.

8.3.4 Weather Data

TMY data used in this study is generated by using 23 years weather data for Antalya between years 1983 and 2005. Since the effects of global warming are becoming more apparent day by day, validity of this TMY data in representing current weather conditions should be checked. Due to increasing trend in weather temperatures cooling load of the buildings calculated with TMY data may be significantly lower compared to actual cooling load. Therefore generating TMY by using more recent data (e.g., years between 2000 - 2008) may be more reasonable and should be investigated.

BIBLIOGRAPHY

Andersson B., Place W. & Kammerud R. (1985). The impact of building orientation on residential heating and cooling. *Energy and Buildings*, 8, 205-224.

Bejan A., Tsatsaronis G. & Moran M. (1996). Thermal design and optimization. USA: John Wiley & Sons.

Bering, B.P., Dubinin, M.M. & Serpinsky, V.V (1972). On thermodynamics of adsorption in micropores. *Journal of Colloid and Interface Science*, 38(1), 185-194.

Cacciola G. & Restuccia G. (1994). Progress on adsorption heat pumps. *Heat Recovery Systems and CHP*, 14(4), 409-420.

Cacciola G. & Restuccia G. (1995). Reversible adsorption heat pump: a thermodynamic model. *International Journal of Refrigeration*, 18(2), 100-106.

Cacciola G., Restuccia G. & van Benthem G.H.W. (1997). Influence of the adsorber heat exchanger design on the performance of the heat pump system. *Applied Thermal Engineering*, 19, 255-269.

Casals X.G. (2006). Solar Cooling Economic Considerations: Centralized Versus Decentralized Options. *Journal of Solar Energy Engineering*, 128, 231-236.

Chua H.T., Ng K.C., Wang W., Yap C. & Wang X.L. (2004). Transient modeling of a two-bed silica gel-water adsorption chiller. *International Journal of Heat & Mass Transfer*, 47, 659-669.

Chunnanond, K. & Aphornratana,S. (2004). Ejectors: application in refrigeration technology *Renewable & Sustainable Energy Reviews*, 8, 129-155.

Critoph R.E. (1988). Performance limitations of adsorption cycles for solar cooling. *Solar Energy*, 41(1), 21-31.

Critoph R.E. & Zhong Y. (2005). Review of trends in solid sorption refrigeration and heat pumping technology. *Proceedings of IMechE*, 219, Part E.

Çengel, Y., Boles, M. (2002). Thermodynamics: an engineering approach. Dubuque, Iowa: McGraw-Hill.

Daou, K., Wang, R.Z. & Xia, Z.Z (2006). Desiccant cooling air conditioning: a review. *Renewable and Sustainable Energy Reviews*, 10, 55-77.

Di J., Wu J.Y., Xia Z.Z. & Wang R.Z. (2007). Theoretical and experimental study on characteristics of a novel silica gel-water chiller under the conditions of variable heat source temperature. *International Journal of Refrigeration*, 30, 515-526.

Dieng A.O. (2001). Literature review on solar adsorption technologies for ice-making and air-conditioning purposes and recent developments in solar technology. *Renewable and Sustainable Energy Reviews*, 5, 313-342.

Dubinin M. M. and Radushkevitch L. V. (1947). The equation of the characteristic curve of activated charcoal. *Proceedings of Academy of Sciences of USSR*, 55, 331

Dubinin, M.M. and Stoeckli, J. (1980). Homogeneous and heterogeneous micropore structures in carbonaceous adsorbents. *Journal of Colloid and Interface Science*, 75, 34-42.

Duffie J.A., Beckman W.A. (2003). Solar Engineering of Thermal Processes. United States: Wiley-Interscience.

Elsafty A. & Al-Daini A.J. (2001). Economical comparison between a solarpowered vapour absorption air-conditioning system and a vapour compression system in the Middle East. *Renewable Energy*, 25, 569-583.

European Solar Thermal Industry Federation. 2006. About solar thermal industry

Finkelstein J.M. & Schafer R.E. (1971). Improved goodness-of-fit tests. *Biometrika*, 58(3), 641-645.

Florides G.A., Tassou S.A., Kalogirou S.A., Wrobel L.C. (2002). Review of solar and low energy cooling technologies for buildings. *Renewable and Sustainable Energy Reviews*, 6, 557-572.

German Solar Energy Society (2005). Planning and installing solar thermal systems: a guide for installers, architects, and engineers. Zrinski, Crotia: James & James.

Gorbach A., Stegmaier M. & Eigenberger G. (2004). Measurement and modeling of water vapor adsorption on zeolite 4A- equilibria and kinetics. *Adsorption*, 10, 29-46.

Günerhan H. & HepbaşlıA. (2007). Determination of the optimum tilt angle of solar collectors for building applications. *Building and Environment*, 42, 779-783.

Hall I. J., Prairie R., Anderson H. & Boes E. (1978). Generation of typical meteorological years for 26 SOLMET stations. SAND78-1601, Sandia National Laboratories, ALbuquerque, NM.

Hamamoto Y., Alam K.C.A., Saha B.B., Koyama S., Akisawa A. & Kashiwagi T. (2006). Study on adsorption refrigeration cycle utilizing activated carbon fibers. Part I. Adsorption characteristics. *International Journal of Refrigeration*, 29, 305-314.

Hartley L.E., Martinez-Lozano J.A., Utrillas M.P., Tena F. & Pedros R. (1999). The optimization of the angle of inclination of a solar collector to maximize the incident solar radiation. *Renewable Energy*, 17, 291-309.

Haywood D., Raine J.K. & Gschwendtner M.A. (2002). Stirling-cycle heat-

pumps and refrigerators - A realistic alternative? . *Proceedings of the IRHACE Technical Conference, Christchurch, 26th April 2002*, 111-118.

Henning, H.M. (2007). Solar assisted air-conditioning in buildings, A handbook for planners, 2nd ed. Wien, Austria: Springer-Verlag.

Hewitt H.C. & Griggs E.I. (1976). Optimal mass flow rates through flat plate solar collector panels. *American Society of Mechanical Engineers, Winter Annual Meeting, New york, N.Y., December 5-10, 1976*, 10p.

Hondeman H. (2000). Electrical compression cooling versus absorption cooling-a comparison. *IEA Heat Pump Centre Newsletter*, 18(4), 23-25.

Hutson N.D. & Yang R.T. (1997). Theoretical basis for the Dubinin-Radushkevitch (D-R) adsorption isotherm equation. *Adsorption*, 3, 189-195.

International Energy Agency. (2004). World Energy Outlook 2004.

International Energy Agency. (2002). Ongoing research relevant for solar assisted air conditioning systems technical report. *IEA Solar Heating and Cooling Task 25: Solar-assisted air-conditioning of buildings.*

Infinia Corporation: A Stirling technology company. http://www.infiniacorp.com/applications/clean_energy.htm accessed in 22 July 2007.

Jensen J.B. (2008). Optimal Operation of Refrigeration Cycles. PhD. thesis. Norwegian University of Science and Technology.

Kalogirou S. A. (2004). Solar thermal collectors and applications. Progress in Combustion and Energy Science, 30, 231-295.

Kalogirou S. A. (1997). Survey of solar desalination systems and system selection. *Energy*, 22, 69-81.

Keeney K. R. & Braun J. E. (1997). Application of Building Precooling to Reduce Peak Cooling Requirements. *ASHRAE Transactions*, 103, 463-469.

Khattab N. M. (2006). Simulation and optimization of a novel solar-powered adsorption refrigeration module. *Solar Energy*, 80, 823-833.

Khudhair A. M. & Farid M. M. (2004). A review on energy conservation in building applications with thermal storage by latent heat using phase change materials. *Energy Conversion and Management*, 45, 263-275.

Klein S.A. et al. (2006). TRNSYS 16.01 User's Manual. University of Wisconsin, Solar Energy Laboratory.

Leite, A. P. F. (1998). Thermodynamic analysis and modeling of an adsorption-cycle system for refrigeration from low-grade energy sources. *Journal of the Brazilian Society of Mechanical Sciences*, 20(4), 518-531.

Lucas L., IIR news, International Journal of Refrigeration 21(2) (1988), pp. 88.

Ma Q., Wang R.Z., Dai Y.J. & Zhai X.Q. (2006). Performance analysis on a hybrid air-conditioning system of a green building. *Energy and Buildings*, 38, 447-453.

McQuiston F.C., Parker J.D. & Spitler J.D. (2005). Heating, ventilating, and air conditioning : analysis and design. Hoboken, N.J.: John Wiley & Sons.

Mills, D. (2004). Advances in solar thermal electricity technology. *Solar Energy*, 76, 19-31.

Miltkau T. & Dawoud B. (2002). Dynamic modeling of the combined heat and mass transfer during the adsorption/desorption of water vapor into/from a zeolite layer of an adsorption heat pump. *International Journal of Thermal Sciences*, 41, 753-762.

Moran M.J., Shapiro H.N., Munson B.R. & DeWitt D.P. (2003). Introduction to thermal systems engineering: thermodynamics, fluid mechanics and heat transfer. United States: John Wiley & Sons, Inc.

Ng K.C., Chua H.T., Chung C.Y., Loke C.H., Kashiwagi T., Akisawa A. & Saha B.B. (2001). Experimental investigation of the silica gel-water adsorption isotherm characteristics. *Applied Thermal Engineering*, 21, 1631-1642.

National Renewable Energy Laboratory (NREL) (1995). User's manual for TMY2s (Typical Meteorological Years).

Papadopoulos A.M., Oxizidis S., Kyriakis N. (2003). Perspectives of solar cooling in view of the development in the air conditioning sectors. *Renewable and Sustainable Energy Reviews*, 7, 419-438.

Pasos E., Meunier F. & Gianola J.C. (1986). Thermodynamic performance improvement of an intermittent solar-powered refrigeration cycle using adsorption of methanol on activated carbon. *Heat Recovery Systems*, 6(3), 259-264.

Philibert C. (2005). The present and future use of solar thermal energy as a primary source of energy, InterAcademy Council.

Polanyi M. 1963. The potential theory of adsorption. *Science*, 141, 1010-1013.

Pons M. & Grenier PH. (1986). A phenomenological adsorption equilibrium law extracted from experimental and theoretical considerations applied to the activated carbon + methanol pair. *Carbon*, 24(5), 615-625.

Pons M. & Poyelle F. (1999). Adsorptive machines with advanced cycles for heat pumping or cooling applications. *International Journal of Refrigeration*, 22, 27-37.

Pridasawas W. (2003). Solar cooling. Assignment for PhD course: Solar Heating. Technical University of Denmark.

Pridasawas W. (2006). Solar-driven refrigeration systems with focus on the ejector cycle. PhD thesis. Royal Institute of Technology.

Qu T.F., Wang W. & Wang R.Z. (2002). Study of the effects of mass and heat recovery on the performances of activated carbon/ammonia adsorption refrigeration cycles. *Journal of Solar Energy Engineering*, 124, 283-290.

Refrigeration. (2007). In Encyclopedia Britannica. Retrieved February 12, 2007, from Encyclopedia Britannica Online: http://search.eb.com/eb/article-9063037

Riffat S.B. & Ma X. (2003). Thermoelectrics: a review of present and potential applications. *Applied Thermal Engineering*, 23, 913-935.

Rona N. (2004). Solar air conditioning systems; focus on components and their working principles. M.Sc. thesis. Chalmers University of Technology.

Saha B.B, Boelman E.C. & Kashiwagi T. (1995). Computer simulation of a silica gel-water adsorption refrigeration cycle- The influence of operating conditions on cooling output and COP. *ASHRAE Transactions*, 101, 348-357.

Saha B.B, El-Sharkawy I.I., Chakraborty A. & Koyama S. (2007). Study on an activated carbon fiber–ethanol adsorption chiller: Part I – system description and modeling. *International Journal of Refrigeration*, 30, 86-95.

Saha S.K. & Mahanta D.K. (2001). Thermodynamic optimization of solar flat-plate collector. *Renewable Energy*, 23, 181-193.

Sakoda A. & Suzuki M. (1984). Fundamental study on solar powered adsorption cooling system. *Journal of Chemical Engineering of Japan*, 17(1), 52-57.

Santamouris M. & Asimakopoulos D. (1996). Passive cooling of buildings. James and James (Science Publisher) Ltd.

Sawaqed N.M., Zurigat Y. H. & Al-Hinai H. (2005). A step-by-step application of Sandia method in developing typical meteorological years for different locations in Oman.*International Journal of Energy Research*, 29, 723-737.

Sayigh A.A.M. & McVeigh J.C. (1992). Solar air conditioning and refrigeration. Great Britain: Pergamon Press plc.

Sϕrensen B., (2004). Renewable energy: It's physics, engineering, use, environmental impacts, economy and planning aspects, 3rd edition. USA: Elsevier Inc.

Srikhirin P., Aphornratana S. & Chungpaibulpatana S. (2001). A review of absorption refrigeration technologies. *Renewable and Sustainable Energy Reviews*, 5, 343-372.

Srivastava N.C. & Eames I.W. (1997). A review of solid-vapor adsorption refrigeration and heat pump system developments. *Applied Thermal Engineering*, 70, 116-127.

Srivastava N.C. & Eames I.W. (1998). A review of adsorbents and adsorbates in solid-vapor adsorption heat pump systems. *Journal of the Institute of Energy*, 18, 707-714.

Sumathy K., Yeung K.H. & Yong L. (2003). Technology development in the solar adsorption refrigeration systems. *Progress in Energy and Combustion Science*, 29, 301-327.

Suzuki, M. (1990). Adsorption Engineering. Japan: Kodansha Ltd. & Elsevier Science Publishers B. V.

Syed A., Maidment G.G., Tozer R.M. & Missenden J.F. (2002). A study of the economic perspectives of solar cooling schemes. *Proceedings of the CIBSE National Technical Conference*, Chartered Institution of Building Services Engineers, London.

Szarzynski S., Feng Y. & Pons M. (1997). Study of different internal vapor transports for adsorption cycles with heat regeneration. *International Journal of Refrigeration*, 20(6), 390-401.

Tamainot-Telto Z. & Critoph R.E. (1997). Adsorption refrigerator using monolithic carbon–ammonia pair. *International Journal of Refrigeration*, 20(2), 146-155.

Tamainot-Telto Z. & Critoph R.E. (2000). Thermophysical properties of monolithic carbon. *International Journal of Heat and Mass Transfer*, 43, 2053-2058.

Tchernev D.I. (1978). Natural zeolites: Occurrence, properties, use. Oxford: Pergamon Press, Ltd. pp. 479-485.

Tsoutsos T., Anagnostou J., Pritchard C., Karagiorgas M. & Agoris D. (2003).

Solar cooling technologies in Greece. An economic viability analysis. *Applied Thermal Engineering*, 23, 1427-1439.

Trieb, F., Lagniβ, O. & Klaiβ, H. (1997). Solar electricity generation - a comparative view of technologies, costs and environmental impact. *Solar Energy*, 59, 89-99.

Türkiye İstatistik Kurumu, http://www.tuik.gov.tr, accessed on August 17, 2008.

US Department of Energy, Energy Efficiency and Renewable Energy (2007). Retrieved August 13, 2007, http://www.eere.energy.gov/buildings/energyplus/weatherdata_sources.html

Üner M. (1998). Obtaining and validating typical weather data for yearly computer simulation of heating/cooling systems in Turkey. MSc. thesis. Middle East Technical University.

Wang L., Zhu D. & Tan Y. (1999a). Heat transfer enhancement of the adsorber of an adsorption heat pump. *Adsorption*, 5, 279-286.

Wang, R.Z. & Wang, Q.B. (1999b). Adsorption mechanism and improvements of the adsorption equation for adsorption refrigeration pairs. *International Journal of Energy Research*, 23, 887-898.

Wang, S.K. (2001a). Handbook of air conditioning and refrigeration, 2nd edition. United States of America.

Wang, R.Z. (2001b). Adsorption refrigeration research in Shanghai Jiao Tong University. *Renewable and Sustainable Energy Reviews*, 5, 1-37.

Wang, R.Z. (2001c). Performance improvement of adsorption cooling by heat and mass recovery operation. *International Journal of Refrigeration*, 24, 602-611.

Wang, R.Z. & Wang, W. (2005). Investigation of non-equilibrium adsorption character in solid adsorption refrigeration cycle. *Heat Mass Transfer*, 41, 680-684.

Wang, R.Z. & Wang, L. (2005). Adsorption refrigeration- green cooling driven by low grade thermal energy. *Chinese Science Bulletin*, 50(3), 193-204.

Wang D.C., Xia Z.Z., Wu J.Y., Wang R.Z., Zhai H. & Dou W.D. (2005). Study of a novel silica gel-water adsorption chiller. Part I. Design and performance prediction. *International Journal of Refrigeration*, 28, 1073-1083.

Wikipedia (2008). http://en.wikipedia.org/wiki/Zeolite, accessed on September 15, 2008.

Wigginton, M., Harris, J. (2002). Intelligent skins. Oxford: Butterworth-Heinemann.

Wongsuwan, W., Kumar, S., Neveu P., & Meunier, F. (2001). A review of chemical heat pump technology and applications. *Applied Thermal Engineering*, 21, 1489-1519.

Zhang X.J., & Wang R.Z. (2002). A new combined adsorption-ejector refrigeration and heating hybrid system powered by solar energy. *Applied Thermal Engineering*, 22, 1245-1258.

APPENDIX A

MATLAB CODE OF HEAT & MASS RECOVERY ADSORPTION CYCLE

```
%This is the Matlab code of the ideal heat & mass recovery
%adsorption refrigeration cycle using zeolite-water pair.
%Emre DEMIROCAK, 2007

clc
clear all
close

tic

K = 273.15; %conversion constant Celcius to Kelvin
Tev = 10+K;
Tcond = 40+K;
%Tgen = 200+K;
delT = .1;
dT = delT*2;
Mz = 1;     %mass of zeolite in kg. Bed1 and Bed2 have equal masses
Cz = 0.920; %specific heat of zeolite [kJ/kg K]
Cw = 4.187; %specific heat of water [kJ/kg K]
Cv = 1.85;  %specific heat of water vapor [kJ/kg K]

Pcond = T2P(Tcond-K);
Pev = T2P(Tev-K);
```

```
k=100;
%Maximum Adsorbate/Adsorbent ratio is found by using evaporator
%temperature (Tev) and adsorption equilibrium equation function AdsW.

run = 40;
Qreg = zeros(run,1);
Qads = zeros(run,1);
Qsa = zeros(run,1);
Qsve = zeros(run,1);
Qe = zeros(run,1);
Qa = zeros(run,1);
Qa1 = zeros(run,1);
Qic1 = zeros(run,1);
Qd1 = zeros(run,1);
Qtot = zeros(run,1);
COP = zeros(run,2);
Ta1 = zeros(run,1);
T1new = zeros(run,1);
Thot = zeros(run,1);
count = zeros(run,1);
count2 = zeros(run,1);
WWmin = zeros(run,1);
sayac = zeros(run,1);
Temp = zeros(run,1);
Tint = zeros(run,1);
Ta2new = zeros(run,1);
P_hot = zeros(run,1);
P_cool = zeros(run,1);

threshold = 0.01;
regtemp = 59;   %initial regeneration temperature

for i = 1:run

  Tgen = regtemp+K+i;

  Wmin = AdsW1_TP(Tgen,Pcond);
  %assuming adsorption temp (Ta2) is equal to Tcond
  Wmax = AdsW1_TP(Tcond,Pev);
  Tg1 = AdsW3_PW(Pcond,Wmax);
  Ta2 = AdsW3_PW(Pev,Wmax);
  Ta1(i) = AdsW3_PW(Pev,Wmin);
  WWmin(i) = Wmin;

  T1new(i) = Ta2; %Bed 1 is assumed to be cool

  count2(i) = (Tgen-Ta1(i))/delT;
  Qdes = 0;
  Qsd = 0;
```

```
W2 = Wmin;
W1 = Wmax;
Ta2new(i) = Ta2; %used in modeling mass recovery

%Mass Recovery Process
for T=Tgen:-delT:(Ta1+delT)
    delW = (Cz + W2*Cw)*delT / AdsH(W2);
    Wnew = W2-delW;
    if ((abs((W2-Wnew)/W2)) > threshold)
        delW = (Cz + (W2-delW/2)*Cw)*delT / AdsH(W2-delW/2);
        Wnew = W2-delW;
    end
    P_hot(i) = AdsW2_TW(T,Wnew);

    A = (AdsH(W1+delW/2)*delW)/(Cz + (W1+delW/2)*Cw);
    T_cool = Ta2new(i) + A;
    Ta2new(i) = T_cool;
    P_cool(i) = AdsW2_TW(T_cool,W1+delW/2);

    W1 = W1+delW/2;
    W2 = W2-delW/2;

    if(P_cool(i) > P_hot(i))
        break
    end

end

T1new(i) = AdsW3_PW(P_cool(i),W1);
Tint(i) =  T1new(i);
Tg1 = AdsW3_PW(Pcond,W1);
Tgen = AdsW3_PW(P_hot(i),W2);
Wmin = W2;
Wmax = W1;


%Heat Recovery Process
for T=Tgen:-delT:(Ta2+delT)
   Thot(i) = T;
   Qic = 0;
   if (T > T1new(i) && T1new(i) < Tg1) %defines isosteric cooling

       %Isosteric cooling process for BED2 (3->4) in P-T-w diagram
       Qic = Mz*(Cz + Cw*Wmin)*(delT);
       Qic1(i) = Qic1(i) + Qic;

       %Isosteric heating process for BED1 (1->2) in P-T-w diagram
       T1new(i) = T1new(i) + Qic / (Mz*(Cz + Cw*Wmax));
       count(i) = count(i)+1;
```

```
   elseif (T > T1new(i) && T1new(i) > Tg1)

      %Resorption process (2->3) in P-T-w diagram
      W_before = AdsW1_TP(T,Pev);
      W_after  = AdsW1_TP((T-delT),Pev);

      %Average heat of desorption for each step
      H_avg = (AdsH(W_before) + AdsH(W_after))/2;
      %heat relased as a result of desorption
      Qads(i) = Mz*H_avg*(W_after-W_before);
      %heat released as a result of sensible cooling
      Qsa(i) = Mz*(Cz + Cw*(W_after-W_before))*delT;
      %heat absorbed as a result of heating up the vapor from
      %evaporation to adsorption temperature
      Qsve(i) = Mz*(W_after-W_before)*Cv*((0.5*(b(W_after)/...
          (log(Pev)-a(W_after)))+(b(W_before)/...
          (log(Pev)-a(W_before))))-Tev);

      Qa(i) = Qads(i) + Qsa(i) - Qsve(i);
      Qa1(i) = Qa1(i) + Qads(i) + Qsa(i) - Qsve(i);

      for Tvar=T1new(i):(dT/k):(T1new(i)+dT)
          if (Qa(i) > Qd1(i))
            W_before = AdsW1_TP(Tvar,Pcond);
            W_after  = AdsW1_TP((Tvar+dT/k),Pcond);
            %Average heat of desorption for each step
            H_avg = (AdsH(W_before) + AdsH(W_after))/2;
            %heat of desorption
            Qdes = Qdes + Mz*H_avg*(W_before-W_after);
            %sensible heat
            Qsd = Qsd + Mz*(Cz + Cw*(W_before-W_after))*(dT/k);
            Qd1(i) = Qdes + Qsd;
            sayac(i) = sayac(i)+1;
          else
              break
          end
      end

   T1new(i) = T1new(i)+ (sayac(i)*(dT/k));

   else
       break  %recovery process finished
   end
   Temp(i) = T;

end

Qreg(i) = Qic1(i) + Qa1(i);
```

```
%intermiitent cycle (heat necessary without heat recovery)

  Tgen = regtemp+K+i;
  %Wmax = AdsW1_TP(Tcond, Pev);
  Wmin = AdsW1_TP(Tgen,Pcond);
  %Tg1 = AdsW3_PW(Pcond,Wmax);

  Qih = 0;
  Qdes = 0;
  Qsd = 0;

  %Heat that must be supplied to the adsorbent for its isosteric heating
  Qih = Qih + Mz*(Cz + Cw*Wmax)*(Tg1-Tint(i));

  for T=Tg1:delT:(Tgen-delT)

      W_before = AdsW1_TP(T,Pcond);
      W_after  = AdsW1_TP((T+delT),Pcond);

      %Average heat of desorption for each step
      H_avg = (AdsH(W_before) + AdsH(W_after))/2;
      %heat of desorption
      Qdes = Qdes + Mz*H_avg*(W_before-W_after);

      Qsd = Qsd + Mz*(Cz + Cw*(W_before-W_after))*delT;

  end

%From Cacciola & Restuccia "influence of HEX design...
  LH2O = 3172-2.4425*Tev;
  Qe(i) = Mz*(W1-W2)*(LH2O - Cw*(Tcond-Tev));
  Qd = Qdes + Qsd;
  Qtot(i) = Qd + Qih - Qreg(i);

  COP(i,1) = Tgen-K;
  COP(i,2) = Qe(i)/Qtot(i);

  Qd=0;

end

toc

t = toc/60 %#ok<NOPTS>

i = 1:run;
g = plot(COP(i,1),COP(i,2),'-');
xlabel('Regeneration Temperature (\circC)')
ylabel('COP')
title('Zeolite 4A-Water Pair, T_{ev}=10\circC, T_{cond}=40\circC ')
```

```
set(g,'LineWidth',1)
grid on
legend('Cacciola et al., 1997','Location','SouthEast')
```

APPENDIX B

BUILDING FILE USED IN TYPE 56 IN TRNSYS

```
**********************************************************************
*  TRNBuild   1.0.89
**********************************************************************
*   BUILDING DESCRIPTIONS FILE TRNSYS
*   FOR BUILDING:   C:\Documents and Settings\Emre\Desktop\Folders...
*   \MyProjects\080328_TwoStorey - BuildingCoolingLoad_5zones\...
*   Building Description\e1.bui
*   GET BY WORKING WITH TRNBuild 1.0 for Windows
**********************************************************************
*
*---------------------------------------------------------------------
*  C o m m e n t s
*---------------------------------------------------------------------
*---------------------------------------------------------------------
*  P r o j e c t
*---------------------------------------------------------------------
*+++ PROJECT
*+++ TITLE=TRNSYS MANUAL VOL.6 EXAMPLE (PAGE 6-71)
*+++ DESCRIPTION=COOLING LOAD WILL BE CALCULATED FOR THIS BUILDING
*+++ CREATED=D. EMRE DEMIROCAK
*+++ ADDRESS=UNDEFINED
*+++ CITY=ANTALYA
*+++ SWITCH=UNDEFINED
*---------------------------------------------------------------------
*  P r o p e r t i e s
*---------------------------------------------------------------------
PROPERTIES
```

```
 DENSITY=1.204 : CAPACITY=1.012 : HVAPOR=2454.0 : SIGMA=2.041e-007 :
 RTEMP=293.15
*--- alpha calculation -------------------
 KFLOORUP=7.2 : EFLOORUP=0.31 : KFLOORDOWN=3.888 : EFLOORDOWN=0.31
 KCEILUP=7.2 : ECEILUP=0.31 : KCEILDOWN=3.888 : ECEILDOWN=0.31
 KVERTICAL=5.76 : EVERTICAL=0.3
*
*++++++++++++++++++++++++++++++++++++++++++++++++++++++++++++++++++++++++++++
TYPES
*++++++++++++++++++++++++++++++++++++++++++++++++++++++++++++++++++++++++++++
*
*---------------------------------------------------------------------
*  L a y e r s
*---------------------------------------------------------------------
LAYER WALL_BOARD
 CONDUCTIVITY=   1.33 : CAPACITY=      1 : DENSITY=   1000
LAYER MINERAL_WO
 CONDUCTIVITY=   0.13 : CAPACITY=    0.9 : DENSITY=     80
LAYER SPRUCE_PIN
 CONDUCTIVITY=   0.47 : CAPACITY=      2 : DENSITY=    600
LAYER PLYWOOD
 CONDUCTIVITY=   0.54 : CAPACITY=    1.2 : DENSITY=    800
LAYER POLY_VINYL
 CONDUCTIVITY=   0.83 : CAPACITY=      1 : DENSITY=   1500
LAYER PLSTRGPS20
 CONDUCTIVITY= 2.6172 : CAPACITY=   0.84 : DENSITY=   1602
LAYER INSUL125
 CONDUCTIVITY= 0.1548 : CAPACITY=   0.84 : DENSITY=     91
LAYER AIRSPACE
 RESISTANCE=    0.044
LAYER STUCCO25
 CONDUCTIVITY= 2.4912 : CAPACITY=   0.84 : DENSITY=   1858
LAYER COMMONLEAF
 CONDUCTIVITY=   0.47 : CAPACITY=   1.88 : DENSITY=    600
LAYER PLASTERBOA
 CONDUCTIVITY=    1.9 : CAPACITY=   0.84 : DENSITY=   1200
LAYER EXTRUDEDPO
 CONDUCTIVITY=    0.1 : CAPACITY=   1.47 : DENSITY=     30
LAYER LIGHTCONCR
 CONDUCTIVITY=    0.5 : CAPACITY=   0.84 : DENSITY=   1200
*---------------------------------------------------------------------
*  I n p u t s
*---------------------------------------------------------------------
INPUTS TEMPERATURE VENTILATION HUMIDITY
*---------------------------------------------------------------------
*  S c h e d u l e s
*---------------------------------------------------------------------
SCHEDULE SCHED001
 HOURS =0.0  11.0  22.0  24.0
 VALUES=0 1. 0 0
```

```
SCHEDULE WORKDAY
 HOURS =0.0  8.0  18.0  24.0
 VALUES=0 1. 0 0
SCHEDULE SCHED002
 HOURS =0.0  1.0  18.0  24.0
 VALUES=1. 0 1. 1.
*-------------------------------------------------------------------
*  W a l l s
*-------------------------------------------------------------------
WALL EXTERNAL_WALL
 LAYERS   = WALL_BOARD MINERAL_WO SPRUCE_PIN PLYWOOD POLY_VINYL
 THICKNESS= 0.006      0.102      0.051      0.006   0.013
 ABS-FRONT= 0.6   : ABS-BACK= 0.6
 HFRONT   = 11 : HBACK= 64
WALL WTYPE98
 LAYERS   = PLSTRGPS20 INSUL125 AIRSPACE STUCCO25
 THICKNESS= 0.02       0.125    0        0.025
 ABS-FRONT= 0.6   : ABS-BACK= 0.6
 HFRONT   = 11 : HBACK= 60
WALL CEILING
 LAYERS   = WALL_BOARD WALL_BOARD WALL_BOARD
 THICKNESS= 0.125      0.125      0.125
 ABS-FRONT= 0.6   : ABS-BACK= 0.6
 HFRONT   = 11 : HBACK= 64
WALL WTYPE39
 LAYERS   = PLSTRGPS20 AIRSPACE STUCCO25
 THICKNESS= 0.02       0        0.025
 ABS-FRONT= 0.6   : ABS-BACK= 0.6
 HFRONT   = 11 : HBACK= 60
WALL GROUND
 LAYERS   = COMMONLEAF PLASTERBOA EXTRUDEDPO LIGHTCONCR
 THICKNESS= 0.015      0.06       0.06       0.15
 ABS-FRONT= 0.6   : ABS-BACK= 0.6
 HFRONT   = 11 : HBACK= 11
*-------------------------------------------------------------------
*  W i n d o w s
*-------------------------------------------------------------------
WINDOW INS2_AR_1
 WINID=2001: HINSIDE=11: HOUTSIDE=64: SLOPE=90: SPACID=0: WWID=0:
 WHEIG=0 : FFRAME=0.15 : UFRAME=8.17 : ABSFRAME=0.6 : RISHADE=0 :
 RESHADE=0 : REFLISHADE=0.5 : REFLOSHADE=0.1 : CCISHADE=0.5
*-------------------------------------------------------------------
*  D e f a u l t  G a i n s
*-------------------------------------------------------------------
GAIN PERS_ISO02
 CONVECTIVE=156 : RADIATIVE=78 : HUMIDITY=0.081
GAIN COMPUTER03
 CONVECTIVE=420 : RADIATIVE=84 : HUMIDITY=0
GAIN LIGHT01_01
 CONVECTIVE=72 : RADIATIVE=648 : HUMIDITY=0
```

```
GAIN PERS_ISO01
 CONVECTIVE=144 : RADIATIVE=72 : HUMIDITY=0.059
GAIN LIGHT02_03
 CONVECTIVE=43.2 : RADIATIVE=388.8 : HUMIDITY=0
GAIN LIGHT02_04
 CONVECTIVE=43.2 : RADIATIVE=388.8 : HUMIDITY=0
*-------------------------------------------------------------------
*  O t h e r  G a i n s
*-------------------------------------------------------------------
*-------------------------------------------------------------------
*  C o m f o r t
*-------------------------------------------------------------------
*-------------------------------------------------------------------
*  I n f i l t r a t i o n
*-------------------------------------------------------------------
INFILTRATION INFIL001
 AIRCHANGE=0.6
*-------------------------------------------------------------------
*  V e n t i l a t i o n
*-------------------------------------------------------------------
VENTILATION VENTIL
 TEMPERATURE=OUTSIDE
 AIRCHANGE=0.2
 HUMIDITY=OUTSIDE
*-------------------------------------------------------------------
*  C o o l i n g
*-------------------------------------------------------------------
COOLING COOL_NO_HUMID
 ON=26
 POWER=999999999
 HUMIDITY=100
COOLING COOL_HUMID
 ON=26
 POWER=999999999
 HUMIDITY=60
*-------------------------------------------------------------------
*  H e a t i n g
*-------------------------------------------------------------------
HEATING HEAT_NO_HUMID
 ON=20
 POWER=999999999
 HUMIDITY=0
 RRAD=0
HEATING HEAT_HUMID
 ON=20
 POWER=999999999
 HUMIDITY=60
 RRAD=0
*
*-------------------------------------------------------------------
```

```
*  Z o n e s
*-------------------------------------------------------------------
ZONES LIVING ATTIC 1ST_ROOM 2ND_ROOM BATHROOM
*-------------------------------------------------------------------
*  O r i e n t a t i o n s
*-------------------------------------------------------------------
ORIENTATIONS NORTH SOUTH EAST WEST HORIZONTAL NSLOPE SSLOPE
*
*+++++++++++++++++++++++++++++++++++++++++++++++++++++++++++++++++++
BUILDING
*+++++++++++++++++++++++++++++++++++++++++++++++++++++++++++++++++++
*
*-------------------------------------------------------------------
*  Z o n e  LIVING  /  A i r n o d e  LIVING
*-------------------------------------------------------------------
ZONE LIVING
AIRNODE LIVING
WALL=EXTERNAL_WALL: SURF= 1: AREA=37: EXTERNAL: ORI=NORTH: FSKY=0.5
WINDOW= INS2_AR_1: SURF= 41: AREA= 2: EXTERNAL: ORI=NORTH: FSKY=0.5
WALL=EXTERNAL_WALL: SURF= 2: AREA=18: EXTERNAL: ORI=SOUTH: FSKY=0.5
WINDOW=INS2_AR_1: SURF=5: AREA= 3: EXTERNAL : ORI=SOUTH : FSKY=0.5
WINDOW=INS2_AR_1: SURF=6: AREA= 3: EXTERNAL : ORI=SOUTH : FSKY=0.5
WALL=EXTERNAL_WALL: SURF=3: AREA= 12: EXTERNAL: ORI=EAST: FSKY=0.5
WINDOW=INS2_AR_1 : SURF=8: AREA= 3: EXTERNAL : ORI=EAST : FSKY=0.5
WALL =EXTERNAL_WALL:SURF=4: AREA= 17: EXTERNAL: ORI=WEST: FSKY=0.5
WINDOW =INS2_AR_1 : SURF=9: AREA= 4: EXTERNAL: ORI=WEST : FSKY=0.5
WALL  =WTYPE39    : SURF=30 : AREA= 12 : ADJACENT=BATHROOM : FRONT
WALL  =WTYPE39    : SURF=32 : AREA= 6 : INTERNAL
WALL  =CEILING    : SURF=22 : AREA= 10 : ADJACENT=ATTIC : BACK
WALL  =WTYPE39    : SURF=23 : AREA= 24 : ADJACENT=1ST_ROOM : FRONT
WALL  =WTYPE39    : SURF=26 : AREA= 15 : ADJACENT=2ND_ROOM : FRONT
WALL  =GROUND     : SURF=40 : AREA= 40 : BOUNDARY=10
 REGIME
 GAIN        = PERS_ISO02 : SCALE= 2
 GAIN        = COMPUTER03 : SCALE= SCHEDULE 1*SCHED001
 GAIN        = LIGHT01_01 : SCALE= SCHEDULE 1*SCHED002
 INFILTRATION= INFIL001
 COOLING     = COOL_HUMID
 CAPACITANCE = 144: VOLUME=120: TINITIAL=20: PHINITIAL=50: WCAPR= 1
*-------------------------------------------------------------------
*  Z o n e  ATTIC  /  A i r n o d e  ATTIC
*-------------------------------------------------------------------
ZONE ATTIC
AIRNODE ATTIC
WALL =WTYPE98:SURF= 10:AREA= 28.284 :EXTERNAL :ORI=NSLOPE :FSKY=0.5
WALL =WTYPE98:SURF= 11:AREA= 28.284 :EXTERNAL :ORI=SSLOPE :FSKY=0.5
WALL =WTYPE98:SURF=  7:AREA= 6.25 :EXTERNAL :ORI=EAST :FSKY=0.5
WALL =WTYPE98:SURF= 12:AREA= 6.25 :EXTERNAL :ORI=WEST :FSKY=0.5
WALL =CEILING:SURF= 13:AREA= 10 :ADJACENT=LIVING :FRONT
WALL =CEILING:SURF= 35:AREA= 6 :ADJACENT=BATHROOM :FRONT
```

```
WALL =CEILING:SURF= 33:AREA= 12 :ADJACENT=2ND_ROOM :BACK
WALL =CEILING:SURF= 39:AREA= 12 :ADJACENT=1ST_ROOM :BACK
 REGIME
 INFILTRATION= INFIL001
 VENTILATION = VENTIL
 CAPACITANCE = 60:VOLUME= 50: TINITIAL= 20: PHINITIAL= 50: WCAPR= 1
*-------------------------------------------------------------------
*  Z o n e  1ST_ROOM  /  A i r n o d e  1ST_ROOM
*-------------------------------------------------------------------
ZONE 1ST_ROOM
AIRNODE 1ST_ROOM
WALL =EXTERNAL_WALL:SURF=14:AREA=9 :EXTERNAL : ORI=WEST : FSKY=0.5
WALL =EXTERNAL_WALL:SURF=15:AREA=10 :EXTERNAL : ORI=SOUTH : FSKY=0.5
WINDOW=INS2_AR_1: SURF= 16 : AREA=2 :EXTERNAL : ORI=SOUTH : FSKY=0.5
WALL =WTYPE39    : SURF= 24 : AREA= 24 :ADJACENT=LIVING : BACK
WALL =WTYPE39    : SURF= 36 : AREA= 9 :ADJACENT=2ND_ROOM : BACK
WALL =CEILING    : SURF= 37 : AREA=  12 :ADJACENT=ATTIC : FRONT
 REGIME
 GAIN        = PERS_ISO01 : SCALE= 1
 GAIN        = LIGHT02_03 : SCALE= SCHEDULE 1*SCHED002
 INFILTRATION= INFIL001
 COOLING     = COOL_HUMID
 CAPACITANCE = 43.2:VOLUME= 36: TINITIAL=20: PHINITIAL= 50:WCAPR= 1
*-------------------------------------------------------------------
*  Z o n e  2ND_ROOM  /  A i r n o d e  2ND_ROOM
*-------------------------------------------------------------------
ZONE 2ND_ROOM
AIRNODE 2ND_ROOM
WALL =EXTERNAL_WALL: SURF= 20: AREA=9:EXTERNAL:ORI=EAST :FSKY=0.5
WALL =EXTERNAL_WALL: SURF= 21: AREA=10:EXTERNAL:ORI=SOUTH :FSKY=0.5
WINDOW=INS2_AR_1: SURF= 25 : AREA=2 :EXTERNAL :ORI=SOUTH :FSKY=0.5
WALL =WTYPE39    : SURF= 29 : AREA=9 : ADJACENT=BATHROOM : BACK
WALL =WTYPE39    : SURF= 27 : AREA=15 : ADJACENT=LIVING : BACK
WALL =CEILING    : SURF= 28 : AREA=12 : ADJACENT=ATTIC : FRONT
WALL =WTYPE39    : SURF= 34 : AREA=9 : ADJACENT=1ST_ROOM : FRONT
 REGIME
 GAIN        = PERS_ISO01 : SCALE= 1
 GAIN        = LIGHT02_04 : SCALE= 1
 COOLING     = COOL_HUMID
 CAPACITANCE = 43.2:VOLUME= 36:TINITIAL= 20: PHINITIAL=50: WCAPR= 1
*-------------------------------------------------------------------
*  Z o n e  BATHROOM  /  A i r n o d e  BATHROOM
*-------------------------------------------------------------------
ZONE BATHROOM
AIRNODE BATHROOM
WALL =WTYPE39    : SURF= 31 : AREA= 12 : ADJACENT=LIVING : BACK
WALL =CEILING    : SURF= 38 : AREA= 6 : ADJACENT=ATTIC : BACK
WALL =WTYPE39    : SURF= 17 : AREA= 9 : ADJACENT=2ND_ROOM : FRONT
WALL =EXTERNAL_WALL:SURF=18: AREA=6 : EXTERNAL :ORI=EAST :FSKY=0.5
WALL =EXTERNAL_WALL:SURF=19: AREA=9 : EXTERNAL :ORI=NORTH :FSKY=0.5
```

```
 REGIME
 CAPACITANCE = 0.12:VOLUME= 0.1:TINITIAL=20: PHINITIAL=50: WCAPR= 1
*-------------------------------------------------------------------
*  O u t p u t s
*-------------------------------------------------------------------
OUTPUTS
 TRANSFER : TIMEBASE=1.000
 AIRNODES = LIVING
 NTYPES =  10 : QLATD - latent energy demand of zone,
  humidification(-), dehumidifcation (+)
        =  11 : QLATG - latent energy gains including ventilation,
         infiltration, couplings, internal latent Gains and
         vapor adsorbtion in walls
        =   9 : RELHUM - relativ humidity of zone air
        =   1 : TAIR - air temperature of zone
        =   2 : QSENS - sensible energy demand of zone, heating(-),
         cooling(+)
 AIRNODES = 1ST_ROOM
 NTYPES =   9 : RELHUM - relativ humidity of zone air
        =  10 : QLATD - latent energy demand of zone,
         humidification(-),
         dehumidifcation (+)
        =  11 : QLATG - latent energy gains including ventilation,
           infiltration,
         couplings, internal latent Gains and vapor adsorbtion
           in walls
        =   1 : TAIR - air temperature of zone
        =   2 : QSENS - sensible energy demand of zone, heating(-),
           cooling(+)
 AIRNODES = 2ND_ROOM
 NTYPES =   9 : RELHUM - relativ humidity of zone air
        =  10 : QLATD-latent energy demand of zone,humidification(-),
         dehumidifcation (+)
        =  11 : QLATG - latent energy gains including ventilation,
         infiltration, couplings, internal latent Gains and
         vapor adsorbtion in walls
        =   1 : TAIR - air temperature of zone
        =   2 : QSENS - sensible energy demand of zone, heating(-),
         cooling(+)
 AIRNODES = BATHROOM
 NTYPES =   1 : TAIR - air temperature of zone
 AIRNODES = ATTIC
 NTYPES =   1 : TAIR - air temperature of zone
*-------------------------------------------------------------------
*  E n d
*-------------------------------------------------------------------
END

_EXTENSION_WINPOOL_START_
WINDOW 4.1  DOE-2 Data File : Multi Band Calculation
```

```
Unit System : SI
Name        : TRNSYS 15 WINDOW LIB
Desc        : Insulating,Ar, 1.4 71/59
Window ID   : 2001
Tilt        : 90.0
Glazings    : 2
Frame       : 11                        2.270
Spacer      :  1 Class1                 2.330  -0.010   0.138
Total Height: 1219.2 mm
Total Width :  914.4 mm
Glass Height: 1079.5 mm
Glass Width :  774.7 mm
Mullion     : None
Gap         Thick   Cond  dCond    Vis   dVis   Dens   dDens     Pr     dPr
1 Argon      16.0 0.01620  5.000  2.110  6.300  1.780 -0.0060  0.680 0.00066
2               0       0      0      0      0      0       0      0       0
3               0       0      0      0      0      0       0      0       0
4               0       0      0      0      0      0       0      0       0
5               0       0      0      0      0      0       0      0       0
Angle     0    10    20    30    40    50    60    70    80    90 Hemis
Tsol  0.426 0.428 0.422 0.413 0.402 0.380 0.333 0.244 0.113 0.000 0.354
Abs1  0.118 0.118 0.120 0.123 0.129 0.135 0.142 0.149 0.149 0.000 0.132
Abs2  0.190 0.192 0.198 0.201 0.200 0.199 0.199 0.185 0.117 0.000 0.191
Abs3      0     0     0     0     0     0     0     0     0     0     0
Abs4      0     0     0     0     0     0     0     0     0     0     0
Abs5      0     0     0     0     0     0     0     0     0     0     0
Abs6      0     0     0     0     0     0     0     0     0     0     0
Rfsol 0.266 0.262 0.260 0.262 0.269 0.286 0.326 0.422 0.621 1.000 0.314
Rbsol 0.215 0.209 0.207 0.210 0.219 0.237 0.272 0.356 0.560 0.999 0.260
Tvis  0.706 0.710 0.701 0.688 0.670 0.635 0.556 0.403 0.188 0.000 0.590
Rfvis 0.121 0.115 0.114 0.118 0.132 0.163 0.228 0.376 0.649 1.000 0.203
Rbvis 0.103 0.096 0.093 0.096 0.108 0.132 0.179 0.286 0.520 0.999 0.162
SHGC  0.589 0.593 0.591 0.586 0.574 0.551 0.505 0.405 0.218 0.000 0.518
SC: 0.55
Layer ID#         9052     9065        0        0        0        0
Tir              0.000    0.000        0        0        0        0
Emis F           0.840    0.140        0        0        0        0
Emis B           0.840    0.840        0        0        0        0
Thickness(mm)      4.0      4.0        0        0        0        0
Cond(W/m2-C     ) 225.0    225.0        0        0        0        0
Spectral File     None     None     None     None     None     None
Overall and Center of Glass Ig U-values (W/m2-C)
Outdoor Temperature         -17.8 C      15.6 C      26.7 C      37.8 C
Solar  WdSpd  hcout hrout  hin
(W/m2) (m/s)     (W/m2-C)
0    0.00  12.25  3.25  7.62  1.54 1.54  1.31 1.31  1.35 1.35  1.47 1.47
0    6.71  25.47  3.21  7.64  1.62 1.62  1.36 1.36  1.40 1.40  1.53 1.53
783    0.00  12.25  3.39  7.99  1.69 1.69  1.54 1.54  1.51 1.51  1.54 1.54
783    6.71  25.47  3.30  7.81  1.79 1.79  1.63 1.63  1.58 1.58  1.59 1.59
*** END OF LIBRARY ***
```

```
*****************************************************************************
*WinID  Description              Design  U-Value g-value T-sol Rf-sol T-vis
*****************************************************************************
  2001  Insulating,Ar, 1.4 71/59  4/16/4     1.4  0.589  0.426  0.266  0.706
_EXTENSION_WINPOOL_END_
```

APPENDIX C

TRNSYS DECK FILE OF THE INTEGRATED MODEL

```
VERSION 16.1
**********************************************************************
*** TRNSYS input file (deck) generated by TrnsysStudio
*** on Pazar, Austos 24, 2008 at 16:53
*** from TrnsysStudio project: C:\Documents and Settings\YILMAZ\...
*** Desktop\080819_tez\080730_TwoStorey - BuildingCoolingLoad_5zones\...
*** cooling_model_deneme7_1.tpf
***
*** If you edit this file, use the File/Import TRNSYS Input File
*** function in TrnsysStudio to update the project.
***
*** If you have problems, questions or suggestions please contact
*** your local TRNSYS distributor or mailto:software@cstb.fr
***
**********************************************************************


**********************************************************************
*** Units
**********************************************************************

**********************************************************************
*** Control cards
**********************************************************************
* START, STOP and STEP
CONSTANTS 3
START=0
```

```
STOP=8760
STEP=1
* User defined CONSTANTS

SIMULATION   START  STOP  STEP ! Start time End time Time step
TOLERANCES 0.001 0.001 ! Integration  Convergence
LIMITS 100 30 30 ! Max iterations Max warnings Trace limit
DFQ 1 ! TRNSYS numerical integration solver method
WIDTH 72 ! TRNSYS output file width, number of characters
LIST  ! NOLIST statement
! MAP statement
SOLVER 0 1 1 ! Solver statement Minimum relaxation factor Maximum
relaxation factor
NAN_CHECK 0 ! Nan DEBUG statement
OVERWRITE_CHECK 0 ! Overwrite DEBUG statement
TIME_REPORT 0 ! disable time report
EQSOLVER 0 ! EQUATION SOLVER statement

* EQUATIONS "Turn"
*
EQUATIONS 5
TURN = 0
AA_N = 180 + TURN
AA_S = TURN
AA_E = -90 + TURN
AA_W = 90 + TURN
*$UNIT_NAME Turn
*$LAYER Main
*$POSITION 87 50

*------------------------------------------------------------------------


* EQUATIONS "Radiation"
*
EQUATIONS 24
AISZ = [109,10]
AISA = [109,11]
IT_H = Max([109,12],0)
IB_H = Max([109,13],0)
ID_H = [109,14]
AI_H = [109,16]
IT_N = [109,18]
AI_N = [109,22]
IB_N = [109,19] * LT(AI_N,90)
IT_S = [109,24]
IB_S = [109,25]
AI_S = [109,28]
IT_E = [109,30]
IB_E = [109,31]
```

```
AI_E = [109,34]
IT_W = [109,36]
IB_W = [109,37]
AI_W = [109,40]
IT_NS = [109,42]
IB_NS = [109,43]
AI_NS = [109,46]
IT_SS = [109,48]
IB_SS = [109,49]
AI_SS = [109,52]
*$UNIT_NAME Radiation
*$LAYER Main
*$POSITION 530 128

*------------------------------------------------------------------


* Model "Weather data" (Type 109)
*

UNIT 109 TYPE 109  Weather data
*$UNIT_NAME Weather data
*$MODEL .\Weather Data Reading and Processing\Standard Format\TMY2\...
Type109-TMY2.tmf
*$POSITION 185 128
*$LAYER Main #
PARAMETERS 4
2 ! 1 Data Reader Mode
30 ! 2 Logical unit
4 ! 3 Sky model for diffuse radiation
1 ! 4 Tracking mode
INPUTS 15
0,0 ! [unconnected] Ground reflectance
0,0 ! [unconnected] Slope of surface-1
0,0 ! [unconnected] Azimuth of surface-1
0,0 ! [unconnected] Slope of surface-2
0,0 ! [unconnected] Azimuth of surface-2
0,0 ! [unconnected] Slope of surface-3
0,0 ! [unconnected] Azimuth of surface-3
0,0 ! [unconnected] Slope of surface-4
0,0 ! [unconnected] Azimuth of surface-4
0,0 ! [unconnected] Slope of surface-5
0,0 ! [unconnected] Azimuth of surface-5
0,0 ! [unconnected] Slope of surface-6
0,0 ! [unconnected] Azimuth of surface-6
0,0 ! [unconnected] Slope of surface-7
0,0 ! [unconnected] Azimuth of surface-7
*** INITIAL INPUT VALUES
0.2 90 AA_N 90 AA_S 90 AA_E 90 AA_W 45 AA_N 45 AA_S 30 AA_S
*** External files
```

```
ASSIGN "Weather Data\Antalya.tm2" 30
*|? Weather data file |1000
*-------------------------------------------------------------------

* Model "Psychrometrics" (Type 33)
*

UNIT 331 TYPE 33  Psychrometrics
*$UNIT_NAME Psychrometrics
*$MODEL .\Physical Phenomena\Thermodynamic Properties\Psychrometrics\
Dry Bulb and Relative Humidity Known\Type33e.tmf
*$POSITION 294 253
*$LAYER Main #
PARAMETERS 3
2 ! 1 Psychrometrics mode
1 ! 2 Wet bulb mode
1 ! 3 Error mode
INPUTS 3
109,1  ! Weather data:Ambient temperature ->Dry bulb temp.
109,2  ! Weather data:relative humidity ->Percent relative humidity
0,0 ! [unconnected] Pressure
*** INITIAL INPUT VALUES
20 50 1
*-------------------------------------------------------------------

* Model "Sky temperature" (Type 69)
*

UNIT 69 TYPE 69  Sky temperature
*$UNIT_NAME Sky temperature
*$MODEL .\Physical Phenomena\Sky Temperature\
calculate cloudiness factor\Type69b.tmf
*$POSITION 443 201
*$LAYER Main # #
PARAMETERS 2
0 ! 1 mode for cloudiness factor
0 ! 2 height over sea level
INPUTS 4
331,7  ! Psychrometrics:Dry bulb temperature ->Ambient temperature
331,8  ! Psychrometrics:Dew point temperature. ->Dew point
temperature at ambient conditions
109,13  ! Weather data:beam radiation on horitonzal ->Beam radiation
on the horizontal
109,14  ! Weather data:sky diffuse radiation on horizontal ->Diffuse
radiation on the horizontal
*** INITIAL INPUT VALUES
0 0 0 0
*-------------------------------------------------------------------

* Model "Building" (Type 56)
```

```
*

UNIT 56 TYPE 56  Building
*$UNIT_NAME Building
*$MODEL .\Loads and Structures\Multi-Zone Building\
With Standard Output Files\Type56a.tmf
*$POSITION 698 128
*$LAYER Main # #
*$#
PARAMETERS 6
31 ! 1 Logical unit for building description file (.bui)
1 ! 2 Star network calculation switch
0.5 ! 3 Weighting factor for operative temperature
32 ! 4 Logical unit for monthly summary
33 ! 5 Logical unit for hourly temperatures
34 ! 6 Logical unit for hourly loads
INPUTS 27
331,7  ! Psychrometrics:Dry bulb temperature -> 1- TAMB
331,6  ! Psychrometrics:Percent relative humidity  -> 2- RELHUMAMB
69,1  ! Sky temperature:Fictive sky temperature -> 3- TSKY
IT_N ! Radiation:IT_N -> 4- IT_NORTH
IT_S ! Radiation:IT_S -> 5- IT_SOUTH
IT_E ! Radiation:IT_E -> 6- IT_EAST
IT_W ! Radiation:IT_W -> 7- IT_WEST
IT_H ! Radiation:IT_H -> 8- IT_HORIZONTAL
IT_NS ! Radiation:IT_NS -> 9- IT_NSLOPE
IT_SS ! Radiation:IT_SS -> 10- IT_SSLOPE
IB_N ! Radiation:IB_N -> 11- IB_NORTH
IB_S ! Radiation:IB_S -> 12- IB_SOUTH
IB_E ! Radiation:IB_E -> 13- IB_EAST
IB_W ! Radiation:IB_W -> 14- IB_WEST
IB_H ! Radiation:IB_H -> 15- IB_HORIZONTAL
IB_NS ! Radiation:IB_NS -> 16- IB_NSLOPE
IB_SS ! Radiation:IB_SS -> 17- IB_SSLOPE
AI_N ! Radiation:AI_N -> 18- AI_NORTH
AI_S ! Radiation:AI_S -> 19- AI_SOUTH
AI_E ! Radiation:AI_E -> 20- AI_EAST
AI_W ! Radiation:AI_W -> 21- AI_WEST
AI_H ! Radiation:AI_H -> 22- AI_HORIZONTAL
AI_NS ! Radiation:AI_NS -> 23- AI_NSLOPE
AI_SS ! Radiation:AI_SS -> 24- AI_SSLOPE
0,0 ! [unconnected]  25- TEMPERATURE
0,0 ! [unconnected]  26- VENTILATION
0,0 ! [unconnected]  27- HUMIDITY
*** INITIAL INPUT VALUES
0 0 0 0 0 0 0 0 0 0 0 0 0 0 0 0 0 0 0 0 0 0 0 0 0 0 0
*** External files
ASSIGN "Building Description\e1.bui" 31
*|? Building description file (*.bui) |1000
ASSIGN "T56_std-Output_20m2_3500_500_1_year.sum" 32
```

```
*|? Monthly Summary File |1000
ASSIGN "T56_std-temp_20m2_3500_500_1_year.prn" 33
*|? Hourly Temperatures |1000
ASSIGN "T56_std-q_20m2_3500_500_1_year.prn" 34
*|? Hourly Loads |1000
*------------------------------------------------------------------------

* Model "Printer" (Type 25)
*

UNIT 8 TYPE 25  Printer
*$UNIT_NAME Printer
*$MODEL .\Output\Printer\TRNSYS-Supplied Units\Type25a.tmf
*$POSITION 839 128
*$LAYER Outputs #
PARAMETERS 10
STEP ! 1 Printing interval
START ! 2 Start time
STOP ! 3 Stop time
35 ! 4 Logical unit
2 ! 5 Units printing mode
0 ! 6 Relative or absolute start time
-1 ! 7 Overwrite or Append
-1 ! 8 Print header
0 ! 9 Delimiter
1 ! 10 Print labels
INPUTS 23
56,5 ! Building: 5- QSENS_LIVING ->Input to be printed-1
56,1 ! Building: 1- QLATD_LIVING ->Input to be printed-2
56,10 ! Building: 10- QSENS_1ST_ROOM ->Input to be printed-3
56,7 ! Building: 7- QLATD_1ST_ROOM ->Input to be printed-4
56,15 ! Building: 15- QSENS_2ND_ROOM ->Input to be printed-5
56,12 ! Building: 12- QLATD_2ND_ROOM ->Input to be printed-6
Q_tot_cooling_load ! Equa-2:Q_tot_cooling_load ->Input to be printed-7
10,1 ! Flat Plate Collector:Outlet temperature ->Input to be printed-8
16,1 ! Hot Storage:Temperature at outlet ->Input to be printed-9
15,1 ! Pump2:Outlet fluid temperature ->Input to be printed-10
16,20 ! Hot Storage:Temperature at HX Outlet ->Input to be printed-11
12,1 ! Auxiliary Heater:Outlet fluid temperature ->
Input to be printed-12
12,5 ! Auxiliary Heater:Rate of energy delivery to fluid stream ->
Input to be printed-13
17,3 ! Adsorption Chiller:output-3 ->Input to be printed-14
17,4 ! Adsorption Chiller:output-4 ->Input to be printed-15
109,1 ! Weather data:Ambient temperature ->Input to be printed-16
10,3 ! Flat Plate Collector:Useful energy gain ->Input to be printed-17
16,23 ! Hot Storage:Energy delivered to HX ->Input to be printed-18
16,5 ! Hot Storage:Energy delivered to flow  ->Input to be printed-19
22,1 ! Integrator:Result of integration-1 ->Input to be printed-20
22,2 ! Integrator:Result of integration-2 ->Input to be printed-21
```

```
21,1 ! Integrator-2:Result of integration-1 ->Input to be printed-22
21,2 ! Integrator-2:Result of integration-2 ->Input to be printed-23
*** INITIAL INPUT VALUES
Q_Sens.1stZone Q_LatD.1stZone Q_Sens.2ndZone Q_LatD.2ndZone
Q_Sens.3rdZone
Q_LatD.3rdZone Q_Tot.Building T_coll.out T_storage.out T_HX.in
T_HX.out
T_aux.out Q_aux.stream COP SF T_Ambient Qu_coll Qu_hx Qu_storage
Int_Qu
Int_Aux Int2_Qu Int2_Aux
*** External files
ASSIGN "***.out" 35
*|? Output File for printed results |1000
*-------------------------------------------------------------------

* Model "Plotter" (Type 65)
*

UNIT 9 TYPE 65  Plotter
*$UNIT_NAME Plotter
*$MODEL .\Output\Online Plotter\Online Plotter Without File\Type65d.tmf
*$POSITION 796 245
*$LAYER Main #
PARAMETERS 12
10 ! 1 Nb. of left-axis variables
10 ! 2 Nb. of right-axis variables
0.0 ! 3 Left axis minimum
160 ! 4 Left axis maximum
0.0 ! 5 Right axis minimum
20000.0 ! 6 Right axis maximum
1 ! 7 Number of plots per simulation
12 ! 8 X-axis gridpoints
0 ! 9 Shut off Online w/o removing
-1 ! 10 Logical unit for output file
0 ! 11 Output file units
0 ! 12 Output file delimiter
INPUTS 20
56,4 ! Building: 4- TAIR_LIVING ->Left axis variable-1
56,17 ! Building: 17- TAIR_ATTIC ->Left axis variable-2
56,9 ! Building: 9- TAIR_1ST_ROOM ->Left axis variable-3
16,22 ! Hot Storage:Average HX temperature ->Left axis variable-4
16,3 ! Hot Storage:Average tank temperature ->Left axis variable-5
16,1 ! Hot Storage:Temperature at outlet ->Left axis variable-6
12,1 ! Auxiliary Heater:Outlet fluid temperature ->Left axis variable-7
10,1 ! Flat Plate Collector:Outlet temperature ->Left axis variable-8
15,1 ! Pump2:Outlet fluid temperature ->Left axis variable-9
16,20 ! Hot Storage:Temperature at HX Outlet ->Left axis variable-10
16,12 ! Hot Storage:Tank energy storage rate ->Right axis variable-1
16,5 ! Hot Storage:Energy delivered to flow  ->Right axis variable-2
16,23 ! Hot Storage:Energy delivered to HX ->Right axis variable-3
```

```
10,3 ! Flat Plate Collector:Useful energy gain ->Right axis variable-4
56,15 ! Building: 15- QSENS_2ND_ROOM ->Right axis variable-5
56,12 ! Building: 12- QLATD_2ND_ROOM ->Right axis variable-6
13,3 ! Pump1:Power consumption ->Right axis variable-7
15,3 ! Pump2:Power consumption ->Right axis variable-8
Q_tot_cooling_load ! Equa-2:Q_tot_cooling_load ->Right axis variable-9
12,5 ! Auxiliary Heater:Rate of energy delivery to fluid stream ->
Right axis variable-10
*** INITIAL INPUT VALUES
TAIR_LIVING TAIR_ATTIC TAIR_1stRoom Tavg_hx Tavg_storage Tstorage_out
Taux_out Tcoll_out Tchiller_out Thx_out Qstorage_rate Qflow_rate
Qhx_rate
Qu_coll QSENS_2ndRoom QLAT_2ndRoom pump1_power pump2_power
QTOT_cool.load
Aux_rate
LABELS  3
"Temperatures"
"Heat transfer rates"
"Graph 1"
*------------------------------------------------------------------------

* Model "Flat Plate Collector" (Type 1)
*

UNIT 10 TYPE 1  Flat Plate Collector
*$UNIT_NAME Flat Plate Collector
*$MODEL .\Solar Thermal Collectors\Quadratic Efficiency Collector\
2nd-Order Incidence Angle Modifiers\Type1b.tmf
*$POSITION 180 392
*$LAYER Main #
PARAMETERS 11
1 ! 1 Number in series
20 ! 2 Collector area
4.190 ! 3 Fluid specific heat
1 ! 4 Efficiency mode
40.0 ! 5 Tested flow rate
0.80 ! 6 Intercept efficiency
13.0 ! 7 Efficiency slope
0.05 ! 8 Efficiency curvature
2 ! 9 Optical mode 2
0.2 ! 10 1st-order IAM
0.0 ! 11 2nd-order IAM
INPUTS 9
13,1 ! Pump1:Outlet fluid temperature ->Inlet temperature
13,2 ! Pump1:Outlet flow rate ->Inlet flowrate
109,1 ! Weather data:Ambient temperature ->Ambient temperature
109,48 ! Weather data:total radiation on tilted surface-6 ->
Incident radiation
109,12 ! Weather data:total radiation on horizontal ->
Total horizontal radiation
```

```
109,14 ! Weather data:sky diffuse radiation on horizontal ->
Horizontal diffuse radiation
0,0 ! [unconnected] Ground reflectance
109,52 ! Weather data:angle of incidence for tilted surface -6 ->
Incidence angle
109,53 ! Weather data:slope of tilted surface-6 ->Collector slope
*** INITIAL INPUT VALUES
20.0 2500 10.0 0. 0.0 0.0 0.2 45.0 0.
*-----------------------------------------------------------------

* Model "Auxiliary Heater" (Type 6)
*

UNIT 12 TYPE 6  Auxiliary Heater
*$UNIT_NAME Auxiliary Heater
*$MODEL .\HVAC\Auxiliary Heaters\Type6.tmf
*$POSITION 491 372
*$LAYER Water Loop #
PARAMETERS 4
100000.0 ! 1 Maximum heating rate
4.19 ! 2 Specific heat of fluid
0.0 ! 3 Overall loss coefficient for heater during operation
1.0 ! 4 Efficiency of auxiliary heater
INPUTS 5
16,1  ! Hot Storage:Temperature at outlet ->Inlet fluid temperature
16,2  ! Hot Storage:Flow rate at outlet ->Fluid mass flow rate
19,1  ! Controller2:Output control function ->Control Function
0,0 ! [unconnected] Set point temperature
0,0 ! [unconnected] Temperature of surroundings
*** INITIAL INPUT VALUES
20.0 100.0 1 60.0 20.0
*-----------------------------------------------------------------

* Model "Pump1" (Type 3)
*

UNIT 13 TYPE 3  Pump1
*$UNIT_NAME Pump1
*$MODEL .\Hydronics\Pumps\Single Speed\Type3b.tmf
*$POSITION 138 488
*$LAYER Water Loop #
PARAMETERS 5
3500 ! 1 Maximum flow rate
4.190 ! 2 Fluid specific heat
60.0 ! 3 Maximum power
0.05 ! 4 Conversion coefficient
0.5 ! 5 Power coefficient
INPUTS 3
16,20 ! Hot Storage:Temperature at HX Outlet->Inlet fluid temperature
16,21  ! Hot Storage:HX flow rate ->Inlet mass flow rate
```

```
14,1  ! Controller1:Output control function ->Control signal
*** INITIAL INPUT VALUES
20.0 100.0 1.0
*-------------------------------------------------------------------

* Model "Controller1" (Type 2)
*

UNIT 14 TYPE 2  Controller1
*$UNIT_NAME Controller1
*$MODEL .\Controllers\Differential Controller w_ Hysteresis\...
for Temperatures\Solver 0 (Successive Substitution) Control Strategy\...
Type2b.tmf
*$POSITION 287 488
*$LAYER Controls #
*$# NOTE: This control strategy can only be used with solver 0...
(Successive substitution)
*$#
PARAMETERS 2
5 ! 1 No. of oscillations
200 ! 2 High limit cut-out
INPUTS 6
10,1 ! Flat Plate Collector:Outlet temperature ->
Upper input temperature Th
16,1 ! Hot Storage:Temperature at outlet ->
Lower input temperature Tl
16,20 ! Hot Storage:Temperature at HX Outlet ->
Monitoring temperature Tin
14,1 ! Controller1:Output control function ->Input control function
0,0 ! [unconnected] Upper dead band dT
0,0 ! [unconnected] Lower dead band dT
*** INITIAL INPUT VALUES
20 10 20 0 2 2
*-------------------------------------------------------------------

* Model "Hot Storage" (Type 534)
*

UNIT 16 TYPE 534  Hot Storage
*$UNIT_NAME Hot Storage
*$MODEL .\Storage Tank Library (TESS)\Cylindrical Tank\
Vertical Cylinder\Type534.tmf
*$POSITION 353 392
*$LAYER Main #
PARAMETERS 5
37 ! 1 Logical unit for data file
5 ! 2 # of tank nodes
1 ! 3 Number of ports
1 ! 4 Number of immersed heat exchangers
0 ! 5 Number of miscellaneous heat flows
```

```
INPUTS 18
15,1!Pump2:Outlet fluid temperature >Inlet temperature for port
15,2!Pump2:Outlet flow rate->Inlet flow rate for port
10,1!Flat Plate Collector:Outlet temperature->Inlet temperature for HX
10,2!Flat Plate Collector:Outlet flowrate->Inlet flow rate for HX
0,0 ! [unconnected] Top loss temperature
0,0 ! [unconnected] Edge loss temperature for node-1
0,0 ! [unconnected] Edge loss temperature for node-2
0,0 ! [unconnected] Edge loss temperature for node-3
0,0 ! [unconnected] Edge loss temperature for node-4
0,0 ! [unconnected] Edge loss temperature for node-5
0,0 ! [unconnected] Bottom loss temperature
0,0 ! [unconnected] Gas flue temperature
0,0 ! [unconnected] Inversion mixing flow rate
0,0 ! [unconnected] Auxiliary heat input for node-1
0,0 ! [unconnected] Auxiliary heat input for node-2
0,0 ! [unconnected] Auxiliary heat input for node-3
0,0 ! [unconnected] Auxiliary heat input for node-4
0,0 ! [unconnected] Auxiliary heat input for node-5
*** INITIAL INPUT VALUES
20 0 20 0 20 20 20 20 20 20 20 20 -1 0 20 20 20 20
DERIVATIVES 5
55 ! 1 Initial Tank Temperature-1
50 ! 2 Initial Tank Temperature-2
45 ! 3 Initial Tank Temperature-3
40 ! 4 Initial Tank Temperature-4
35 ! 5 Initial Tank Temperature-5
*** External files
ASSIGN "C:\Program Files\Trnsys16\Tess Models\PlugIns\
Example_534_hot.dat" 37
*|?Which file contains the parameter values for this component?|1000
*-----------------------------------------------------------------

* Model "Pump2" (Type 3)
*

UNIT 15 TYPE 3  Pump2
*$UNIT_NAME Pump2
*$MODEL .\Hydronics\Pumps\Single Speed\Type3b.tmf
*$POSITION 429 488
*$LAYER Water Loop #
PARAMETERS 5
500.0 ! 1 Maximum flow rate
4.190 ! 2 Fluid specific heat
60.0 ! 3 Maximum power
0.05 ! 4 Conversion coefficient
0.5 ! 5 Power coefficient
INPUTS 3
17,1  ! Adsorption Chiller:output-1 ->Inlet fluid temperature
17,2  ! Adsorption Chiller:output-2 ->Inlet mass flow rate
```

```
20,1  ! Controller3:Output control function ->Control signal
*** INITIAL INPUT VALUES
20.0 100.0 1.0
*-------------------------------------------------------------------

* EQUATIONS "Equa-2"
*
EQUATIONS 1
Q_tot_cooling_load = [56,1]+[56,5]+[56,7]+[56,10]+[56,12]+[56,15]
*$UNIT_NAME Equa-2
*$LAYER Main
*$POSITION 699 265

*-------------------------------------------------------------------


* Model "Adsorption Chiller" (Type 155)
*

UNIT 17 TYPE 155  Adsorption Chiller
*$UNIT_NAME Adsorption Chiller
*$MODEL .\Utility\Calling External Programs\Matlab\Type155.tmf
*$POSITION 598 372
*$LAYER Main #
PARAMETERS 5
0 ! 1 Mode
4 ! 2 Number of inputs
4 ! 3 Number of outputs
0 ! 4 Calling Mode
0 ! 5 Keep Matlab open after simulation
INPUTS 4
12,1  ! Auxiliary Heater:Outlet fluid temperature ->input-1
12,2  ! Auxiliary Heater:Outlet fluid flow rate ->input-2
Q_tot_cooling_load ! Equa-2:Q_tot_cooling_load ->input-3
12,5!Auxiliary Heater:Rate of energy delivery to fluid stream->input-4
*** INITIAL INPUT VALUES
0 0 0 0
LABELS 1
"IdealAdsChiller.m"
*-------------------------------------------------------------------

* Model "Controller2" (Type 2)
*

UNIT 19 TYPE 2  Controller2
*$UNIT_NAME Controller2
*$MODEL .\Controllers\Differential Controller w_ Hysteresis\generic\...
Solver 0 (Successive Substitution) Control Strategy\Type2d.tmf
*$POSITION 581 466
*$LAYER Controls #
```

```
*$# NOTE: This controller can only be used with Solver 0
(Successive substitution)
*$#
*$#
*$#
*$#
*$#
*$#
*$#
*$#
*$#
PARAMETERS 2
5 ! 1 No. of oscillations
100.0 ! 2 High limit cut-out
INPUTS 6
Q_tot_cooling_load ! Equa-2:Q_tot_cooling_load ->Upper input value
0,0 ! [unconnected] Lower input value
0,0 ! [unconnected] Monitoring value
19,1  ! Controller2:Output control function ->Input control function
0,0 ! [unconnected] Upper dead band
0,0 ! [unconnected] Lower dead band
*** INITIAL INPUT VALUES
20.0 100 20.0 0 2.0 2.0
*-------------------------------------------------------------------

* Model "Controller3" (Type 2)
*

UNIT 20 TYPE 2  Controller3
*$UNIT_NAME Controller3
*$MODEL .\Controllers\Differential Controller w_ Hysteresis\...
for Temperatures\Solver 0 (Successive Substitution) Control Strategy\...
Type2b.tmf
*$POSITION 373 301
*$LAYER Controls #
*$# NOTE: This control strategy can only be used with solver 0
(Successive substitution)
*$#
PARAMETERS 2
5 ! 1 No. of oscillations
100.0 ! 2 High limit cut-out
INPUTS 6
16,3!Hot Storage:Average tank temperature->Upper input temperature Th
0,0 ! [unconnected] Lower input temperature Tl
0,0 ! [unconnected] Monitoring temperature Tin
20,1 ! Controller3:Output control function ->Input control function
0,0 ! [unconnected] Upper dead band dT
0,0 ! [unconnected] Lower dead band dT
*** INITIAL INPUT VALUES
20.0 50 20.0 0 2.0 2.0
```

```
*-------------------------------------------------------------------

* Model "Integrator" (Type 24)
*

UNIT 22 TYPE 24  Integrator
*$UNIT_NAME Integrator
*$MODEL .\Utility\Integrators\Quantity Integrator\Type24.tmf
*$POSITION 90 271
*$LAYER Main #
PARAMETERS 2
24 ! 1 Integration period
0 ! 2 Relative or absolute start time
INPUTS 2
10,3!Flat Plate Collector:Useful energy gain->Input to be integrated-1
12,5 ! Auxiliary Heater:Rate of energy delivery to fluid stream ->
Input to be integrated-2
*** INITIAL INPUT VALUES
0.0 0.0
*-------------------------------------------------------------------

* Model "Integrator-2" (Type 24)
*

UNIT 21 TYPE 24  Integrator-2
*$UNIT_NAME Integrator-2
*$MODEL .\Utility\Integrators\Quantity Integrator\Type24.tmf
*$POSITION 43 197
*$LAYER Main #
PARAMETERS 2
8760 ! 1 Integration period
0 ! 2 Relative or absolute start time
INPUTS 2
10,3!Flat Plate Collector:Useful energy gain->Input to be integrated-1
12,5  ! Auxiliary Heater:Rate of energy delivery to fluid stream ->
Input to be integrated-2
*** INITIAL INPUT VALUES
0.0 0.0
*-------------------------------------------------------------------

END
```